INNATE IMMUNE SENSING OF A BACTERIAL PORE-FORMING TOXIN:
THE ROLE OF THE NLRP3 INFLAMMASOME

by

Jessica Chu

B. S., Carnegie Mellon University, 2004

Submitted to the Graduate Faculty of

University of Pittsburgh School of Medicine in partial fulfillment

of the requirements for the degree of

Doctor of Philosophy

University of Pittsburgh

2010

UNIVERSITY OF PITTSBURGH

SCHOOL OF MEDICINE

This dissertation was presented

by

Jessica Chu

It was defended on

January 28, 2010

and approved by

Lawrence P. Kane, Ph.D., Associate Professor, Department of Immunology

Adriana T. Larregina, M.D., Ph.D., Associate Professor, Department of Dermatology

Bruce A. McClane, Ph.D., Professor, Department of Microbiology and Molecular Genetics

Penelope A. Morel, M.D., Professor, Department of Immunology

Thesis Advisor: Russell D. Salter, Ph.D., Professor, Department of Immunology

INNATE IMMUNE SENSING OF A BACTERIAL PORE-FORMING TOXIN:

THE ROLE OF THE NLRP3 INFLAMMASOME

Jessica Chu, Ph.D.

University of Pittsburgh, 2010

Gram-positive bacterial infections have risen over recent years and current antibiotic treatments are not always sufficient to control these infections. Specifically, antibiotics target bacteria themselves, but not the bacterially secreted proteins that contribute to bacterial pathogenesis and host tissue damage (i.e. virulence factors). These virulence factors may linger after bacteria are eradicated, making their interaction with the host important to understand for the development of novel therapeutics to supplement antibiotics. One class of virulence factors studied in our laboratory is a large pore-forming toxin family known as the cholesterol-dependent cytolysins (CDC). These exotoxins are secreted by over twenty species of gram-positive bacteria and have been shown to contribute to the virulence of the bacteria that secrete them. We are interested in exploring the pathways initiated by CDC in host innate immune cells such as macrophages and dendritic cells. These cells would be expected to first encounter CDC after bacterial infection and therefore, pathways initiated in these cells by CDC could be targeted for the benefit of the host.

We have characterized the mechanism of mature IL-1beta secretion induced by CDC tetanolysin O (TLO) from LPS-primed murine bone marrow-derived macrophages (BMDM). This process is dependent on TLO dose and relies on the caspase-1-containing NLRP3 inflammasome as well as associated signaling pathways, which include ion fluxes and iPLA2 and cathepsin B activities. Furthermore, TLO induces different cell death programs in BMDM

that are dependent on TLO dose. High TLO doses induce conventional necrotic cell death while low TLO doses cause NLRP3 inflammasome-dependent and cathepsin B-dependent necrotic cell death that is characterized by lactate dehydrogenase (LDH) and high mobility group box 1 (HMGB1) release. Both IL-1beta and HMGB1 are pro-inflammatory cytokines that contribute to inflammation and may be useful therapeutic targets, in addition to the inflammasome. Finally, susceptibility to CDC-induced cell killing varies based on cell type. In order to determine pathways that might explain these differences, we created a variant murine dendritic cell line resistant to pore formation. Though this cell line has been characterized to some degree, future studies will be needed to pinpoint the pathways responsible for the phenotype observed.

TABLE OF CONTENTS

PREFACE

From a young age, I found a fascination in learning about the inner workings of living organisms, but it was not until I was a teenager when my mother was diagnosed with and ultimately succumbed to cancer that I began to grasp the importance and impact of scientific research. I would like to dedicate this dissertation to my mom whose long fight against a deadly disease led me down the path of scientific research and discovery in the hopes of benefiting, in some small way, those that continue to struggle with incapacitating and lethal diseases. In addition to my mom's influence in shaping not only my career path, but also the person I am today, I must acknowledge the ever present support of my dad. His continued guidance and advice in both my professional and personal life have contributed to the many successes that I have experienced in my life. Specifically, his perseverance when faced with seemingly insurmountable obstacles has imbued in me optimism and confidence when facing and overcoming challenges. But more importantly, his positive outlook on life has shown me that even failure brings its own rewards. I would also like to acknowledge my step-mother Kathy and step-sister Laura who have always supported me and bring a sense of warmth, positivity, humor, and adventure to our family. Lastly, I would like to thank my boyfriend Justin for his continual support and understanding during frustrating times in my research as well as his enthusiasm in the celebration of my successes.

ACKNOWLEDGEMENTS

My rich and rewarding experience as a graduate student would not have been possible without my mentor Russ Salter. He provided key direction and advice regarding my project, but at the same time gave me freedom to explore the scientific questions we sought to answer. Moreover, his optimism and encouragement when I would come to an impasse in my research motivated me to forge ahead. Finally and most importantly, the concern that he showed in furthering my education and career as well as the interest that he took in my life beyond the lab also meant a great deal.

When I first started working in the Salter lab, it was composed of me and a woman who was to become a good friend – Sarita Singh. I would like to thank Sarita for her help and support in teaching me basic immunology techniques, for her advice about lab and life, and for sharing her delicious Indian cooking with me! Next to join the lab was Mike Thomas. Many thanks goes to him for the countless numbers of critical scientific discussions, the continued technical support, his friendship and quirky sense of humor that lightens the mood of the lab. The lab continues to grow and within the past couple of years has included Chengqun Sun and Michelle Heid. I would like to acknowledge Cheng for his scientific advice, technical support, and positive attitude that brightens the lab atmosphere. Michelle has also contributed to many useful scientific discussions, technical support, and her laughter and enthusiastic energy keep the lab day full of excitement. I would also like to thank her for her friendship. The most recent

1.0   INTRODUCTION

In recent years, the incidence of gram-positive bacterial infections has dramatically risen. Current treatments, which mainly include antibiotics, eradicate the infecting bacteria, but their heavy use can lead to bacterial resistance. Moreover, virulence factors (e.g. toxins) already released into the host remain behind, wreaking havoc on the immune system. New therapies directly targeting these toxins are needed and initial steps must be made to understand their mechanisms of action on immune cells. Additionally, there exists an urgency to develop new gram-positive bacterial treatments in the event of a bioterror attack utilizing toxin-secreting pathogens such as *B. anthracis* (anthrax). Though much data has accumulated on the effects of virulence factors on immune cells, there still remains a gap in knowledge regarding the effects of a family of bacterial exotoxins known as cholesterol-dependent cytolysins (CDC). Specifically, it is important to understand the impact of these toxins on innate immune phagocytes, which would most likely first encounter CDC-secreting bacteria. Particularly, our laboratory is interested in studying the innate immune sensors that recognize these toxin virulence factors and their associated downstream pathways. The next two sections will review the current knowledge regarding this toxin family, including pathways activated in innate immune cells with a focus on the activation of a proinflammatory molecular complex known as the inflammasome.

1.1   CHOLESTEROL-DEPENDENT CYTOLYSINS

There are two major classes of bacterial toxins: endotoxins and exotoxins (Grandel &
Grimminger, 2003). Endotoxins are released from the outer membrane of the cell wall of Gram-
negative bacteria upon lysis or during cell division and are fairly similar regardless of the
bacterial strain. On the other hand, exotoxins are secreted into the surrounding environment by
live bacteria and distinct exotoxins are produced by different genera. These latter toxins
comprise three classes: type I toxins bind surface receptors and initiate signaling, type II toxins
form channels in the lipid bilayer, and type III toxins allow passage of an enzymatic component
into the host cell for modification of a target molecule (Henderson *et al.*, 1997). Of particular
interest is a subclass of type II exotoxins known as the cholesterol-dependent cytolysin (CDC)
family (containing 27 known members (Billington *et al.*, 2000; Palmer, 2001; Shannon *et al.*,
2003; Gelber *et al.*, 2008) – see Figure 1-1), which is specific to gram-positive bacteria.

Bacterial genus	Species	CDC	Abbreviation
Arcanobacterium	*A. pyogenes*	Pyolysin	PLO
Bacillus	*B. alvei*	Alveolysin	ALY
	B. anthracis	Anthrolysin O	ALO
	B. cereus	Cereolysin O	CLY or CLO
	B. laterosporus	Latersporolysin	LSL
	B. thuringiensis	Thuringiolysin O	TLO
Clostridium	*C. bifermentans*	Bifermentolysin	BFL
	C. botulinum	Botulinolysin	BLY
	C. chauvoei	Chauveolysin	CVL
	C. histolyticum	Histolyticolysin O	HTL
	C. novyi type A	Novyilysin O	NVL
	C. perfringens	Perfringolysin O	PFO
	C. sordellii	Sordellilysin	SDL
	C. septicum	Septicolysin O	SPL
	C. tetani	Tetanolysin	TLO or TLY
Gardnerella	*G. vaginalis*	Vaginolysin	VLY
Listeria	*L. ivanovii*	Ivanolysin	ILO
	L. monocytogenes	Listeriolysin O	LLO
	L. seeligeri	Seeligerolysin	LSO
Streptococcus	*S. canis*	Streptolysin O	SLO
	S. equisimilis	Streptolysin O	SLO
	S. intermedius	Intermedilysin	ILY
	S. pneumoniae	Pneumolysin	PLY or PLN
	S. pyogenes	Streptolysin O	SLO
	S. suis	Suilysin	SLY

Figure 1-1: The family of cholesterol-dependent cytolysins.

The 5 bacterial genera represented above are broken down into individual species of bacteria that secrete a specific

cholesterol-dependent cytolysin (CDC). The abbreviations for the full length CDC name are also provided.

1.1.1 CDC structure and pore formation process

Members of the CDC family share 30-60% primary amino acid sequence homology (Billington *et al.*, 2000), which affords them some similarities in function. Most notably, these 471-571 amino acid (47-60 kDa) proteins (Palmer, 2001) are well established in their ability to form pores in host cell membranes, a process that relies on cholesterol binding. Each monomer is rich in β-sheets and contains four domains. Collectively, these domains are responsible for cholesterol-binding (domain 4), oligomerization (domains 1 and 4), membrane insertion (domain 3), and membrane-spanning (domain 2) (Rossjohn *et al.*, 1997; Billington *et al.*, 2000). Domain 4 also contains a conserved undecapeptide sequence that includes three tryptophan residues important for membrane binding and insertion, as well as a cysteine residue, which was originally thought to be required for toxin activation when in a reduced state. Thus, these toxins were formerly known as thiol-activated cytolysins (TACYs), but have been renamed cholesterol-dependent cytolysins (CDC) given that thiol activation may not be required for cytolytic activity (Pinkney *et al.*, 1989; Saunders *et al.*, 1989; Billington *et al.*, 2000).

It has been reported that 40-80 monomers oligomerize to form transmembrane pores up to 30nm in diameter, allowing passage of ions and macromolecules (Billington *et al.*, 2000; Palmer, 2001; Tweten, 2005). The pore formation process begins by toxin binding to membrane cholesterol. The close localization of toxin monomers in cholesterol-rich regions enables them to diffuse laterally and oligomerize into a pre-pore complex that does not insert its transmembrane β-barrel into the membrane to form a full-sized pore until the requisite number of monomers has joined the ring (Shepard *et al.*, 2000; Tilley *et al.*, 2005). However, arc-like oligomers have also been observed to insert into membranes and it has been speculated that arcs

may represent premature insertion of the pre-pore complex. Other pore-forming toxins (PFTs), such as *Aeromonas hydrophila* aerolysin or *Staphylococcus aureus* α-hemolysin (also known as α-toxin), have also been shown to assemble pre-pore complexes before membrane insertion. Unlike CDC, only seven monomers contribute to each pore (Chakraborty *et al.*, 1990; Wilmsen *et al.*, 1992; van der Goot *et al.*, 1993; Valeva *et al.*, 1997).

1.1.2 Unique members of the CDC family

Though cholesterol is the major "receptor" for most CDC, the human late-stage complement receptor CD59 has been identified as the specific receptor for the CDC intermedilysin (ILY) (Giddings *et al.*, 2004) and is required for ILY-induced pore formation. However, it has been shown that the presence of cholesterol is important for the insertion of ILY into the membrane after binding to CD59 (Soltani *et al.*, 2007). Accordingly, the undecapeptide sequence of ILY diverges from the highly conserved sequence of many other CDC in that it lacks a third tryptophan residue. This change in sequence is thought to prevent thiol activation. In addition to ILY, CDC pyolysin (PLO) and seeligerilysin O (LSO) also show variation in the undecapeptide sequence. The recently identified CDC vaginolysin (VLY) has also shown specificity for CD59, and a proline residue in the undecapeptide sequence is critical for pore formation and cytotoxicity (Gelber *et al.*, 2008).

In addition to its cytolytic function, the CDC pneumolysin (PLY) possesses the unique ability to activate complement in the absence of specific antibodies (Mitchell *et al.*, 1991; Rossjohn *et al.*, 1998). This activity is conferred to PLY because of a sequence in domain 4 responsible for binding to the Fc region of IgG. Moreover, domain 4 of PLY forms a β-

sandwich similar to the Fc potion of IgG. Normally, aggregated Fc regions promote complement fixation, suggesting that PLY-Fc aggregates could play a similar role in activating complement.

Lastly, the CDC listeriolysin O (LLO) stands apart from other CDC family members in its ability to help *Listeria monocytogenes* escape from the phagolysosome of phagocytic cells (e.g. macrophages) (Nomura *et al.*, 2007) in order to replicate and spread. This bacterium is acknowledged to be the only true intracellular pathogen to produce a CDC. LLO is highly active at an acidic pH since it must function in the phagolysosome, which is highly acidic. Furthermore, LLO is degraded in the cytosol once the bacteria have escaped due to PEST (peptide sequence rich in proline (P), glutamic acid (E), serine (S), and threonine (T)) sequence recognition. It should also be noted that LLO is capable of binding cholesterol and forming pores in the plasma membrane of the J774 macrophage cell line at non-acidic pH (7.4) (Bavdek *et al.*, 2007). This phenomenon could be physiologically relevant if bystander cells were exposed to the released contents of dead infected cells or to LLO from extracellular Listeria.

1.1.3 Lethal effects of CDC

Lethal doses of CDC lead to irreparable damage and subsequent death. On the organismal level, it has been shown that CDC confer virulence to the bacteria that express them. For example, mice infected intravenously (i.v.) with a PLY-negative pneumococci strain survive longer than those infected with wild type pneumococci (D39 strain) (Benton *et al.*, 1995). Similar findings have been observed with wild type versus mutant pyolysin-secreting *A. pyogenes* strains as well as wild type and mutant PLY-secreting strains (Berry *et al.*, 1995; Jost *et al.*, 1999). However, the role of anthrolysin O (ALO) in the virulence of *B. anthracis* is unclear. It has been shown that immunization of mice with ALO or a genetic toxoid results in protection against the toxin

but not the bacterium itself (Cowan *et al.*, 2007). On the other hand, mice pre-treated with a combination of monoclonal antibodies to recombinant ALO followed by infection with a lethal i.v. dose of *B. anthracis* survived longer than mice not treated with ALO-specific antibodies (Nakouzi *et al.*, 2008). Lastly, the lethal effects of CDC alone can be observed in mice injected i.v. with 100 pmol of various purified CDC that undergo death within seconds (Watanabe *et al.*, 2006). Thus, CDC can elicit rapid death in mice and in many cases contribute to the virulence of the bacteria that secrete them.

As expected from the results of the mouse studies, CDC have lethal effects on the cellular level as well. Initial studies on the cytolytic nature of CDC were conducted using sheep erythrocytes with the release of hemoglobin as a measure of the amount of hemolysis induced. For instance, one such study showed that ALO exhibits dose-dependent hemolytic activity against sheep erythrocytes (Shannon *et al.*, 2003). Another common method to measure cell death is the uptake of cell impermeable fluorescent dyes such as trypan blue or propidium iodide (PI). Mosser and Rest (Mosser & Rest, 2006) showed that certain concentrations of ALO could induce the uptake of trypan blue by neutrophils, THP-1 monocytes, lymphocytes, monocyte-derived macrophages, and several epithelial cell lines. Interestingly, different toxin doses were required to elicit cell death depending on the cell type. It is unclear if surface membrane cholesterol content is the only factor that plays a role or if unknown receptors or pathways also contribute to sensitivity to CDC death.

More extensive studies have been conducted to determine the types of cell death induced by purified CDC or CDC in the context of a bacterial infection. Much of this work has focused on cells of the nervous system as well as on phagocytic cells of the immune system, which are among the first cells to encounter CDC-secreting bacteria. Specifically, macrophages initially

phagocytose invading bacteria at the site of infection. It has been observed that high doses of purified PLY induce apoptosis in macrophages via a TLR4-dependent mechanism (Srivastava *et al.*, 2005). TLR4 is a putative receptor for CDC, as will be discussed in section 1.1.6. In studies with purified LLO, macrophage cell death is characterized by lactate dehydrogenase (LDH) release and phosphatidylserine (PS) flip, which may be indicative of late-stage apoptosis (Zwaferink *et al.*, 2008). However, the role of CDC in macrophage cell death during infection with whole bacteria is less clear cut.

LLO is required for the escape of Listeria from macrophage phagosomes, which leads to caspase-1 activation and subsequent cell death as measured by dye uptake (Cervantes *et al.*, 2008). It is not clear if LLO plays any additional roles in this cell death process apart from enabling Listeria to escape. With a different CDC-secreting pathogen, Goldmann, *et al.* found that *S. pyogenes* infection results in caspase-1-independent, but reactive oxygen species (ROS)– and calpain-dependent oncosis in macrophages (Goldmann *et al.*, 2009). LDH release is dependent on CDC streptolysin O (SLO) expression by *S. pyogenes*, but its role in other aspects of the oncotic cell death process was not determined. Lastly, Group A streptococcus (GAS) infection induces caspase-1-dependent apoptosis. SLO is necessary and sufficient for this cell death process in macrophages, though the dependence of caspase-1 activation on SLO was not studied (Timmer *et al.*, 2009). It appears that the type of cell death that a single cell type (i.e. macrophage) undergoes varies based on the CDC family member and pathogen that secretes it. Other conditions such as CDC dose and presence of other bacterial factors derived from the CDC-producing source most likely also play a role in the skewing of the cell death pathway. To further complicate matters, cell death processes in general encompass distinct pathways that can no longer be referred to simply as apoptosis or necrosis. Instead, a spectrum of unique pathways

that share some similarities have been suggested, including apoptosis, autophagy, pyroptosis, pyronecrosis, and oncosis (Fink & Cookson, 2005; Willingham *et al.*, 2007). To summarize, the role of CDC as an inducer of cell death must be more clearly defined in terms of the type(s) of cell death initiated and the specificity of these death pathways depending on cell type.

1.1.4 Pore sensing and resealing processes

Though high doses of CDC are lethal to cells and ultimately to the host, cells are capable of recovering from sublethal or sublytic doses. This phenomenon was first observed by Walev and collaborators who treated THP-1 monocytes, COS cells, a human keratinocyte (HaCat) or endothelial cell line with various doses of SLO. They then measured the ability of cells to recover their cellular ATP content, which represented recovery of metabolic activity, or to exclude PI dye as a measure of pore resealing activity (Walev *et al.*, 2001a; Walev *et al.*, 2001b). Cells were capable of recovering after treatment with low doses of SLO in a calcium-dependent manner, but could not recover after stimulation with high doses of SLO. It has been reported for toxins that induce smaller pores, such as alpha toxin, that p38 MAPK activity is essential for pore resealing, but SLO-induced pores reseal regardless of p38 activity (Husmann *et al.*, 2006). Instead, a calcium-dependent endocytic process is required for repair of SLO-induced membrane damage (Idone *et al.*, 2008). Thus, different PFTs rely on different mechanisms of membrane repair possibly due to the size of the pores created by these toxins. Interestingly, recovery from aerolysin requires a caspase-1-dependent process for the activation of sterol regulatory element binding proteins (SREBPs) that are involved in lipid biosynthesis (Gurcel *et al.*, 2006). This pathway has not been studied for CDC or alpha toxin.

Though p38 MAPK activation is not required for resealing of CDC pores, it may be important for the sensing of osmotic stress (Uhlik *et al.*, 2003). It has been reported by multiple groups that CDC activate this kinase (Husmann *et al.*, 2006; Ratner *et al.*, 2006; Kloft *et al.*, 2009) and Kloft, *et al.* suggested that loss of cellular potassium in response to CDC leads to the activation of p38 (Kloft *et al.*, 2009). Additionally, Ratner, *et al.* showed that sublytic doses of PLY, SLO, and ALO induced p38 phosphorylation in epithelial cell lines and subsequent downstream IL-8 chemokine release (Ratner *et al.*, 2006). Pore formation and the presence of extracellular divalent cations were essential for p38 activation, which was inhibited by the presence of high molecular weight dextran, an osmoprotectant. These findings suggested to the authors that epithelial cells may sense a breach in membrane integrity induced by CDC and initiate p38 MAPK activation for the sensing of osmotic stress. Furthermore, downstream IL-8 secretion would enable the recruitment of innate immune cells such as neutrophils to the location of the CDC-secreting bacteria as an immune defense mechanism. In addition to p38 activation, CDC have also been implicated in NF-κB activation as a possible result of pore sensing. Walev, *et al.* reported that pore resealing after SLO membrane perforation was followed by NF-κB activation and the release of IL-6 and IL-8 from keratinocytes and endothelial cells (Walev *et al.*, 2001b). Thus, stress activated kinase and transcription factor activation seem to play major roles in the defense of host cells against stress induced by CDC.

CDC have also been shown to elicit ion fluxes, particularly calcium fluxes, in a pore-dependent manner (Our lab (data not shown) and (Gekara *et al.*, 2007)). As discussed above, calcium flux is important for the initiation of endocytosis and pore resealing after CDC disruption of the membrane. Additionally, we have recently discovered that calcium influx is required for a sublytic dose of CDC to induce mature IL-1β release, a process that is presumably

enabled through initial CDC pore formation. Calcium influx may contribute to the activation of the NLRP3 inflammasome, which is required for CDC-induced secretion of IL-1β (see section 1.2 and Chapter 2). Thus, the calcium flux response may serve as a general mechanism for pore-dependent cell sensing of CDC.

1.1.5 Sublytic effects of CDC

As demonstrated above, immune cells are capable of initiating signaling pathways for the benefit of the host upon interaction with CDC. For this to occur, the toxin dose must be sublethal, allowing cells to recover from membrane attack and remain metabolically active long enough to create a proinflammatory environment for the recruitment of other immune cells to the local site of infection. On the other hand, sublytic doses of CDC have also been reported to inhibit key functions of immune cells required to combat bacterial infection. This dichotomy demonstrates that there is a fine line between the ability of the host immune system to respond to a bacterial threat and the ability of the pathogen to use its virulence factors to evade detection. To date, the sublytic effects of many CDC family members (SLO, PLY, LLO, PFO, ALY to name a few) have been characterized and include, but are not limited to: (1) Transcription factor activation (NF-κB, p38 MAPK), (2) Cytokine (IL-1α, IL-1β, TNF-α, IL-6, IL-12, IFN-γ) and chemokine (IL-8, MCP-1) expression in or secretion from human monocytes, human keratinocytes, murine macrophages, murine NK cells, or human epithelial cells, (3) Nitric oxide induction in murine macrophages, and (4) Inhibition of chemotaxis, migration, respiratory burst, and bacteriocidal activity of human neutrophils and monocytes (for a minireview see (Billington *et al.*, 2000)). These sublytic effects of CDC can occur in a pore-dependent manner (discussed in the previous section) or can be elicited through pore-independent processes. One such example of the latter

process is the ability of CDC to activate Toll-like receptor 4 (TLR4). This interaction may be responsible for many of the sublytic effects mentioned above as will be discussed below.

1.1.6 CDC and TLR4 activation

TLR4 is a pattern recognition receptor (PRR) that belongs to a family of transmembrane receptors that recognizes pathogen-associated molecular patterns (PAMPs) present on bacteria and viruses. Commonly characterized TLR agonists are bacterial cell wall components (TLRs 1, 2, 4, 6), flagellins (TLR5), viral dsRNA and poly(I:C) (TLR3), small anti-viral compounds (TLR7), and CpG DNA (TLR9) (Martin & Wesche, 2002; Kumar et al., 2009a). TLR2, binding mostly Gram-positive endotoxins (i.e. PGN), and TLR4, typically binding Gram-negative endotoxins (i.e. LPS), have been described as the prototypes for this type of receptor. Ligation of TLR4 initiates either MyD88-dependent or MyD88-independent signaling pathways that lead to transcription of proinflammatory cytokines (Akira et al., 2001; Medzhitov, 2001; Netea et al., 2004). Several studies have shown that CDC activate TLR4 and this occurs independently of cytolytic activity as TLR4 activity is retained in the presence of cholesterol or for mutant CDC lacking domain 4. For example, NF-κB translocation and pro-inflammatory cytokine (TNF-α, IL-6) secretion occurred when PLY (Malley et al., 2003), ALO (Park et al., 2004a), or seeligeriolysin O (LSO) (Ito et al., 2005) acted on mouse peritoneal macrophages, mouse bone marrow-derived macrophages (BMDM), or mouse peritoneal exudate cells (PECs) and the RAW267.4 mouse macrophage line, respectively. This effect was TLR4-dependent as CDC elicited responses only from macrophages from TLR4-positive mice and not TLR4-deficient mice. Direct binding of CDC to TLR4 was not addressed in these studies, but a study by Srivastava, et al., using ELISA, showed that TLR4 and PLY, but not TLR2 and PLY, were

12

capable of interacting (Srivastava *et al.*, 2005). TLR4 activation by CDC ultimately leads to promotion of inflammation and protection of the host against infection (Malley *et al.*, 2003). All of these studies conducted on mouse macrophages suggest that CDC play an important role in stimulating innate immunity during Gram-positive bacterial infection through TLR4 activation.

1.1.7 Lipid raft aggregation and signaling

Another mode of pore-independent signaling initiated by CDC is through lipid raft aggregation. Gekara, *et al.* observed in J774 macrophages via microscopy that LLO oligomerization aggregated lipid rafts (Gekara *et al.*, 2005). They further demonstrated that LLO could induce the tyrosine phosphorylation of non-receptor tyrosine kinases Lyn and Syk. This lipid raft aggregation and tyrosine phosphorylation process was independent of LLO's cytolytic activity as cholesterol-treated LLO also induced the same effect. The authors put forth a model whereby LLO could directly bind cholesterol in rafts or cholesterol-bound LLO would be targeted to lipid raft regions (Gekara & Weiss, 2004). The clustering of rafts would then lead to the activation of signaling molecules such as kinases, which presumably become activated by the non-specific activation of receptors or the kinases themselves clustered within the rafts. The downstream outcomes of these signaling pathways were not addressed, but it might be expected that typical downstream events of Lyn and Syk signaling would occur. For example, increased phagocytosis in macrophages after Syk signaling might be expected (Tohyama & Yamamura, 2009).

1.1.8 Other CDC-induced signaling pathways

Aside from the CDC-induced signaling pathways and outcomes discussed above, there are a few others that warrant some discussion. In addition to cytokine and chemokine responses, which would be expected to occur downstream of p38 MAPK or NF-κB activation, CDC have been implicated in actin remodeling, microtubule bundling and stabilization, and histone modifications. In the first study, sublytic doses of PLY induced rapid activation of Rho and Rac GTPases that resulted in formation of actin stress fibers, filopodia, and lamellipodia (Iliev *et al.*, 2007). Furthermore, small GTPase activation and actin remodeling could be inhibited by free cholesterol and a voltage-gated calcium channel inhibitor, suggesting that PLY pore formation and calcium influx were critical for these processes. A second study by the same group showed that sublytic doses of PLY induce rapid bundling and increase acetylation of microtubules, which is a hallmark of microtubule stabilization (Iliev *et al.*, 2009). This process depended on cholesterol and Src kinase activity, but not pore formation, calcium influx, cell death, RhoA, Rac1, PKCζ, or actin cytoskeletal changes. The authors postulated that PLY-induced microtubule bundling and stabilization might allow pneumococci to evade host cell phagocytic machinery and phagosome formation. It should be noted that these two aforementioned studies were conducted on neuronal cells and it is unknown if immune cells, specifically phagocytes, respond in a similar way to CDC.

The third study (Hamon *et al.*, 2007) focused on the ability of LLO to cause the dephosphorylation of Ser^{10} on histone H3 and the deacetylation of histone H4 in a cholesterol-dependent manner. Global transcription levels changed as a result of these changes and, interestingly, the same subset of genes appeared to be targets for both H3 and H4 modifications. These studies, in addition to those addressed above, show that sublytic doses of CDC have a

diverse array of effects that are both dependent and independent of CDC-induced pore formation. Many of these studies may account for sublytic effects observed to date, but there may be unknown pathways responsible for these effects, as well as other completely novel pathways that have yet to be discovered. Ultimately, understanding the different pathways induced in immune cells both by sublytic and lytic doses of CDC could provide key direction for the generation of specific antibacterial therapies.

1.2   THE INFLAMMASOME

The innate immune system has evolved to recognize a wide variety of pathogens including viruses, bacteria, and fungi.   Many immune cell types such as macrophages, monocytes, dendritic cells (DC), and neutrophils express germline-encoded receptors known as pattern-recognition receptors (PRRs).   These PRRs recognize conserved motifs on pathogens known as pathogen-associated molecular patterns (PAMPs). A major family of PRRs is the Toll-like receptor (TLR) family, which was briefly reviewed in section 1.1.6.   These receptors recognize a wide variety of pathogen-related cell wall components, RNAs, and DNAs, and localize to the plasma membrane as well as to endocytic compartments where these components would be likely to interact with their receptors.

In recent years, it has been recognized that the immune system, in addition to sensing PAMPs, may also sense danger-associated molecular patterns (DAMPs). Matzinger proposed a 'danger model' where antigen presenting cells (APCs) are activated by endogenous danger or alarm signals released from injured or dying cells exposed to pathogens, toxins, mechanical damage, or cell stress (Matzinger, 2002). These signals can initiate exogenous signaling through receptors such as TLRs for the downstream generation of endogenous pro-inflammatory mediators.   However, it should be noted that the recognition of some DAMPs by TLRs is controversial. For instance, TLR4 recognition of host heat shock proteins has been questioned (Tsan & Gao, 2004). The newly identified cytoplasmic NOD-like receptors (NLRs), another class of PRRs, appear to recognize both PAMPs as well as DAMPs and will be reviewed below.

It should also be mentioned that the RIG-like helicases (RLHs), which include RIG-I and MDA5, sense viral RNA in the cytoplasm, but this family will not be further discussed here.

1.2.1 The NOD-like receptor family

The NOD-like receptor (NLR) family consists of various cytosolic proteins involved in innate immune sensing. These proteins have three major domains: (1) A ligand-sensing, leucine-rich repeat (LRR) domain, (2) A domain conserved in NAIP, CIITA, HET-E and TP-1 (NACHT) for oligomerization, and (3) An effector domain that consists of a pyrin domain (PYD), caspase recruitment domain (CARD), or baculovirus IAP repeat domain (BIR) (Girardin *et al.*, 2002; Inohara *et al.*, 2002; Inohara & Nunez, 2003; Tschopp *et al.*, 2003). The NLR family of proteins can be divided into the NACHT, LRR, and PYD-containing proteins (NALPs, now known as NLR proteins or NLRPs) with 14 members, ICE-protease-activating factor (IPAF, now known as NLRC4) and NAIP, and the nucleotide oligomerization domain (NOD) proteins with 6 members (NODs 1-5 and MHC class II transcription activator CIITA) (Martinon *et al.*, 2009). NLRs combine with other proteins to form molecular platforms involved in proinflammatory responses, namely (1) the NOD signalosome composed of oligomerized NOD1 or NOD2 that activates kinase RIP2 and NF-κB signaling and (2) the inflammasomes that lead to the activation of inflammatory caspases and processing of immature pro-IL-1β and pro-IL-18 to their mature forms (Martinon *et al.*, 2009). There are two steps for the final secretion of mature IL-1β and IL-18. The first step requires TLR priming (e.g. LPS) for the production of the pro forms of both cytokines. In the second step, the inflammasome must be activated such that active caspase-1 can cleave these immature cytokines to their mature forms before release from the cell. There are three prototypical inflammasomes (NLRC4, NLRP1, and NLRP3) that have been fairly well-

17

studied in recent years. Their structure, function, and the stimuli that activate them will be discussed below.

1.2.2 The NLRC4 inflammasome

The NLR family, CARD domain containing 4 (NLRC4) inflammasome, formerly known as the IPAF inflammasome, consists of the NLR IPAF that recruits caspase-1 via homotypic CARD-CARD interactions and may require the adaptor ASC, though its role remains unclear (Martinon *et al.*, 2009). This inflammasome is involved in the recognition of virulence factors from Gram-negative bacteria. Many studies have shown that the NLRC4 inflammasome recognizes Gram-negative bacteria such as *Salmonella typhimurium* (Mariathasan et al., 2004), *Shigella flexneri* (Suzuki *et al.*, 2007), *Legionella pneumophila* (Amer *et al.*, 2006; Lightfield *et al.*, 2008), and *Pseudomonas aeruginosa* (Sutterwala *et al.*, 2007; Miao *et al.*, 2008). Uniquely, recognition of *L. pneumophila* requires both NLRs NAIP5 and IPAF for inflammasome formation (Lightfield *et al.*, 2008). Most Gram-negative pathogens require type III secretion systems (T3SS) or type IV secretion systems (T4SS) for the injection of factors such as flagellin into the host cytosol (Miao *et al.*, 2007). Flagellin is a major component identified so far that activates the NLRC4 inflammasome and this recognition process is independent of TLR5, which recognizes extracellular flagellin (Amer *et al.*, 2006; Franchi *et al.*, 2006).

Recognition of flagellin leads to NLRC4 inflammasome- and ASC-dependent caspase-1 activation and the maturation of IL-1β (Amer *et al.*, 2006; Franchi *et al.*, 2006), which is important for the recruitment of innate immune cells such as neutrophils to the site of local infection (Jones *et al.*, 2005). Flagellin recognition is also critical for NLRC4– and NAIP5-dependent phagosome maturation and restriction of *L. pneumophila* replication inside

18

macrophages (Coers *et al.*, 2007; Lamkanfi *et al.*, 2007; Vinzing *et al.*, 2008). Recently, Akhter, *et al.* have determined that flagellin from *L. pneumophila* activates caspase-7 in a manner dependent on the NLRC4 inflammasome, caspase-1 activation, and NAIP5 (Akhter *et al.*, 2009). The authors observed that caspase-7-deficient macrophages were less able to clear bacterial infection via delivery of intracellular bacteria to lysosomes than wild type macrophages. Caspase-7 has previously been identified as a substrate of caspase-1-containing inflammasomes such as NLRC4 (Lamkanfi *et al.*, 2008). Lastly, NLRC4 has been linked to ASC-independent pyroptosis (Suzuki *et al.*, 2007; Case *et al.*, 2009), a cell death marked by caspase-1 activation, as well as ASC-independent inhibition of autophagy (Suzuki *et al.*, 2007), a normal process where the cell degrades its own components using lysosomal machinery.

1.2.3 The NLRP1 inflammasome

The NLR family, pyrin domain containing 1 (NLRP1) inflammasome, formerly known as the NALP1 inflammasome, consists of NLR family NLRP1, ASC, and caspase-1 (Martinon *et al.*, 2009). Humans have a single *NLRP1* gene whereas mice have three *Nlrp1* paralogs, including *Nlrp1a*, *Nlrp1b*, and *Nlrp1c*. Using a cell-free system, human NLRP1 has been shown to oligomerize with caspase-1 in the presence of microbial muramyl dipeptide (MDP) and form an inflammasome complex that does not require ASC, though ASC can enhance caspase-1 activation (Faustin *et al.*, 2007). The mechanism that MDP uses to trigger NLRP1 oligomerization is unknown. In mice, *Nlrp1b* has been identified as the gene that encodes for a product that is involved in the recognition of metalloprotease lethal toxin (LT) from *B. anthracis* (Boyden & Dietrich, 2006). NLRP1b inflammasome recognition of LT results in ASC-independent caspase-1 activation and involves lysosomal membrane permeabilization (LMP) and

the activity of lysosomal protease cathepsin B (Averette *et al.*, 2009; Newman *et al.*, 2009). Moreover, Newman, *et al.* found that LT-induced LMP led to cytolysis and this cell death could be inhibited with CA-074-Me, a cathepsin B inhibitor. Interestingly, knocking down cathepsin B with siRNA had no effect on LT-induced cell death, suggesting that the pharmacological inhibitor was blocking other cellular proteases. Lastly, recent work by Hsu, *et al.* (Hsu *et al.*, 2008) has shown that NLRP1 complexes with NLR NOD2, a protein that senses MDP, and caspase-1. Interestingly, the authors also showed that *B. anthracis* infection, as well as LT alone, induced IL-1β secretion in a NOD2- and caspase-1-dependent way.

1.2.4 The NLRP3 inflammasome

The NLR family, pyrin domain containing 3 (NLRP3), formerly known as NALP3 and cryopyrin, inflammasome is the most well studied of the inflammasomes. This molecular complex consists of NLRP3, ASC, and caspase-1 with the major downstream pathway being maturation of IL-1β and IL-18 (Martinon *et al.*, 2009). There have been many stimulators of the NLRP3 inflammasome identified to date. Initial studies identified the DAMP adenosine triphosphate (ATP) and K^+ ionophores nigericin and maitotoxin as second stimuli (after TLR priming) to activate caspase-1 and induce IL-1β and IL-18 secretion in a NLRP3-dependent way in murine macrophages (Mariathasan *et al.*, 2006). The authors additionally identified *Staphylococcus aureus* and *Listeria monocytogenes* as inducers of the NLRP3 inflammasome. Interestingly, *L. monocytogenes* was only capable of inducing IL-1β release in the presence of CDC LLO, suggesting that the intracellular bacterium had to escape from the phagosome before recognition by NLRP3. Around the same time, two other studies were published identifying additional second stimuli of the NLRP3 inflammasome. Kanneganti, *et al.* (Kanneganti *et al.*,

2006b) showed that bacterial RNA and small antiviral compounds activated caspase-1 and induced IL-1β and IL-18 secretion in a NLRP3-dependent manner. NLRP3-dependent caspase-1 activation and IL-1β and IL-18 release could also be initiated by gout-associated monosodium urate (MSU) crystals and calcium pyrophosphate dehydrate (CPPD) crystals (Martinon *et al.*, 2006).

As many of these various stimulators of the NLRP3 inflammasome were identified, a looming question as to the mechanism of NLRP3 activation began to dominate. All NLR family proteins contain ligand-sensing leucine-rich repeats (LRRs) that would be expected to recognize PAMPs or DAMPs. However, this has been difficult to directly demonstrate. Thus far, three major pathways in which the inflammasome may become activated have been postulated. All pathways share commonalities such as K^+ efflux and NLRP3 and caspase-1 activation for IL-1β and IL-18 release, but differ in the upstream recognition of PAMPs and DAMPs. The first model was put forth by Kanneganti, *et al.* (Kanneganti *et al.*, 2007) who suggested that PAMPs enter cells through pores or channels in the plasma membrane, formed due to damage from bacterial toxins, cell stress, or DAMPs, and directly interact with NLRP3 within the cytoplasm. The authors showed that various bacterial species alone could not induce caspase-1 activation and required cytosolic entry via pores induced by CDC SLO or hemichannel protein pannexin-1. SLO at the concentrations tested or pannexin-1 channel formation alone were also not capable of inducing caspase-1 activation. However, it should be noted that in another study, SLO was capable of inducing caspase-1 activation in LPS-primed macrophages (Harder *et al.*, 2009). It is unclear if this activation occurred as a direct result of SLO activity or if SLO solely served as a conduit for LPS entry. As for the role of pannexin-1, it is thought that ATP activates its purinergic receptor P2X$_7$, leading to downstream pannexin-1 channel formation (most likely in

endosomes), PAMP escape from endosomes into the cytosol, and subsequent recognition of these PAMPs by the NLRP3 inflammasome. Pelegrin and Surprenant (Pelegrin & Surprenant, 2006) have found a role for pannexin-1 in nigericin and maitotoxin-induced caspase-1 activation, but the mechanism is unclear. At this time, direct or indirect recognition of PAMPs by NLRP3 has not yet been demonstrated.

The second major model of NLRP3 inflammasome activation summarized by Willingham and Ting (Willingham & Ting, 2008) suggested that large particulates or crystals could be phagocytosed and physically disrupt lysosomal membranes leading to cathepsin B release. This protease could then activate NLRP3 through an unknown mechanism and bring about NLRP3 inflammasome activation. This model was supported by two similar studies. Hornung, *et al.* (Hornung *et al.*, 2008) demonstrated that silica crystals and aluminum salt (alum) crystals were phagocytosed by human PBMC and lead to lysosomal destabilization as assessed by the loss of lysosomal acidity. These crystals were also capable of inducing cathepsin B- and NLRP3-dependent IL-1β release. In the other study, Halle, *et al.* (Halle *et al.*, 2008) showed that fibrillar peptide amyloid-β (Aβ) was also phagocytosed and induced lysosomal damage. Using confocal microscopy, they showed that lysosomal disruption led to the release of cathepsin B into the cytoplasm, which was required (as was NLRP3) for caspase-1 activity and IL-1β release. Cathepsin B has been implicated in the activation of caspase-1 either through direct cleavage or via the activity of caspase-11 (Schotte *et al.*, 1998; Vancompernolle *et al.*, 1998). Together, these studies provided a potential pathway in which sterile inflammation could occur in the absence of any pathogenic threat. It might also explain how the NLRP3 inflammasome is capable of recognizing some second stimuli that are unlikely to be recognized by the LRRs of NLRP3 due to sheer physical shape and size.

The third model postulated is known as the frustrated phagocytosis model. This model also focuses on large particulates and crystals, but states that they are too large to be phagocytosed and as a result, undergo "frustrated phagocytosis." Instead of being internalized, these particulates and crystals stay at the cell surface while the cell continually attempts and fails to phagocytose them. This process generates the production of reactive oxygen species (ROS) that are required for the activation of caspase-1 and release of IL-1β. In the context of the inflammasome, this concept was first suggested by Dostert, *et al.* (Dostert *et al.*, 2008) who showed that asbestos, silica, and MSU crystals induced IL-1β secretion from monocytes and macrophages in a NLRP3 inflammasome-dependent manner. Furthermore, asbestos and MSU crystals required K^+ efflux, actin polymerization (most likely for endocytosis), NAPDH oxidase, and the generation of ROS to activate caspase-1 and induce IL-1β secretion. Other studies have also shown a similar pathway induced by non-particulate, NLRP3 inflammasome-activating agents such as ATP and nigericin. Hewinson, *et al.* (Hewinson *et al.*, 2008) demonstrated that ATP causes the generation of reactive oxygen and nitrogen species (RNOS) in a NADPH oxidase- and superoxide dismutase (SOD)-dependent way and this process was required for ATP-induced IL-1β release. Nigericin-induced caspase-1 activation and IL-1β release was also dependent on RNOS generation. Likewise, Meissner, *et al.* (Meissner *et al.*, 2008) showed that SOD1 activity was essential for ATP-induced caspase-1 activation and IL-1β and IL-18 secretion through the control of caspase-1. This control was exerted through redox-sensitive cysteine residues on caspase-1 such that high superoxide production in the absence of SOD1 led to decreased redox potential and inhibition of caspase-1. Thus, this model can apply to both large particulate structures as well as smaller molecules and may serve as a more general method for NLRP3 inflammasome activation.

Though there are limited data, another general mechanism that may tie into NLRP3 inflammasome activation would involve the activation of non-receptor tyrosine kinases such as Syk. A study by Gross, *et al.* (Gross *et al.*, 2009) reported that *Candida albicans* induces IL-1β secretion from bone marrow-derived dendritic cells (BMDC) in a manner dependent on K^+ efflux, ROS production, and the activation of the NLRP3 inflammasome, which includes caspase-1 activation. Furthermore, Syk kinase signaling was required for pro-IL-1β synthesis and caspase-1 activation in this system. Another known second stimulator of the NLRP3 inflammasome, crystalline MSU, has also been shown to induce Syk activation in BMDC (Ng *et al.*, 2008), but the link between Syk and components of the NLRP3 inflammasome was not studied. Lastly, malarial hemozoin has recently been identified as another second stimulator of the NLRP3 inflammasome that results in caspase-1 activation and IL-1β secretion, which is dependent on ROS production, potassium efflux, and cathepsin B (Tiemi Shio *et al.*, 2009). Like *C. albicans* and MSU crystals, malarial hemozoin was also capable of inducing Syk activation and this activity was critical in the release of mature IL-1β.

Lastly, though there is accumulating evidence as to the ways in which the NLRP3 inflammasome may become activated, there is little understanding of the factors that regulate NLRP3 in its inactive state. However, a study by Mayor, *et al.* (Mayor *et al.*, 2007) identified heat shock protein 90 (HSP90) and ubiquitin ligase-associated protein SGT1 as such regulators. In general, both of these proteins were observed to interact with many other NLRs with a particularly strong interaction observed with NLRP3. Specifically, the SGT1-HSP90 complex interacted with the NLRP3 LRR domain and the presence of HSP90 was critical to stabilize NLRP3 and prevent its degradation, presumably by the proteasome. Furthermore, both regulatory proteins were required for NLRP3 inflammasome function after cell stimulation with

known inflammasome stimulators. These data suggested that the SGT1-HSP90 complex maintains NLRP3 in an inactive state until recognition of an activating signal. Subsequently, NLRP3 can dissociate from SGT1 and HSP90 followed by association with caspase-1 and ASC.

In summary, much remains to be elucidated regarding the regulation of NLRP3, but the list of NLRP3 inflammasome activators continues to grow. Not all of the stimulators could be discussed here, but they include: pore-forming agents (ATP (Mariathasan *et al.*, 2006), nigericin (Mariathasan *et al.*, 2006), maitotoxin (Mariathasan *et al.*, 2006), TLO (Chu *et al.*, 2009), SLO (Harder *et al.*, 2009), *S. aureus* α-hemolysin (Craven *et al.*, 2009)), bacteria (*S. aureus* (Mariathasan *et al.*, 2006; Munoz-Planillo *et al.*, 2009), *L. monocytogenes* (Mariathasan *et al.*, 2006), *K. pneumoniae* (Willingham *et al.*, 2009)), viruses (influenza (Kanneganti *et al.*, 2006a; Allen *et al.*, 2009)), aggregated peptides (Aβ (Halle *et al.*, 2008)), crystals and particulates (silica (Dostert *et al.*, 2008), MSU (Dostert *et al.*, 2008), CPPD (Martinon *et al.*, 2006), asbestos (Dostert *et al.*, 2008), alum (Eisenbarth *et al.*, 2008; Li *et al.*, 2008)), yeasts (*C. albicans* (Gross *et al.*, 2009)), and malarial hemozoin (Tiemi Shio *et al.*, 2009) (See also Figure 3-1). The mechanisms of NLRP3 inflammasome activation employed by these stimuli may stand independently or overlap to some degree and include components such as K^+ efflux, Ca^{2+} influx, Syk kinase activation, RNOS generation and associated signaling pathways, and/or lysosomal destabilization and cathepsin B release. Some of these pathways and stimuli are diagrammed in Figure 1-2. The interplay between these pathways and the stimuli that invoke them may become clearer in time. Some of the current work in this field has also begun to focus on NLRP3 function independently of the inflammasome complex as will be briefly discussed in the next section.
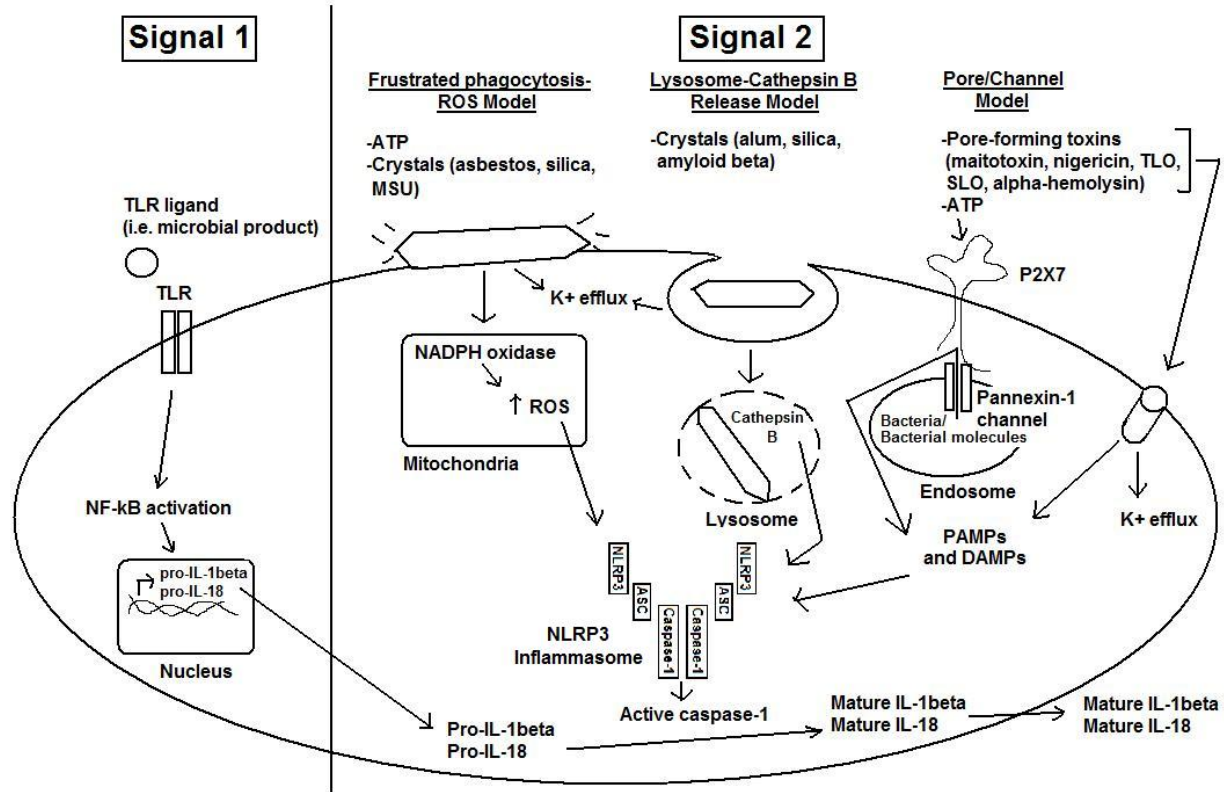
Figure 1-2: NLRP3 inflammasome activation mechanisms.

The release of proinflammatory cytokines IL-1β and IL-18 require two signals for production and release. The first signal is initiated by PAMPs that bind TLRs and initiate the transcription and translation of the inactive pro forms of these cytokines. The second signal includes many stimuli such as large crystals, pore-forming toxins, or ATP that activate the NLRP3 inflammasome for caspase-1 cleavage of these cytokines to their mature forms before release. These second stimuli may activate the inflammasome through a frustrated phagocytosis and ROS production pathway, a lysosomal disruption and cathepsin B release pathway, or a pannexin-1 or toxin-induced channel pathway.

1.2.5 Inflammasome-independent NLRP3 functions

NLRP3 has been described to play a role in a type of cell death known as pyronecrosis. This cell death process is dependent on NLRP3 and cathepsin B, but is caspase-1-independent and characterized by the loss of an intact plasma membrane, which leads to spilling of cellular contents that promote inflammation. It should be noted that pyronecrosis differs from another form of cell death known as pyroptosis (Bergsbaken *et al.*, 2009), a proinflammatory programmed cell death characterized by caspase-1 activation, the secretion of mature IL-1β and IL-18, and cell lysis for the release of inflammatory contents. Initial studies conducted by Willingham, *et al.* (Willingham *et al.*, 2007; Willingham *et al.*, 2009) showed that both *S. flexneri* and *K. pneumoniae* induced pyronecrosis, marked by lactate dehydrogenase (LDH) and high mobility group box 1 (HMGB1) release, in monocytes and macrophages. These studies were particularly novel because they demonstrated that NLRP3 could function independently of its inflammasome function. In another study, it was demonstrated that *S. aureus* α-hemolysin also induced pyronecrotic cell death of monocytes that was marked by NLRP3-dependent, but caspase-1-independent HMGB1 release (Craven *et al.*, 2009). The mechanism of NLRP3 action in pyronecrosis has yet to be defined. It is likely that future studies will address this issue as well as identify unknown inflammasome-independent NLRP3 functions.

1.2.6 The role of IL-1 in immunity

As discussed above, one of the major outcomes of inflammasome activation is the generation of IL-1β. The IL-1 family contains 11 known members including agonists IL-1α, IL-1β, IL-18,

FIL-1ε, IL-1H2, IL-1ε, and IL-33, receptor antagonist IL-1Ra and possibly IL-1Hy2, and anti-inflammatory FIL1δ and IL-1H4/IL-1ζ (Dinarello, 2009). The IL-1 receptor (IL-1R) family is also diverse, consisting of 10 members that serve as ligand-binding α chains and coreceptor β chains, decoy receptors, or inhibitory receptors (Boraschi & Tagliabue, 2006; Dinarello, 2009). Activation of IL-1 and IL-18 receptors results in signaling through adaptors MyD88 and Tollip, IL-1 receptor-associated kinases (IRAKs), and TRAF-6, which leads to downstream activation of transcription factors such as p38 MAPK, JNK, and NK-κB (Dunne & O'Neill, 2003; Dinarello, 2009). These signaling pathways share many similar components to the TLR pathways discussed above.

Once activated, IL-1R signaling pathways induce cyclooxygenase type 2 (COX-2) (Lyons-Giordano *et al.*, 1993; Pang & Knox, 1997), type 2 phospholipase A (Lyons-Giordano *et al.*, 1993), and inducible nitric oxide synthase (iNOS) (Mendes *et al.*, 2001), which together lead to production of prostaglandin-E2 (PGE2) (Pang & Knox, 1997), platelet activating factor (Bussolino *et al.*, 1986), and nitric oxide (NO) (Palmer *et al.*, 1993) [(Dinarello, 2009)]. These changes are manifested as fever, lowered pain threshold, vasodilation, and hypotension. In particular, IL-1β has been shown to increase adhesion molecule expression on mesenchymal and endothelial cells and to induce cytokine secretion, which attracts inflammatory cells (e.g. neutrophils) from the circulation into the tissues that propagate IL-1-induced inflammation (Dinarello, 2009). In terms of adaptive immunity, IL-1 together with an antigen or mitogen can act as a costimulator of T cell function (Lichtman *et al.*, 1988). IL-1 has also been shown to contribute to Th2 polarization using murine models of asthma (Nakae *et al.*, 2003), to induce antibody production (Nakae *et al.*, 2001), and seems to be essential for the generation of Th17 responses in mice and humans (Sutton *et al.*, 2006; Acosta-Rodriguez *et al.*, 2007). IL-1 family

member IL-18 also participates in adaptive immune responses by synergizing with IL-12 and IL-15 for IFN-γ production, a process crucial for Th1 responses. On the other hand, in the absence of IL-12, IL-18 drives Th2 responses (Hoshino *et al.*, 2001; Nakanishi *et al.*, 2001a, b). Thus, IL-1 family members play key roles in inducing inflammation for the generation of robust immune responses.

1.2.7 Diseases associated with IL-1 and the inflammasome

Though IL-1 is critical in eliciting inflammation and subsequent immunity, excessive inflammation can be detrimental to host tissues. Endogenous IL-1 and IL-18 antagonists exist to control inflammation such that damage to the host is limited. For example, IL-1 receptor antagonist (IL-1Ra) specifically targets IL-1α and IL-1β by binding to the IL-1R1 receptor and blocking subsequent signaling (Arend, 1990). These mechanisms are usually sufficient to control inflammation in people with normal IL-1 pathways intact. However, there are patients with autoinflammatory diseases marked by chronic inflammation that can be due to disorders in IL-1β activation as well as problems with NK-κB activation, protein folding, complement, cytokine signaling, and macrophage activation (Masters *et al.*, 2009). These diseases can be distinguished from autoimmune disorders in that they lack associations with class II MHC haplotypes, occur periodically, and can be triggered by environmental sources (Dinarello, 2009). One underlying mechanism for excessive IL-1β production is mutations in the *NLRP3/CIAS1* gene, which encodes the NLRP3 protein. These mutations result in the formation of *CIAS1*-associated periodic syndromes (CAPS) such as familial cold autoinflammatory syndrome (FCAS) (Hoffman *et al.*, 2001), Muckle-Wells syndrome (MWS) (Hoffman *et al.*, 2001), and

neonatal-onset Multi-inflammatory disease (NOMID) (Aksentijevich *et al.*, 2002), which is also known as Chronic Infantile Neurologic Cutaneous Articular Syndrome (CINCA).

Targeting and neutralizing IL-1β has been a major goal in controlling inflammation in patients with IL-1β autoinflammatory disorders. One highly promising treatment to achieve this is a recombinant, nonglycosylated form of IL-1Ra known commercially as anakinra (Mertens & Singh, 2009). So far, it has only been indicated for the treatment of rheumatoid arthritis, but clinical trials suggest that it could benefit patients with autoinflammatory disorders (Leslie *et al.*, 2006; Maksimovic *et al.*, 2008). Thus, conducting basic research on the mechanisms of inflammasome activation and IL-1β secretion could be crucial for the development of additional therapies to target overactive inflammation. These therapies could potentially benefit patients with autoinflammatory disorders as well as those undergoing sepsis due to bacterial infection.

1.3   STATEMENT OF THE PROBLEM

The incidence of bacterial infections is on the rise.   In particular, gram-positive bacterial infections have become a problem in hospitals, where many patients are immunocompromised. Control of infection is often difficult not only because of a compromised immune system, but also because of the increased resistance of bacteria to antibiotic treatments.   As a result of uncontrolled infection in these patients, sepsis can occur, which ultimately leads to mortality. The bacterial factors that contribute to sepsis and gram-positive bacterial infection, in general, have remained unclear, largely due to basic research being focused on gram-negative sepsis. Thus, it is important to understand, on a basic level, how these bacterial products contribute to the virulence and pathogenesis of their gram-positive bacterial source.   Moreover, it is equally important to study the response of the host innate immune system to these bacterial proteins.

At the beginning of our studies, it was known that some cholesterol-dependent cytolysins (CDC) added to the virulence of the bacteria that expressed them.   These CDC were also examined for their ability to elicit host immune responses when applied to immune cells in sublytic amounts.   One effect observed was the ability of CDC to elicit pro-inflammatory cytokine IL-1β from macrophages, but the mechanism of IL-1β release was not identified. Within the past decade, a general mechanism for IL-1β secretion was discovered: activation of a caspase-1-containing inflammasome complex.   We hypothesized that inflammasome complex activation was responsible for CDC-induced IL-1β secretion.   To test this hypothesis, we have employed pharmacological inhibitors against components of an inflammasome pathway and murine macrophages lacking inflammasome components.

31

Another major interest for our laboratory has been to understand the cell death pathways elicited by CDC. Though there is some knowledge regarding these cell death mechanisms, there could be variation due to the host cell type, CDC family member, CDC dose, and CDC in the context of whole bacteria. One such example is that the exposure of different cell types, including many immune cell types, to one specific CDC resulted in differences in susceptibility. We chose to focus our studies on CDC-induced cell death of macrophages and the role that NLRP3, an inflammasome component, might play in the cell death process. NLRP3 has been implicated in a form of cell death known as pyronecrosis and we hypothesized that NLRP3 also played a role in CDC-induced cell death of murine macrophages. Furthermore, to explore additional mechanisms involved in CDC-induced cell death, we isolated and characterized a CDC-resistant murine dendritic cell line. We have addressed these hypotheses herein.

2.0 CHOLESTEROL-DEPENDENT CYTOLYSINS INDUCE RAPID RELEASE OF MATURE IL-1BETA FROM MURINE MACROPHAGES IN A NLRP3 INFLAMMASOME AND CATHEPSIN B-DEPENDENT MANNER

2.1 AUTHORS AND THEIR CONTRIBUTIONS

This study was published in the *Journal of Leukocyte Biology* in the November 2009 issue (86(5): 1227-38.). Copyright permission was granted by the *Journal of Leukocyte Biology* for reuse of this publication within this dissertation. Jessica Chu (Immunology Graduate Program, University of Pittsburgh School of Medicine) generated the majority of the data and prepared the manuscript. L. Michael Thomas (Immunology Graduate Program, University of Pittsburgh School of Medicine) provided help with bone marrow derived macrophage (BMDM) culture, Simon C. Watkins (Departments of Cell Biology and Physiology and Immunology, University of Pittsburgh School of Medicine) and Russell D. Salter (Department of Immunology, University of Pittsburgh School of Medicine) collected the confocal imaging data, and Luigi Franchi (Department of Pathology and Comprehensive Cancer Center, University of Michigan Medical School) and Gabriel Núñez (Department of Pathology and Comprehensive Cancer Center, University of Michigan Medical School) provided the NLRP3 knockout mouse bones and caspase-1 p10 antibody. All authors contributed to the scientific discussion regarding the project, especially Russell D. Salter who also majorly contributed to the critical reading and

2.2   ABSTRACT

Cholesterol-dependent cytolysins (CDC) are exotoxins secreted by many Gram-positive bacteria that bind cholesterol and oligomerize to form pores in eukaryotic cell membranes. We demonstrate that the CDC tetanolysin O (TLO) induces caspase-1 cleavage and the rapid release of IL-1β from LPS-primed murine bone marrow-derived macrophages (BMDM). IL-1β secretion depends on functional toxin pore formation since free cholesterol, which prevents TLO binding to cell membranes, blocks the cytokine release. Secretion of the mature forms of IL-1β and caspase-1 occurs only at lower TLO doses, whereas at higher concentrations cells release the biologically inactive pro-forms. IL-1β release at a low TLO dose requires potassium efflux, calcium influx, and the activities of calcium-independent phospholipase A2, caspase-1, and cathepsin B. Additionally, mature IL-1β release induced by a low TLO dose is dependent on the NLRP3 inflammasome while pro-IL-1β release induced by a high TLO dose occurs independently of NLRP3. These results further elucidate the mechanism of CDC-induced IL-1β release, and suggest a novel immune evasion strategy in which IL-1β-containing macrophages might release primarily inactive cytokine following exposure to high doses of these toxins.

2.3   INTRODUCTION

Cholesterol-dependent cytolysins (CDC) are a class of protein exotoxins that are secreted by over twenty species of Gram-positive bacteria (Billington et al., 2000; Palmer, 2001). Individual subunits bind to cholesterol in eukaryotic cell membranes and oligomerize to form transmembrane pores up to 30 nm in size (Bhakdi et al., 1985; Olofsson et al., 1993; Morgan et al., 1995; Billington et al., 2000; Palmer, 2001). Approximately 40-80 CDC monomers assemble into a pre-pore complex before membrane insertion and final pore conversion, which results in osmotic imbalance that may lead to cell death. Mice injected intravenously with 100 pmol of purified forms of several different CDC underwent almost immediate death (Watanabe et al., 2006), demonstrating the potent biological activities of these toxins. Pneumolysin (PLY)-deficient *S. pneumoniae* have reduced virulence in mice, supporting a potential role for such toxins in bacterial pathogenesis (Berry et al., 1989; Benton et al., 1995).   In contrast, immunization of mice with anthrolysin O (ALO) or a genetic toxoid does not protect against *B. anthracis* infection (Cowan et al., 2007), suggesting that for some CDC-bearing pathogens the toxin plays a less important role. It should be noted that at least one CDC, listeriolysin O (LLO), has a specialized role in allowing escape of Listeria from the phagosome into the cytosol and is maximally active at acidic pH (Geoffroy et al., 1987; Beauregard et al., 1997). While CDC such as ALO can substitute for LLO when manipulated experimentally (Wei et al., 2005), most CDC do not show a marked pH dependence and are believed to function primarily extracellularly following secretion by bacteria, acting on adjacent cells in the infected host.

While all eukaryotic cells are susceptible to toxin-induced lysis, the amounts required for killing vary widely between cell types (Mosser & Rest, 2006). This may be due to differential ability of distinct cell types to repair membranes damaged by pores. Evidence for membrane

repair after toxin damage has been obtained by measuring cytoplasmic adenosine triphosphate (ATP) levels, which decrease drastically after exposure to sublethal concentrations of toxin before a return to normal levels (Walev *et al.*, 2001b; Husmann *et al.*, 2006). At higher lytic levels of toxin, recovery of ATP levels is not observed. The mechanism of repair involves removal of pores from the plasma membrane via an endocytic process (Idone et al., 2008). Cells that have been exposed to sublytic doses of toxin and then recover may be altered phenotypically, and there are numerous examples of such sublethal effects of CDC (Billington et al., 2000).

In immune cells, exposure to CDC toxins at concentrations that are not lytic induce release of cytokines and chemokines (Henderson et al., 1997; Billington et al., 2000). Cytokine and chemokine secretion are particularly important for the recruitment and activation of inflammatory immune cells to the local site of bacterial infection. One major cytokine family that plays a role in the inflammation process is the IL-1 family. Included in this family are IL-1α and IL-1β, which are both released after treatment of cells with CDC. Specifically, LLO induces the release of IL-1α from murine macrophages (Nishibori et al., 1996), while both streptolysin O (SLO) and PLY cause the secretion of IL-1β from human monocytes (Hackett & Stevens, 1992; Houldsworth *et al.*, 1994). The mechanism by which CDC induce release of IL-1 has not been fully characterized to date.

IL-1α and IL-1β, as well as IL-18 and IL-33, are stored inside cells such as macrophages and dendritic cells as precursors whose synthesis is induced by exposure to TLR ligands (signal 1) (Arend et al., 2008). Unlike many other cytokines, efficient release requires exposure of cells to a second stimulus to initiate processing and the nonclassical secretion of the active cytokine. The second stimuli lead to the activation of inflammasome complexes, which consist of members

of the Nod-like receptor (NLR) family, for the activation of inflammatory caspases such as caspase-1 (for a review see (Franchi et al., 2009; Martinon et al., 2009; Pedra et al., 2009)). The best known examples of these caspase-1-activating platforms are the NLRP1, NLRP3, and NLRC4 inflammasomes, which lead to the processing of the pro-form of IL-1β to its mature form. To date, multiple second stimuli for these various inflammasomes have been identified (for a review see (Martinon et al., 2009)) and select ones will be discussed below.

One of the best studied second stimuli is ATP, which acts by binding to the purinergic receptor $P2X_7$, initiating calcium influx and potassium efflux via its ion channel function (Ferrari et al., 2006). Calcium is also released from intracellular stores during this process and contributes to cytokine release (Brough et al., 2003). Potassium efflux leads to activation of calcium-independent phospholipase A_2 ($iPLA_2$) (Andrei et al., 2004) and the NLRP3 inflammasome, which contains dimeric caspase-1, adaptor ASC, and NLRP3 (also known as cryopyrin or NALP3) (Sutterwala et al., 2006). Activation of this inflammasome leads to cleavage of caspase-1, which cleaves inactive pro-IL-1β to generate active mature IL-1β for release from the cell. Additionally, $P2X_7$ activation causes recruitment of pannexin-1 protein to form a non-selective pore for passage of molecules up to ~900Da across membranes (Pelegrin & Surprenant, 2006; Locovei *et al.*, 2007). This pannexin-1 pore is thought to allow ion fluxes as well as the passage of bacterial products from inside endosomes or phagosomes into the cytosol for the subsequent activation of one or more inflammasome complexes (Kanneganti et al., 2007).

An additional stimulus that can activate the NLRP3 inflammasome and initiate IL-1β release is the potassium ionophore nigericin, which exerts its effects primarily through a potassium efflux mechanism (Mariathasan et al., 2006). Much like ATP, it also relies on the activity of caspase-1, but acts independently of $P2X_7$ (Le Feuvre et al., 2002). Other stimuli

37

inducing IL-1β release from myeloid cells through a NLRP3 and caspase-1 dependent mechanism include uric acid crystals (Martinon et al., 2006), silica crystals (Dostert et al., 2008; Hornung et al., 2008), aluminum salt crystals (Hornung et al., 2008), and amyloid-β fibrils (Halle et al., 2008). All of these can be phagocytosed by macrophages, and appear to disrupt lysosomes, resulting in leakage of their contents into the cytosol (Willingham & Ting, 2008). It was recently reported that cathepsin B is required for release of IL-1β following stimulation with silica crystals, aluminum salt crystals, or amyloid-β (Halle et al., 2008; Hornung et al., 2008), which supports a scenario in which mislocalized cathepsin B is involved in aspects of NLRP3 inflammasome activation or subsequent IL-1β release. In fact, other groups have shown that cathepsin B activates caspase-11, which in turn acts as an upstream activator of caspase-1 (Schotte et al., 1998; Wang et al., 1998).

In this report, we describe the mechanism of rapid IL-1β release after exposure of LPS-primed murine bone marrow-derived macrophages (BMDM) to the CDC tetanolysin O (TLO). Cytokine release occurs maximally within 2 hours of initial treatment with little additional release occurring by 20 hours post-treatment. Though TLO-induced IL-1β secretion is dependent on functional toxin pore formation, this alone is not sufficient for the processing and secretion of IL-1β. Lower TLO doses are required for release of mature IL-1β, as well as for the cleavage and release of mature caspase-1, as opposed to higher doses that enable the release of the inactive pro-IL-1β. Similarly to ATP and nigericin, TLO-induced release is dependent on potassium efflux, calcium influx, and the activities of iPLA$_2$, caspase-1, and cathepsin B as determined by pharmacological inhibition. Moreover, TLO-induced release of mature IL-1β is dependent on the NLRP3 inflammasome and independent of the NLRC4 inflammasome based

on studies employing BMDM deficient in NLRP or NLRC4. In summary, we further elucidate a mechanism for CDC-induced release of IL-1β.

2.4   MATERIALS AND METHODS

Reagents - Tetanolysin (TLO) was obtained from Biomol International (Plymouth Meeting, PA). Toxin was reduced with 10mM DTT (Sigma, St. Louis, MO) for 10min, 37°C before use unless indicated and untreated control samples were incubated in the same buffer lacking toxin. Adenosine triphosphate (ATP), nigericin, lipopolysaccharide (LPS), cholesterol, and pepstatin A were purchased from Sigma-Aldrich (St. Louis, MO), z-VAD-fmk/pan-caspase inhibitor VI, BAPTA-AM, Z-FF-fmk/cathepsin L inhibitor I, and CA-074 Me/cathepsin B inhibitor IV from EMD Biosciences (Gibbstown, NJ), Ac-YVAD-cmk/caspase-1 inhibitor II and bromoenol lactone (BEL) from Axxora, LLC (San Diego, CA), and triton X-100 from Fisher Scientific (Pittsburgh, PA). Purified anti-mouse IL-1α and IL-1β capture antibodies, biotin-conjugated anti-mouse IL-1α and IL-1β detection antibodies, and recombinant IL-1α were acquired from eBioscience (San Diego, CA). Purified and biotin-conjugated anti-mouse TNF-α antibodies, recombinant TNF-α, recombinant IL-1β, avidin-HRP, and 3, 3', 5, 5'-tetramethyl benzidine (TMB) were obtained from Biolegend (San Diego, CA).

Bone marrow-derived macrophage preparation – The following protocol was adapted from (Davies & Gordon, 2005). Tibiae and femurs from wild type (gifts from Dr. Lisa Borghesi, University of Pittsburgh), NLRP3$^{-/-}$, or NLRC4$^{-/-}$ (provided by Dr. Gabriel Núñez, University of Michigan) C57BL/6 mice were collected. Bone marrow cells were extracted using a 27 gauge needle and passed through a 21 gauge needle to obtain a homogenous mixture. Cells were plated

in petri dishes (Day 1) in DMEM (Mediatech, Inc., Herndon, VA) supplemented with 20% Gemcell™ FBS (Gemini Bio-Products, West Sacramento, CA), 2mM L-glutamine, 500U Penicillin/500µg Streptomycin (Lonza Inc., Walkersville, MD), 1mM sodium pyruvate (MP Biomedicals, Solon, OH), and 30% L cell supernatant. L cell supernatant was generated by incubating L cell fibroblasts (CCL-1 from ATCC, Manassas, VA) in DMEM supplemented with 10% Gemcell™ FBS, 2mM L-glutamine, 500U Penicillin/500µg Streptomycin, 1X non-essential amino acids (Irvine Scientific, Santa Ana, CA), and 1mM sodium pyruvate until confluent. Supernatant was collected and filtered through a 0.22um filter. Differentiation media for BMDM was changed every 3-4 days and BMDM were used for experiments Days 8-22. For experiments, BMDM were cultured in IMDM (Lonza, Inc.) containing 10% Gemcell™ FBS, 2mM L-glutamine, and 500U Penicillin/500µg Streptomycin.

Western blotting – 2×10^6 BMDM (plated the day before) were treated for 4 h in serum-containing IMDM with 1µg/ml LPS, various concentrations of TLO, or were left untreated. In some cases, following LPS priming, BMDM were incubated for 30 min in serum-free media with DTT control buffer, various doses of TLO, 3mM ATP, 20µM nigericin, or 1% triton X-100. Where indicated, 1ml supernatants were collected and TCA/cholic acid-precipitated as described by Qu and colleagues (Qu et al., 2007). Cells were harvested, washed, and lysed or directly lysed in wells with NP-40 lysis buffer containing a protease inhibitor cocktail (Sigma). Bradford assay (Bio-rad, Hercules, CA) was conducted to determine protein concentration of lysates and 20-50µg of protein lysate was run on SDS-PAGE gels along with concentrated supernatants (where indicated). Proteins were transferred to PVDF membrane using Towbin buffer transfer or the iBlot™ system (Invitrogen) and probed for IL-1β with mouse anti-IL-1β primary antibody (3ZD, National Cancer Institute Biological Resources Branch, Frederick Cancer Research and

Development Center) and goat anti-mouse IgG-HRP secondary antibody (Santa Cruz Biotechnology, Santa Cruz, CA) using the SNAP i.d. system (Millipore). Membranes were also probed for caspase-1 with rabbit anti-caspase-1 primary antibody and donkey anti-rabbit IgG-HRP secondary antibody (Biolegend). In some cases, the same blot was stripped with Restore Plus Western Blot Stripping Buffer (Thermo Scientific) according to the manufacturer's protocol and reprobed with rabbit anti-β-actin primary antibody (Biolegend) and donkey anti-rabbit IgG-HRP secondary antibody. Western blotting luminol reagent (Santa Cruz Biotechnology) was applied and membranes were imaged and analyzed (densitometry) with Kodak Image Station 4000MM (Molecular Imaging Systems, Carestream Health, Inc.). The net intensity of a single IL-1β protein band in a supernatant sample is expressed as a percentage of the total net intensities of IL-1β protein bands in all the supernatant samples for a given blot.

Preparation of ELISA supernatants – 1×10^5 BMDM were plated/well of 24-well plates overnight in IMDM. The next day, the spent media was removed and BMDM were primed with 1ug/ml LPS for 4 h. LPS was then removed and 300μl of the indicated treatments were added for the indicated times. Since TLO pore forming activity is inhibited by free cholesterol present in FBS, TLO treatments were added in IMDM lacking FBS for 5 min followed by addition of 10% FBS. Cholesterol inhibition of TLO activity was conducted by pre-mixing 1ug/ml free cholesterol with TLO before addition to cells. For all other inhibitor experiments, inhibitors were pre-incubated with BMDM for 1 h after LPS removal prior to the addition of TLO, ATP, or nigericin. Inhibitors were prepared in serum-free IMDM containing 0.01% BSA. Supernatants were collected, centrifuged 10000 rpm for 10min, and stored at -20°C before analysis by ELISA.

ELISA – High-bind polystyrene 96-well plates (Greiner Bio-One, Monroe, NC) were coated with 100μl/well of 1μg/ml of purified anti-mouse IL-1α, 4μg/ml of purified anti-mouse

41

IL-1β, or 1X purified anti-mouse TNF-α capture antibody overnight. Wells were washed three times with 200μl/well wash buffer (0.05% Tween® 20 in PBS) and this step was repeated in between each of the following incubations: (1) 200μl/well of filtered 1% BSA in PBS for 1 h, RT. (2) 100μl/well of standards or supernatant samples for 2 h, RT. (3) 100μl/well of 1μg/ml biotinylated anti-mouse IL-1α, 6μg/ml biotinylated anti-mouse IL-1β, or 1X biotinylated anti-mouse TNF-α detection antibody for 1 h, RT. (4) 100μl/well of 1:5000 avidin-HRP for 30min, RT. (5) 100μl/well of TMB substrate for 10min (IL-1α, TNF-α) or 20min (IL-1β) at RT. (6) 50μl/well of 1M sulfuric acid to stop the reaction. OD values were read at 450nm with a 570nm subtracted correction using a BioTek® PowerWave™ XS Microplate Spectrophotometer and data was analyzed using Gen5™ Data Analysis Software (BioTek® Instruments, Inc. Winooski, VT).

LDH release assay – 4.5×10^5 BMDM were plated/35mm dish overnight in IMDM. The next day, spent media was removed and BMDM were treated with 1ug/ml LPS for 4 h. Cells were then washed with PBS and incubated for 30 min with DTT control buffer or various TLO concentrations in phenol red-free IMDM. 1% triton X-100 was used as a control of complete cell lysis and maximal LDH release. Supernatants were collected and assayed in duplicate for LDH content using the LDH Cytotoxicity Assay Kit from Cayman Chemical Company (Ann Arbor, MI). % cytotoxicity was calculated as follows: ((Mean OD value of experimental sample – Mean blank OD) / (Mean OD value of triton X-100 control sample – Mean blank OD)) * 100. BMDM from these experiments were harvested from dishes using CellStripper™ (Mediatech, Inc.) and stained with 5μM YO-PRO-1 dye (Invitrogen, Carlsbad, CA) before analysis using a BD Biosciences (San Jose, CA) LSR II flow cytometer and accompanying FACSdiva™

software. BMDM were also stained with YO-PRO-1 after 5 min of DTT control buffer or TLO treatments.

Cy5 labeling of toxin – A monofunctional NHS-Ester Cy5 (GE Healthcare, Piscataway, NJ) vial was resuspended in 20μl PBS and diluted 1:100. 2.5μg TLO (2.5μl) or 2.5μg BSA control (2.5μl) was labeled with 0.5μl of PBS (control unlabeled TLO) or 0.5μl of 1:100 Cy5 (TLO-Cy5) for 10min, RT, in the dark. To quench each reaction, 2.5μg of BSA was added and incubated 10min, RT, in the dark.

Toxin binding & pore formation flow cytometry assay – 4.5×10^5 BMDM were plated/35 mm petri dish overnight in IMDM. The next day, spent media was removed and BMDM were treated with 1ug/ml LPS for 4 h. LPS was then removed and 1ml of each indicated inhibitor was added for 1 h. Inhibitors were prepared in serum-free IMDM containing 0.01% BSA. Then, TLO, TLO-Cy5, or BSA-Cy5 was added to cells in the presence or absence of 1μg/ml cholesterol for 5 min. Cells were harvested from dishes and stained with 5μM YO-PRO-1 dye before analysis by flow cytometry. FlowJo (Tree Star, Inc., Ashland, OR) was used for data analysis. A similar protocol was followed for BMDM treated with unlabeled TLO in the presence or absence of 1μg/ml cholesterol.

Live cell microscopy – 1×10^5 BMDM were plated/35 mm collagen-coated glass bottom culture dish (MatTek Corporation, Ashland, MA) overnight in IMDM. The next day, cells were primed with 1μg/ml LPS for 4 h. Cells were washed with serum-free IMDM and incubated for 15 min with 0.5μM LysoTracker™ Green in serum-free IMDM. BMDM were treated with a final concentration of 1.8nM TLO-Cy5 in serum-free media. In indicated experiments, TLO-Cy5 was pre-incubated with 1μg/ml cholesterol before addition to cells. Live cell imaging was performed using a Nikon TI inverted microscope with a 60X 1.49 NA oil immersion optic, a

NikonPiezo driven XYZ stage, a Prairie Sweptfield confocal head and Prairie Technology (Madison, WI) laser bench. Images were collected using a QuantEM backthinned 512B camera (Photometrics, Tucson AZ). Cells were maintained at 37^oC in the microscope with a Tokai Hit Environmental Stage (Tokyo Japan). Software control of the microscope was with Elements (Nikon, Melville NY). Data analysis was performed using Metamorph software.

Graphical and Statistical Analysis – All graphing analyses were completed using Microsoft Excel (Microsoft, Redmond, WA). Statistical analysis (Student's paired t-test) was conducted with GraphPad Prism (GraphPad Software, Inc., San Diego, CA). P-values were denoted as follows: p-value $\leq$ 0.05 = *, p-value $\leq$ 0.01 = **, and p-value > 0.05 was not significant (ns).

2.5   RESULTS

2.5.1 TLO-induced IL-1β release occurs via a TLR-independent mechanism

Previous studies reporting IL-1 induction by CDC did not fully characterize the mechanism involved. Since CDC have been reported to activate toll-like receptor 4 (TLR4) (Malley *et al.*, 2003; Park *et al.*, 2004a; Ito *et al.*, 2005; Srivastava *et al.*, 2005; Shoma *et al.*, 2008), we considered whether non-lytic doses of TLO could prime BMDM to synthesize pro-IL-1β similarly to LPS. Release of IL-1β might be expected to occur at low levels following such treatment, particularly if some cell death occurred over the time course of the experiment. To test this, western blotting was first used to measure pro-IL-1β levels in lysates of cells exposed to varying doses of TLO or 1μg/ml LPS. At all concentrations of TLO tested, after a 4 h period, no

44

pro-IL-1β could be detected while large amounts were induced by LPS (Figure 2-1). In addition, there was little to no detectable release of IL-1β from TLO-primed cells over this 4 h time period as measured by a sensitive ELISA assay to test culture supernatants (detection limit 16pg/ml) (data not shown). Thus, TLO cannot replace LPS for the priming of cells to synthesize pro-IL-1β.
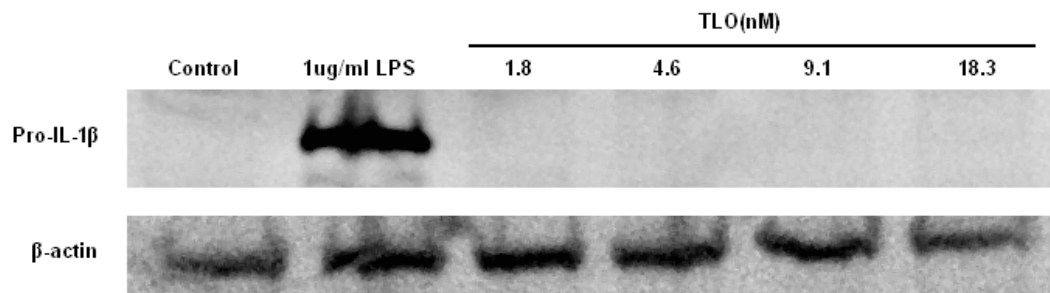
Figure 2-1: TLO cannot replace LPS as signal 1.

BMDM were treated with control (DTT-containing buffer), 1μg/ml LPS, 1.8nM TLO (100ng/ml TLO), 4.6nM TLO (250ng/ml TLO), 9.1nM TLO (500ng/ml TLO), or 18.3nM TLO (1μg/ml TLO) for 4 h in serum-containing media. Lysates were prepared from these cells, 50μg of protein run on an SDS-PAGE gel, and western blot conducted for IL-1β protein. Only LPS treatment induces the detectable expression of 35kDa pro-IL-1β. Data shown is a representative example of two independent experiments.

We next tested if LPS-primed cells could release IL-1 after exposure to TLO. A time course of IL-1β (Figure 2-2A) as well as IL-1α (Figure 2-2B) release demonstrates the rapid rates at which these cytokines are exported after TLO exposure, with near maximal secretion seen by 2 hours. Non-primed BMDM, as well as cells exposed to TLO for 4 h without LPS, could not be induced to secrete IL-1β following addition of TLO, ATP, or nigericin (data not shown). This rapid secretion contrasts to the release of another pro-inflammatory cytokine, TNF-α, from LPS-primed BMDM that have been exposed to control buffer, TLO, ATP, or nigericin for up to 2 hours (Figure 2-2C). LPS priming induces background levels of TNF-α as seen for the control, but additional treatment with TLO, ATP, or nigericin does not raise these levels significantly above background. These results are consistent with TLO acting to induce rapid release of IL-1β and IL-1α, and suggest that this occurs independently of TLR activation. The kinetics of the response were similar to those for ATP and nigericin, suggesting possible mechanistic similarities.
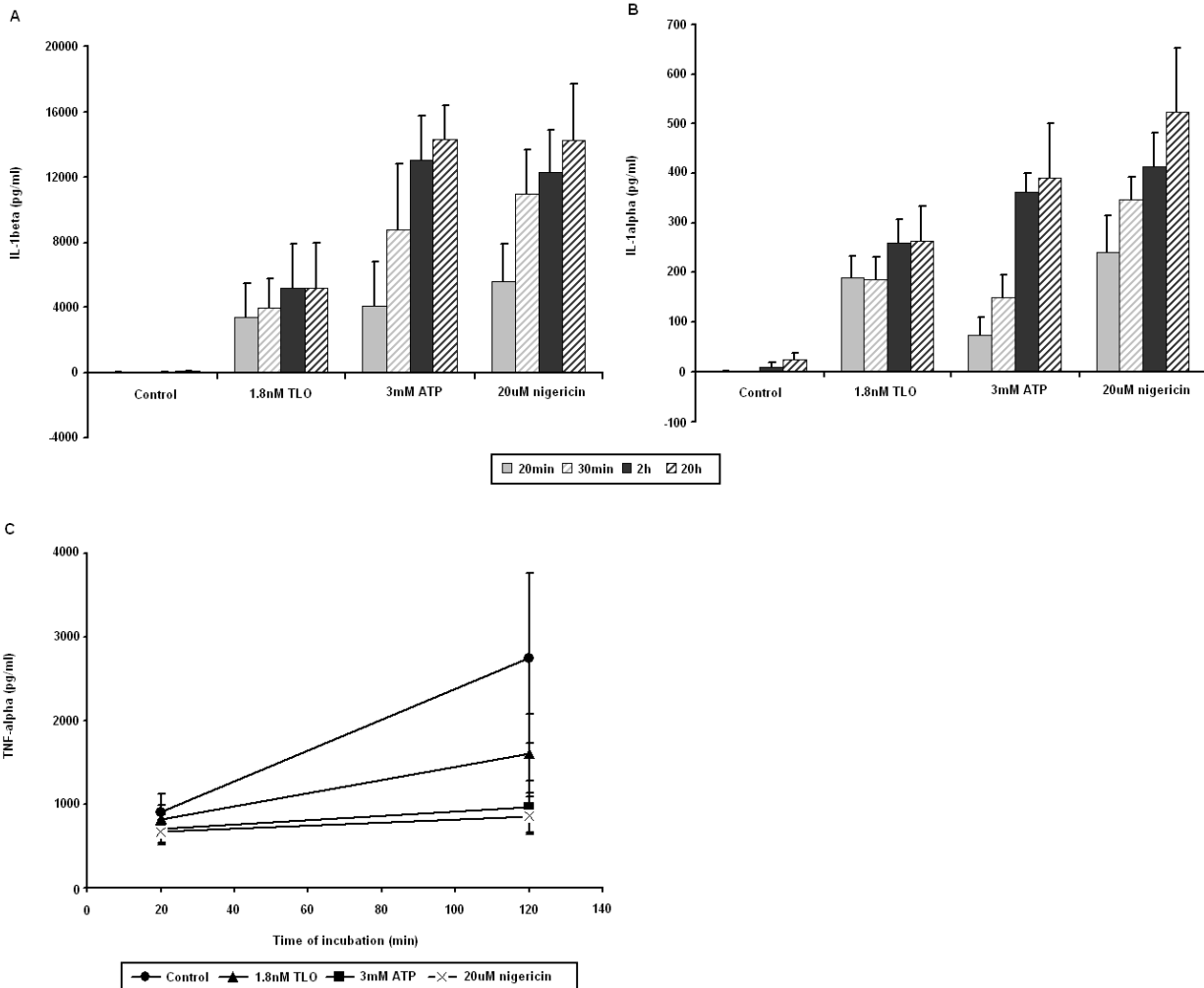
Figure 2-2: LPS-primed BMDM treated with TLO rapidly release IL-1β and IL-1α.

(A) IL-1β and (B) IL-1α content in supernatants from 4 h LPS-primed BMDM treated with control (DTT-containing buffer), 1.8nM TLO, 3mM ATP, and 20μM nigericin for 20 min, 30 min, 2 h, or 20 h was measured by ELISA. The majority of IL-1β and IL-1α are released by 2 h post-treatment. Data represents mean +/- SEM for 3 independent experiments each for IL-1β and IL-1α. (C) TNF-α content in supernatants from 4 h LPS-primed BMDM treated with control (DTT-containing buffer), 1.8nM TLO, 3mM ATP, and 20μM nigericin for 20 min or 2 h was measured by ELISA. Significant levels of TNF-α are not induced by TLO, ATP, or nigericin above control background levels. Data represents mean +/- SEM for 3 independent experiments.

47

2.5.2 Pore formation is required for TLO-induced IL-1β secretion

To further address the mechanism of CDC-induced cytokine release, we determined whether TLO pore formation was required to induce IL-1β release. Free cholesterol was added to TLO at a concentration shown previously to inhibit its ability to bind cholesterol on cell membranes and subsequently form pores (Mosser & Rest, 2006). Cholesterol-inhibited TLO was not able to induce IL-1β release from BMDM (Figure 2-3). To confirm that pore formation was blocked under these conditions, uptake of YO-PRO-1 dye, which does not cross intact cell membranes but readily enters permeabilized cells (Solini et al., 1999; Locovei et al., 2007), was measured (Figure 2-3, *inset*). Thus, TLO-induced pore formation is required for the release of IL-1β.
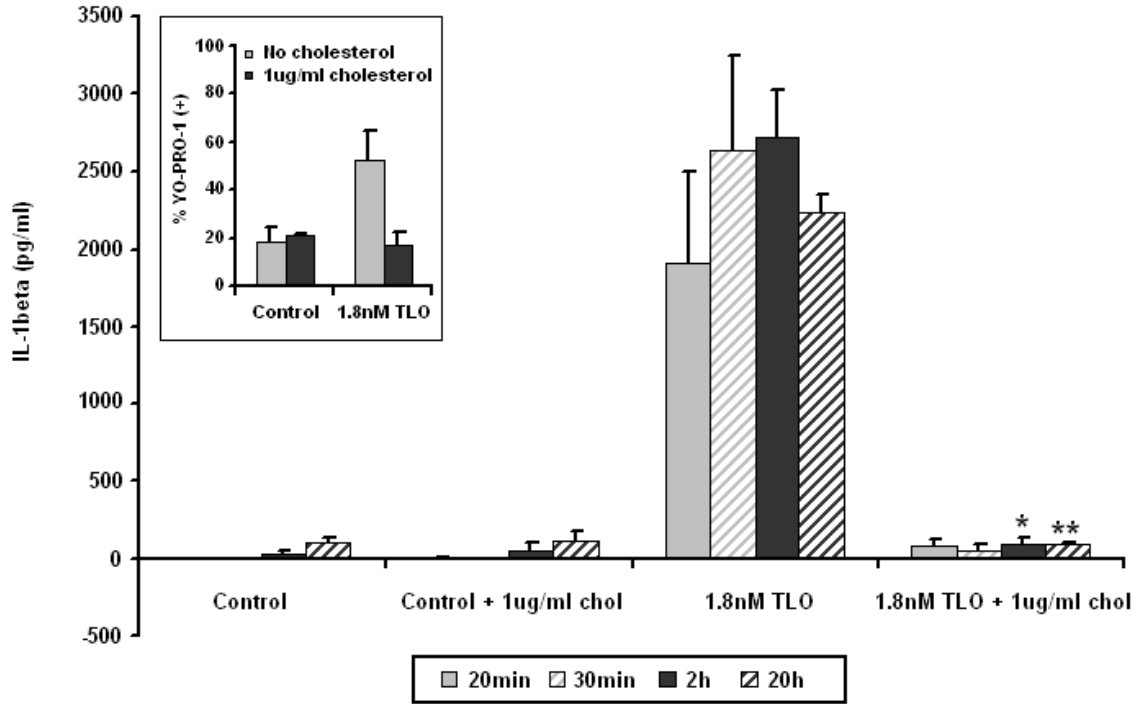
Figure 2-3: TLO-induced pore formation is required for IL-1β release from BMDM.

Four-hour LPS-primed BMDM were treated with control (DTT-containing buffer), control plus 1µg/ml cholesterol, 1.8nM TLO, or 1.8nM TLO plus 1µg/ml cholesterol for 20 min, 30 min, 2 h, or 20 h. Supernatants were collected and assayed by ELISA for IL-1β. Free cholesterol inhibits TLO- induced IL-1β release. Data represents mean +/- SEM for 3 independent experiments. Student's paired t-test was applied for comparison of 1.8nM TLO group with cholesterol versus without cholesterol; * = $p \leq 0.05$, ** = $p \leq 0.01$. *Inset:* 4 h LPS-primed BMDM were treated with DTT control buffer or 1.8nM TLO in the presence or absence of 1µg/ml cholesterol for 5 min. TLO-induced perforation as measured by YO-PRO-1 dye uptake was assessed by flow cytometry. Free cholesterol blocks TLO from forming pores and allowing dye uptake. Data represents mean +/- SEM for 2 independent experiments.

2.5.3 Lower TLO doses are required for the release of mature IL-1β

A straightforward explanation for the above results might be that TLO exposure could passively lead to release of IL-1β from BMDM through toxin-induced pores. To begin to test this possibility, toxin-induced pore formation in BMDM membranes, measured by YO-PRO-1 uptake, was compared to toxin-induced passive spilling of intracellular contents as measured by LDH release. BMDM became perforated within 5 min of treatment by even the lowest dose of TLO tested (0.9nM TLO) and the percentage of cells perforated increased in a dose-dependent manner (Figure 2-4A). These cells appeared to undergo membrane recovery by 30 min post-treatment as dye uptake did not change from background for all TLO concentrations tested (Figure 2-4B). Significant LDH release was not evident until exposure of BMDM to a much higher dose of 18.3nM TLO (Figure 2-4C). Thus, it appears that though cells become perforated starting at low levels of toxin, a high threshold of toxin must be reached before passive release of intracellular components occurs. IL-1β release in response to varying concentrations of TLO was then measured by ELISA (Figure 2-4D). Maximal secretion of IL-1β occurred at 9.1nM, a concentration that resulted in less than 10% LDH release. Strikingly, high levels of TLO that resulted in correspondingly higher LDH release induced lower levels of IL-1β secretion.
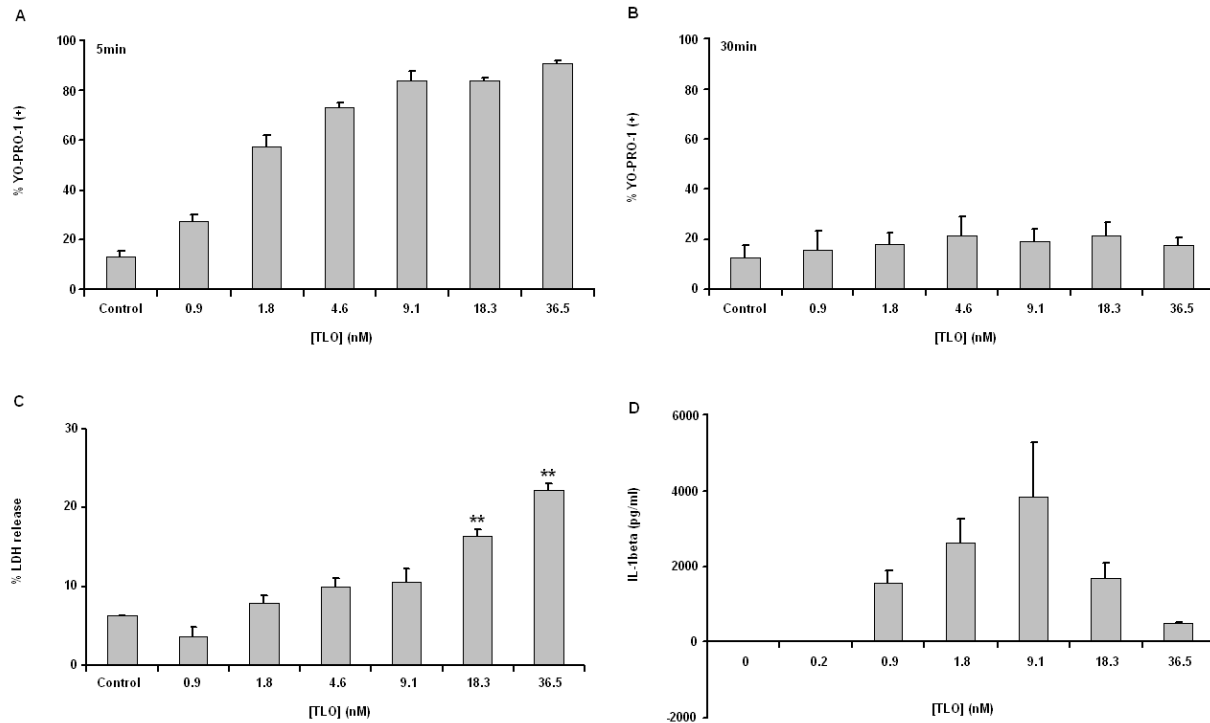
Figure 2-4: Determination of sublytic versus lytic CDC doses.

(A-B) Four-hour LPS-primed BMDM were treated with DTT control buffer or a range of TLO doses in serum-free media for 5 min or 30 min. BMDM were harvested and stained with YO-PRO-1 dye as a measure of TLO-induced perforation and dye uptake was assessed by flow cytometry. BMDM are perforated after 5 min of exposure to 0.9nM TLO and this process occurs in a dose-dependent manner. By 30 min post-TLO treatment, BMDM are no longer perforated. Data represents mean +/- SEM for 3 independent experiments for each time point. (C) Supernatants were collected from 4 h LPS-primed BMDM treated for 30 min with DTT control buffer or various TLO doses in serum-free media. TLO-induced passive spilling of contents (i.e. LDH) was determined by taking the ratio of LDH released from TLO-treated BMDM to LDH released from triton X-100-treated BMDM (see *Materials and Methods*). In comparison to perforation at lower doses of TLO, BMDM do not release LDH until much higher doses (18.3nM) of TLO. Data represents mean +/- SEM for 3 independent experiments. Student's paired t-test was applied for comparison of control versus TLO conditions; ** = $p \leq 0.01$. (D) Four-hour LPS-primed BMDM were treated with a range of concentrations of TLO for 30 min. Supernatants were collected and assayed by ELISA for IL-1β. Release of IL-1β from BMDM occurs after treatment with 0.9nM TLO to 36.5nM TLO. Data represents mean +/- SEM for 3 independent experiments.

We next determined whether IL-1β released from cells was processed to the mature bioactive form by analyzing supernatants using western blotting. A majority of the IL-1β was fully processed in supernatants from cells treated with 1.8nM TLO, whereas in supernatants from cells treated with 9.1nM or 18.3nM TLO, much of the IL-1β was in the pro-form and less mature form was detected (Figure 2-5A). We also confirmed that 3mM ATP and 20μM nigericin induced the release of mostly mature IL-1β while 1% triton X-100 lysed cells for complete release of pro-IL-1β content. Since caspase-1 is known to cleave pro-IL-1β to its mature form and undergo cleavage and release itself after activation, we further tested for release of the p20 caspase-1 cleavage product after exposure to TLO. Mature p20 caspase-1 release only occurred at the low 1.8nM TLO dose while pro-caspase-1 was released from cells treated with high 9.1nM or 18.3nM TLO doses (Figure 2-5B). ATP and nigericin controls also induced caspase-1 cleavage, but mature caspase-1 stayed inside the cells after ATP treatment while nigericin treatment induced most of it to be secreted from the cells. Triton X-100 caused complete lysis and release of pro-caspase-1 stores. We found the same pattern of IL-1β content in these samples (data not shown). Thus, cleavage of pro-caspase-1 for release of mature caspase-1 and secretion of mature bioactive IL-1β by BMDM occur selectively at concentrations of toxin that are sublytic.

53
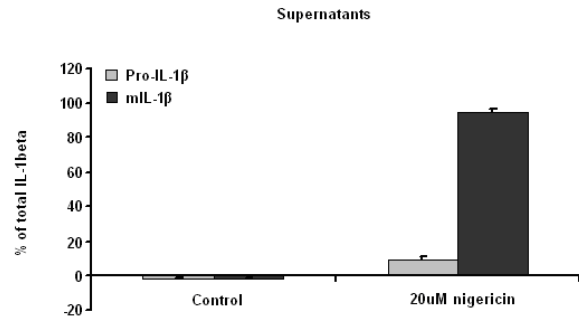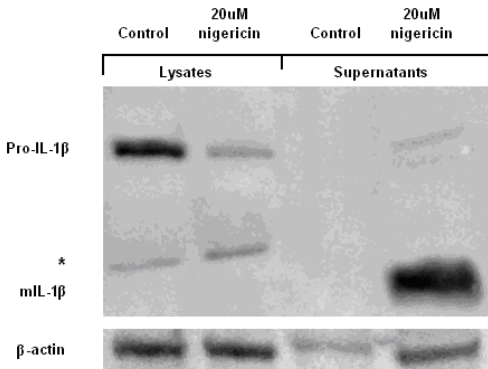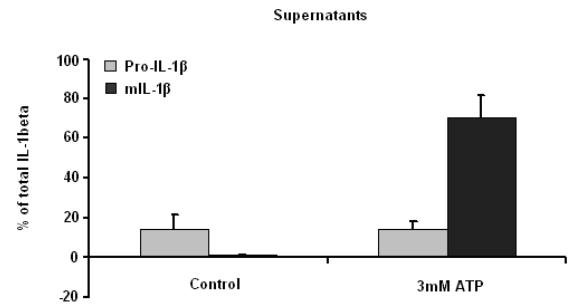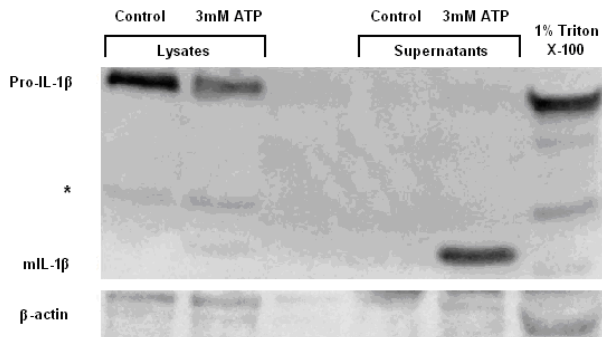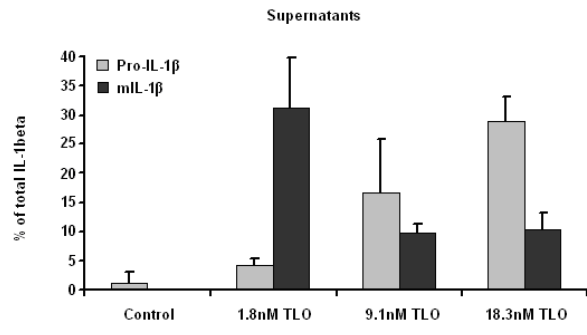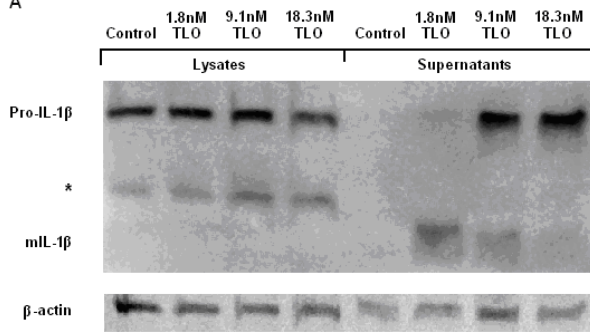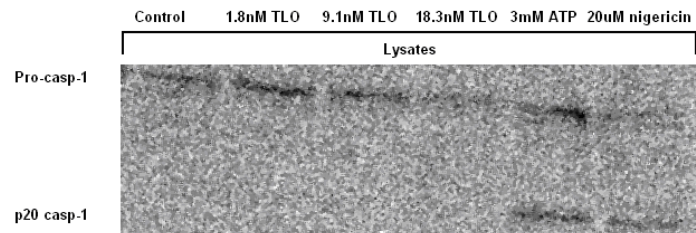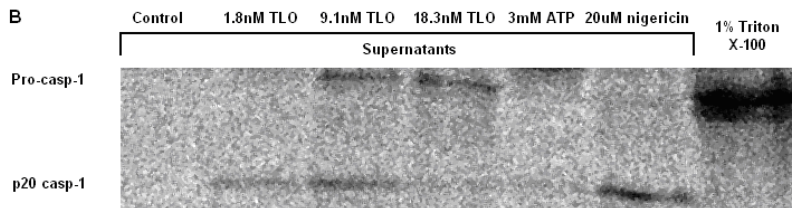
Figure 2-5: Lower concentrations of TLO are required to elicit mature IL-1β release from BMDM.

(A) Four-hour LPS-primed BMDM were treated with control (DTT-containing buffer), 1.8nM, 9.1nM, and 18.3nM doses of TLO, 3mM ATP, 1% triton X-100, and 20μM nigericin for 30 min in serum-free IMDM. 20μg of whole cell protein lysate or entire 1ml TCA/cholic acid precipitated supernatants were run on an SDS-PAGE gel and western blot conducted for mature (17kDa) or pro- (35kDa) IL-1β protein. Supernatants from 1.8nM TLO-treated BMDM contain mostly mature IL-1β while 9.1nM and 18.3nM TLO-treated BMDM supernatants contain mostly pro-IL-1β. ATP and nigericin controls induce the release of mostly mature IL-1β while triton X-100 lyses cells for release of pro-IL-1β. Data shown in the left panels are representative examples of three independent experiments. The right panels show the densitometry (see *Materials and Methods*) of the pro- and mature IL-1β bands in supernatants expressed as mean % of total IL-1β in supernatants +/- SEM for 3 independent experiments. The asterisk (*) refers to a non-specific protein band. (B) BMDM were treated as in part A. 20μg of whole cell protein lysate or entire 1ml TCA/cholic acid precipitated supernatants were run on an SDS-PAGE gel and western blot conducted for pro-caspase-1 (45kDa) or the cleaved p20 caspase-1 subunit (20kDa). Supernatants from 1.8nM TLO-treated BMDM contain mostly p20 caspase-1 while 9.1nM and 18.3nM TLO-treated BMDM supernatants contain pro-caspase-1. ATP and nigericin controls induce the cleavage of pro-caspase-1 with release of the p20 subunit from nigericin-treated cells and retained p20 for ATP-treated cells. Triton X-100 lyses cells for release of pro-caspase-1. Data shown is a representative example of two independent experiments.

2.5.4 IL-1β induced by low doses of TLO requires potassium efflux, calcium influx, and the activities of calcium-independent phospholipase A$_2$, caspase-1, and cathepsin B

To further elucidate the mechanism of IL-1β secretion induced by sublytic doses of TLO, we used a pharmacologic approach to inhibit different processes known to play a role in IL-1β secretion induced by other stimuli. Potassium efflux from cells, shown to be important for both ATP and nigericin-induced IL-1β release, can be inhibited by addition of excess exogenous KCl to the medium. Figure 2-6A demonstrates that KCl also inhibited IL-1β release induced by TLO. It has also been shown that IL-1β secretion induced by ATP requires calcium influx. Treatment

54

of BMDM with intracellular calcium chelator BAPTA-AM (Figure 2-6B) prior to TLO exposure blocked IL-1β secretion similarly to that for ATP and nigericin. Another event that occurs during ATP-induced IL-1β release is the activation of $iPLA_2$, which is also involved in TLO-induced IL-1β secretion as determined with the $iPLA_2$ inhibitor BEL (Figure 2-6C). Lastly, ion fluxes and $iPLA_2$ activity are thought to be involved in the activation of caspase-1, which in turn cleaves pro-IL-1β to the mature form before its release. Pan-caspase inhibitor z-VAD-fmk and caspase-1-specific inhibitor Ac-YVAD-cmk each inhibited TLO-induced IL-1β secretion (Figure 2-6D). Similar inhibition was seen with ATP and nigericin controls. All of the above pharmacological inhibitors were tested for toxicity against BMDM using YO-PRO-1 dye uptake (data not shown). It was found that BMDM exposed to 50mM KCl, 30μM BAPTA-AM, 10μM BEL, 20μM z-VAD-fmk, 100μM Ac-YVAD-cmk, 100μM pepstatin A, 100μM CA-074-Me, or 10μM Z-FF-fmk for 1 hour did not take up YO-PRO-1 above background levels observed for untreated BMDM. Thus, the inhibitors used at these concentrations were not toxic to BMDM. Overall, these results demonstrate that sublytic TLO doses induce IL-1β secretion through similar mechanisms to that for ATP and nigericin.

It was recently reported that IL-1β released from cells exposed to silica and alum crystals, and also amyloid-β fibrils, required cathepsin B activity (Halle et al., 2008; Hornung et al., 2008). Both groups proposed the novel hypothesis that cathepsin B localization to the cytosol might participate in IL-1β processing. We therefore investigated the role of cathepsin B activity in toxin-induced IL-1β release by utilizing the highly selective cathepsin B inhibitor CA-074-Me. IL-1β release induced by a low dose of TLO was substantially blocked by this inhibitor (Figure 2-6E). We also tested the contribution of other cathepsins in IL-1β release by using specific inhibitors pepstatin A (Figure 2-6E) and Z-FF-fmk (Figure 2-6F) to inhibit cathepsin D

and cathepsin L activities, respectively. Little if any effect on TLO-induced IL-1β was observed with these inhibitors, suggesting that cathepsin D and L do not participate in toxin-induced cytokine release. ATP and nigericin showed a similar dependence on cathepsin B, with a partial contribution of cathepsin L evident for both of these stimuli. These results demonstrate that cathepsin B activity is required for release of IL-1β induced by sublytic TLO doses.
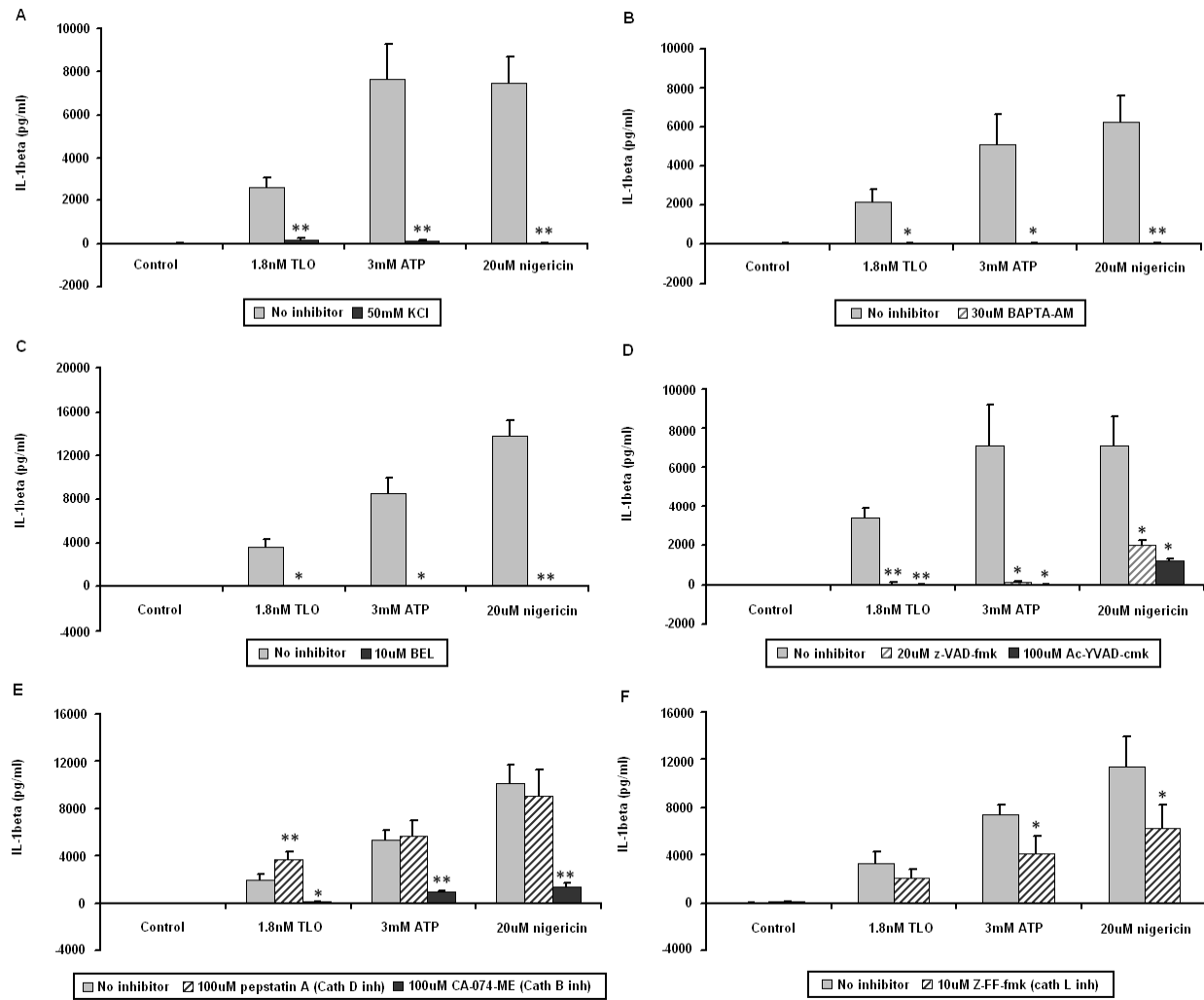
Figure 2-6: TLO-induced IL-1β release from BMDM relies on K⁺ efflux, Ca²⁺ influx and the activities of iPLA₂, caspase-1, and cathepsin B.

Four-hour LPS-primed BMDM were treated with no inhibitor (buffer only) versus 50mM KCl (K⁺ efflux inhibitor) (A), 30μM BAPTA-AM (intracellular calcium chelator) (B), 10μM BEL (iPLA₂ inhibitor) (C), 20μM z-VAD-fmk (pan-caspase inhibitor) or 100μM Ac-YVAD-cmk (caspase-1 inhibitor) (D), 100μM pepstatin A (cathepsin D inhibitor) or 100μM CA-074-Me (cathepsin B inhibitor) (E), or 10μM Z-FF-fmk (cathepsin L inhibitor) (F) for 1 h. Control (DTT-containing buffer), 1.8nM TLO, 3mM ATP, or 20μM nigericin treatments were then added for 30 min. Supernatants were collected and assayed by ELISA for IL-1β. KCl, BAPTA-AM, BEL, z-VAD-fmk, and Ac-YVAD-cmk almost completely abrogate IL-1β secretion induced by TLO, ATP, and nigericin. Cathepsin B inhibitor CA-074-Me has a major effect on IL-1β secretion induced by all three stimuli while the other cathepsins

play a lesser role. It should be noted that all inhibitors were not toxic to cells as assessed by YO-PRO-1 dye uptake (data not shown). Data represents mean +/- SEM for 5 independent experiments for parts A, D, and E, 6 independent experiments for part B, 3 independent experiments for part C, and 4 independent experiments for part F. Student's paired t-test was applied for comparison of no inhibitor versus inhibitor conditions; * = p $\leq$ 0.05, ** = p $\leq$ 0.01.

2.5.5 TLO-induced mature IL-1β release is dependent on the NLRP3 inflammasome

Since ion fluxes, iPLA$_2$, caspase-1, and the release of IL-1β have all been linked to inflammasome activation, specifically the NLRP3 inflammasome, we sought to determine if NLRP3 played a role in TLO-induced IL-1β secretion. To test this, we compared the response of wild type, NLRP3-deficient, and NLRC4-deficient BMDM to a low dose of TLO (1.8nM). We observed that 1.8nM TLO induced mature IL-1β release from LPS-primed wild type BMDM as well as NLRC4$^{-/-}$ BMDM, but not NLRP3$^{-/-}$ BMDM (Figure 2-7A). Similar results were obtained with the nigericin control while triton X-100 lysis caused release of pro-IL-1β regardless of an NLRC4 or NLRP3 deficiency. Furthermore, a high dose of TLO (18.3nM) induced release of the pro form from both wild type and NLRP3$^{-/-}$ BMDM (Figure 2-7B). Taken together, these results demonstrate NLRP3 dependence for mature IL-1β release caused by a low dose of TLO, but NLRP3 independence for pro-IL-1β secretion after exposure to a high TLO dose.
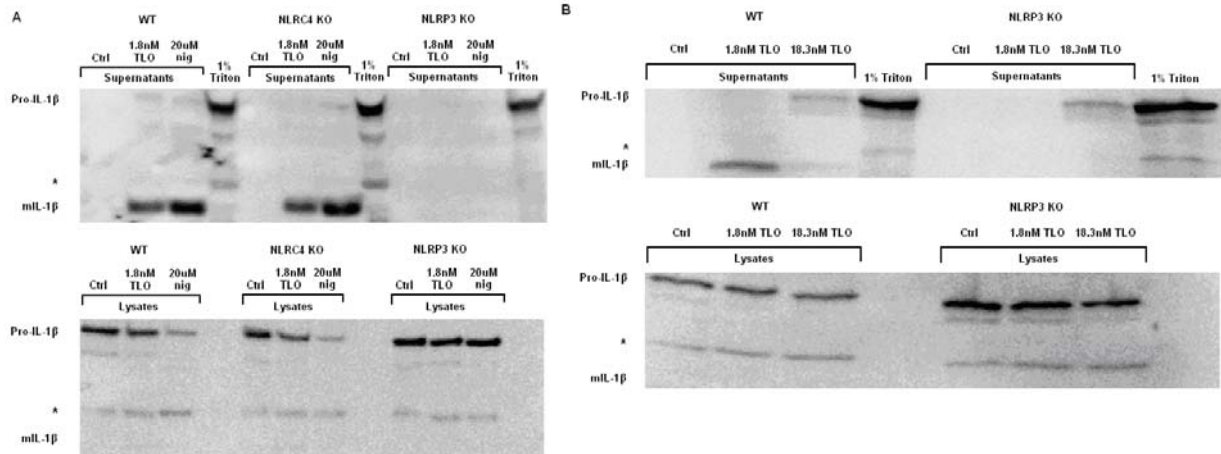
Figure 2-7: IL-1β release induced by low TLO doses is NLRP3-dependent.

(A) Four-hour LPS-primed wild type, NLRC4$^{-/-}$, or NLRP3$^{-/-}$ BMDM were treated with control (DTT-containing buffer), 1.8nM TLO, 20uM nigericin, or 1% triton X-100 for 30 min in serum-free IMDM. 20μg of whole cell protein lysate or entire 1ml TCA/cholic acid precipitated supernatants were run on an SDS-PAGE gel and western blot conducted for mature (17kDa) or pro- (35kDa) IL-1β protein. Mature IL-1β was released from wild type and NLRC4$^{-/-}$ BMDM after exposure to the low TLO dose and nigericin, but not from NLRP3$^{-/-}$ BMDM. Triton X-100 lysis caused release of pro-IL-1β stores from all cell types, including NLRP3$^{-/-}$ BMDM. Data shown is a representative example of two independent experiments. The asterisk (*) refers to a non-specific protein band. (B) Four-hour LPS-primed wild type or NLRP3$^{-/-}$ BMDM were treated with control (DTT-containing buffer), 1.8nM TLO (low dose), 18.3nM TLO (high dose), or 1% triton X-100 for 30 min in serum-free IMDM. 20μg of whole cell protein lysate or entire 1ml TCA/cholic acid precipitated supernatants were run on an SDS-PAGE gel and western blot conducted for mature (17kDa) or pro- (35kDa) IL-1β protein. Mature IL-1β was released from wild type BMDM after exposure to the low TLO dose, but not from NLRP3$^{-/-}$ BMDM. The high TLO dose as well as Triton X-100 caused release of pro-IL-1β stores from both wild type and NLRP3$^{-/-}$ BMDM. Data shown is a representative example of three independent experiments. The asterisk (*) refers to a non-specific protein band.

59

2.5.6 Toxin-induced pore formation is necessary but not sufficient for IL-1β release

We hypothesized based on the above results that pore formation would not be sufficient to induce IL-1β release by TLO in the absence of other components of the signaling pathway we identified. First, we assessed the ability of toxin to bind BMDM in the presence and absence of cholesterol, using live cell confocal imaging to characterize the interaction. Cy5-labeled TLO was generated for this purpose and BMDM were labeled with LysoTracker™ green as a marker of internal compartments. Active TLO-Cy5 (non-cholesterol treated) bound predominantly to the surface of BMDM (Figure 2-8A). On the other hand, BMDM internalized cholesterol-bound TLO-Cy5 to mostly non-acidic compartments, as there was little co-localization observed with LysoTracker™ green-labeled vesicles (Figure 2-8B). To next test if binding and pore formation could occur in the presence of inhibitors of IL-1β release, the interaction between Cy5-labeled TLO and BMDM was measured by flow cytometry. Pore formation was measured by uptake of YO-PRO-1 dye. Fluorescently-labeled TLO binds to cells and perforates them, as evidenced by increased YO-PRO-1 uptake (Figure 2-8C) and increased Cy5 signal (Figure 2-8D), relative to cells exposed to labeled BSA used as a control. In the presence of BAPTA-AM or KCl, which impairs IL-1β secretion as previously discussed, binding of TLO and subsequent pore formation is essentially unaffected. It can again be seen that Cy5-labeled TLO pre-incubated with cholesterol associates with BMDM despite the lack of pore forming activity. Taken together with the microscopy data, these results show that cholesterol-bound TLO can be efficiently internalized by BMDM without causing deleterious effects and without inducing biological responses such as IL-1β secretion. Overall, these results demonstrate that TLO-induced pore formation is required, but not sufficient for IL-1β release from BMDM.

60
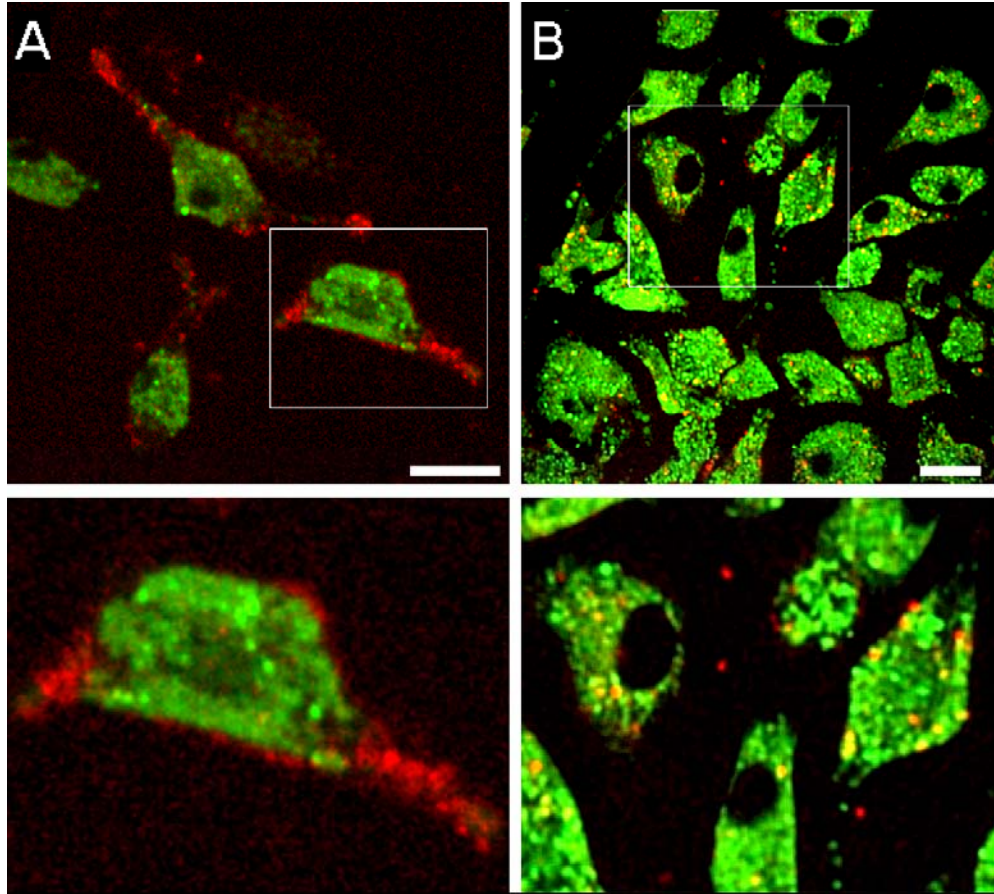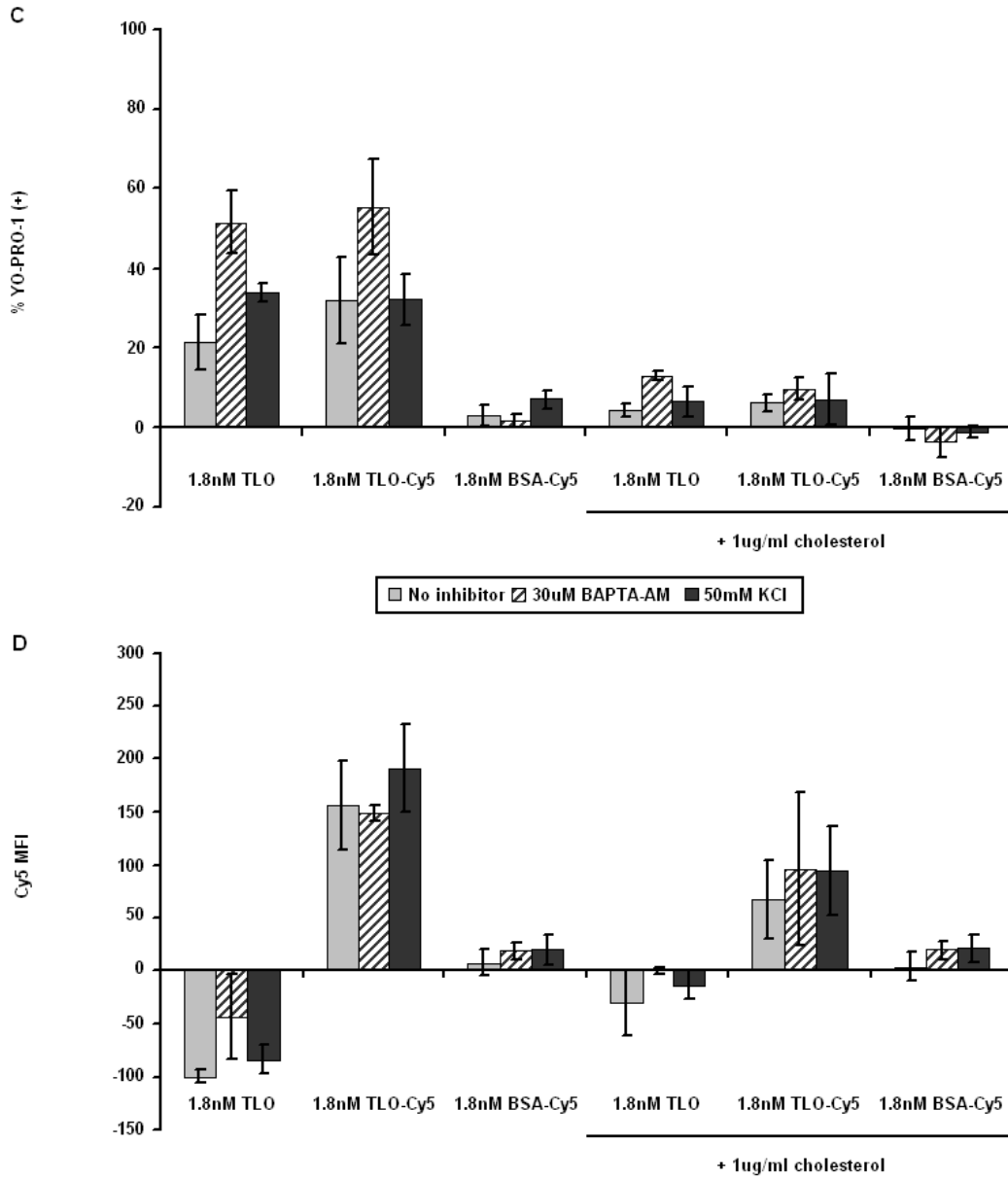
Figure 2-8: TLO binding and pore formation still occur in the presence of inhibitors of IL-1β secretion.

(A-B) Four-hour LPS-primed BMDM were labeled with LysoTracker™ Green dye (green) for intracellular tracking purposes and then treated with 1.8nM TLO-Cy5 (red) inactivated with 1μg/ml cholesterol or left untreated. BMDM were imaged by live cell microscopy to track active or cholesterol-inactivated TLO-Cy5 after addition. These midplane sections taken at 10 min post treatment show that active toxin binds primarily to the surface of BMDM (A) while cholesterol-bound toxin is internalized by BMDM (B). The bottom panels show magnifications of boxed cells displayed in the top panels. The white bar scales indicate a 10μm length. (C-D) Four-hour LPS-primed BMDM

were treated with no inhibitor (buffer only), 50mM KCl, or 30μM BAPTA-AM for 1 h followed by addition of control (DTT-containing buffer), 1.8nM TLO, 1.8nM TLO-Cy5, or 1.8nM BSA-Cy5 in the presence or absence of 1μg/ml cholesterol for 5 min. BMDM were analyzed by flow cytometry for TLO-induced pore formation (YO-PRO-1 uptake) (A) and TLO binding (Cy5 signal) (B). BMDM bind to pore-inducing TLO-Cy5, but not control BSA-Cy5 in the absence of IL-1β inhibitors as well as in the presence of BAPTA-AM or KCl. Data represents mean +/- SEM for 3 independent experiments. Control background values were subtracted out from the data.

2.6   DISCUSSION

We show here that TLO, a toxin of the CDC family, induces the rapid release of IL-1β from LPS-primed murine BMDM. Release of this cytokine typically requires two stimuli: (1) TLR pathway activation to generate the inactive IL-1β precursor and (2) a stimulator of the inflammasome for the activation of caspase-1 to cleave pro-IL-1β to its mature form before release. It has been observed that signal 1 (e.g. LPS) alone or signal 2 (e.g. ATP) alone stimulates IL-1β release from macrophages at low levels (pg/ml range for *in vitro* cultures) usually over long time periods (up to 24 h) (Mehta et al., 2001; Shoma et al., 2008). However, when both signals are applied sequentially, IL-1β can be secreted from macrophages in much greater amounts (ng/ml range) within 30 min (Kahlenberg et al., 2005; Sutterwala et al., 2006). Our results are consistent with TLO acting as a type of signal 2, and are inconsistent with TLO providing signal 1 to BMDM.

Shoma, *et al.* recently reported that the CDC pneumolysin (PLY) induced the release of IL-1β and IL-1α from murine peritoneal macrophages, a TLR4-dependent process not inhibited by cholesterol (Shoma et al., 2008). The PLY doses used in those experiments were similar to those for TLO used in our experiments. Additionally, other groups have found that PLY induces

63

IL-1β secretion from monocytes (Houldsworth et al., 1994) and that CDC listeriolysin O (LLO) induces IL-1 (type not defined) release from peritoneal macrophages (Yoshikawa et al., 1993), a process also unaffected by free cholesterol. In contrast, we tested whether TLO could induce release of IL-1β from LPS-primed BMDM, which carry pre-formed stores of the cytokine. Our results demonstrate that TLO-induced pore formation, requiring binding of the toxin to cellular cholesterol, stimulates the rapid release of large amounts of cytokine through a mechanism dependent on K^+ efflux, Ca^{2+} influx, and the activation of iPLA2, NLRP3, caspase-1, and cathepsin B. It should be noted that there was some variation in the amounts of TLO-induced IL-1β (mean amount per experiment ranged from 1975-3973 pg/ml; minimum = 803 pg/ml, maximum = 7569 pg/ml). The variability is most likely due to several factors, including differences in macrophage preparation, length of macrophage culture (up to three weeks), sample collection day, and assay day.

It appears that TLO-induced pore formation causes K^+ efflux and subsequent IL-1β release. However, mature IL-1β release only occurs when pore formation is balanced by the ability of cells to maintain function, required presumably for the activation of appropriate signaling pathways that will lead to the activation of caspase-1, the protease responsible for the conversion of inactive pro-IL-1β to active mature IL-1β. Evidence for this is seen at low concentrations of TLO, which induced release of primarily mature IL-1β as well as generation of mature caspase-1, whereas higher doses caused release of predominantly the pro-forms of caspase-1 and IL-1β, which are biologically inactive. We suggest that at high concentrations of toxin, a cell may undergo rapid release of cellular contents (e.g. pro-caspase-1 and pre-formed pro-IL-1β stores) through a passive process, outpacing the ability of the cell to activate caspase-1, required for processing of the pro- to mature form. This finding may explain a difference

between our results and those of Kanneganti, *et al.*, who reported that CDC streptolysin O (SLO) does not activate caspase-1 (Kanneganti et al., 2007). In their study, SLO was used at a high dose of 5μg/ml or 72.5nM.

In addition to a requirement for K^+ efflux, we also identified calcium influx and the activities of $iPLA_2$, NLRP3, and caspase-1 as key players in TLO-induced IL-1β release. To our knowledge, this is the first study to address the mechanism of CDC-induced IL-1β release and to differentiate the effects of low versus high doses of toxin. Non-cholesterol binding, pore-forming toxins (PFTs) from other families such as *A. hydrophila* aerolysin, which binds to GPI-anchored protein receptors, and *S. aureus* alpha toxin that binds specific lipid clusters (Gonzalez et al., 2008) also require K+ efflux for their downstream effects (Walev et al., 1995; Gurcel et al., 2006; Kloft et al., 2009). Aerolysin has been implicated in the activation of the NLRP3 and NLRC4 inflammasomes as well as caspase-1 for the activation of Sterol Regulatory Element Binding Proteins (SREBPs), which promote cell survival after cell membrane injury (Gurcel et al., 2006). However, this study utilized non-immune cells and the role of aerolysin in IL-1β processing and release was not addressed. Alpha toxin has also been shown to induce IL-1β secretion from LPS-primed monocytes, but the mechanism of release is unclear (Bhakdi et al., 1989; Walev et al., 1995). It should be stressed that although these other toxins may share some similarities to CDC in their ability to form pores in cells and initiate K+ efflux, they also differ in the size of the pore they induce (2nm for aerolysin and alpha toxin; 30nm for CDC) (Gonzalez et al., 2008) and therefore could have divergent downstream pathways. One such example is the response of cells to alpha toxin-mediated versus CDC-mediated cell injury. It has been observed that membrane repair after CDC-induced injury involves a p38-independent mechanism and occurs in less than 1 hour, compared to alpha toxin-mediated repair, which requires p38 activity

and may take many hours for full recovery (Bhakdi *et al.*, 1996; Husmann *et al.*, 2006). Thus, it will be interesting to see if IL-1β processing and release mechanisms are similar or disparate for PFTs that form small pores (alpha toxin, aerolysin) versus large ones (CDC).

While the involvement of ion fluxes and the activities of iPLA$_2$, NLRP3, and caspase-1 in IL-1β release induced by ATP and nigericin is well established (Lich et al., 2006), the mechanism for direct activation of the NLRP3 inflammasome complexes has remained unclear. Recent studies (Halle *et al.*, 2008; Hornung *et al.*, 2008) have suggested that cathepsin B may activate the NLRP3 inflammasome either directly or indirectly through other factors. In their studies, they show that IL-1β-inducing stimuli such as silica crystals, alum salt crystals, and amyloid-β fibrils are phagocytosed, and that these cargos disrupt lysosomal integrity. This would allow subsequent release of cathepsin B into the cytosol, which is proposed to cause activation of the NLRP3 inflammasome by an unknown mechanism. We also observe a dependence on cathepsin B activity for TLO-induced IL-1β secretion. Studies are underway to determine if this toxin relies on similar pathways as silica crystals, alum salt crystals, and amyloid-β fibrils, which lead to active cytosolic cathepsin B.

In addition to understanding how caspase-1 is directly activated in this system, there is much interest in determining the general mechanism by which mature IL-1β is secreted from cells. IL-1β lacks signal sequences for localization to the Golgi and other classical secretory compartments and therefore must be secreted by non-classical means. The data available suggest several possible pathways for IL-1β release, including release of exosomes carrying mature IL-1β after fusion of multivesicular bodies with the plasma membrane, Ca^{2+}-dependent secretory lysosome exocytosis, microvesicle shedding from the plasma membrane, and direct translocation of cytosolic cytokine through unknown plasma membrane transporters to the extracellular

environment (Qu et al., 2007). It is possible that multiple pathways may be involved for a single cell type or that a particular pathway is designated to each specific cell type. At this time, it is unknown what pathway(s) TLO utilizes to cause the export of mature IL-1β.

This is the first study to identify the mechanism of IL-1β release induced by a family of cholesterol-binding, large pore-forming toxins and to tease apart differences in the IL-1β response to lower versus higher toxin doses. This IL-1β release mechanism may differ from that for other families of PFTs that bind different receptors, form much smaller pores, and utilize different pathways to achieve the same goal (i.e. pore resealing processes). Moreover, to our knowledge this is the first observation of cathepsin B involvement in IL-1β release induced by a PFT. In summary, we find that low TLO concentrations induce the rapid release of relatively high amounts of active mature IL-1β from LPS-primed murine macrophages in a process dependent on toxin-induced perforation, potassium efflux, calcium influx, and activation of iPLA$_2$, NLRP3, caspase-1, and cathepsin B. On the other hand, high TLO doses induce the release of inactive pro-IL-1β, which may be an evasion mechanism employed by bacteria during infection. This study addresses in detail the mechanisms of CDC-induced rapid IL-1β release and may help to explain the effects of these toxins in bacterial infections and the subsequent host immune responses.

3.0 NLRP3 INFLAMMASOME-DEPENDENT AND NLRP3 INFLAMMASOME-INDEPENDENT HMGB1 RELEASE INDUCED BY A BACTERIAL PORE-FORMING TOXIN

3.1 ABSTRACT

The NLRP3 inflammasome is a pro-inflammatory caspase-1-containing complex involved in the maturation of pro-inflammatory cytokines IL-1β and IL-18. NLRP3, independent of its inflammasome functions, has been demonstrated to play a role in a cathepsin B-dependent, caspase-1-independent necrotic cell death process known as pyronecrosis. We have previously shown that the cholesterol-dependent, pore-forming toxin tetanolysin O (TLO) causes IL-1β release from LPS-primed murine bone marrow-derived macrophages (BMDM) in a NLRP3 inflammasome- and cathepsin B-dependent manner. The work contained herein supports an additional role for TLO in the necrosis of LPS-primed BMDM. Both a low and a high TLO dose induce release of lactate dehydrogenase (LDH) and high mobility group box 1 (HMGB1) and this release is NLRP3-dependent for the low toxin dose. Low dose TLO-induced HMGB1 release is also dependent on the activities of caspase-1 and cathepsin B, suggesting a novel form of cell death that is distinct from caspase-1-independent pyronecrosis. We also observe via fixed cell microscopy that TLO causes relocalization of HMGB1 from the nucleus to the cytoplasm in LPS-primed BMDM and that NLRP3 plays a role in HMGB1 release from the cells. To our

knowledge, this is the first study to visualize HMGB1 localization in cells lacking NLRP3. These results provide some understanding as to how HMGB1 release is regulated and could eventually lead to new therapeutic approaches to target HMGB1, which contributes to many inflammatory diseases.

3.2   INTRODUCTION

The NLR (nucleotide binding domain, leucine rich repeat-containing) family of proteins plays a significant role in innate immune sensing of danger signals derived both from pathogens and the host (Martinon *et al.*, 2009). In particular, NLR family member NLRP3 has been well studied for its ability to promote inflammatory responses. Genetic mutations in the *NLRP3/CIAS1* human gene encoding for this protein lead to autoinflammatory diseases known as *CIAS1*-associated periodic syndromes (CAPS) that include familial cold autoinflammatory syndrome (FCAS) (Hoffman *et al.*, 2001), Muckle-Wells syndrome (MWS) (Hoffman *et al.*, 2001), and neonatal-onset multi-inflammatory disease (NOMID) (Aksentijevich *et al.*, 2002), which is also known as Chronic Infantile Neurologic Cutaneous Articular Syndrome (CINCA). NLRP3 oligomerizes to form a platform for the activation of caspase-1, known as the NLRP3 inflammasome, which ultimately leads to pro-inflammatory IL-1β and IL-18 secretion (Cassel *et al.*, 2009). Cells must be exposed to a TLR priming signal for the generation of pro-IL-1β and pro-IL-18 followed by a second NLRP3 inflammasome-activating signal that enables the activation of caspase-1 and release of the mature forms of these cytokines. To date, many pathogen-, host-, and environmental toxin-related second stimuli have been identified (Figure 3-

1). Some of these studies also implicated lysosomal protease cathepsin B activity in IL-1β release, but the mechanism of action is unclear.

Class of inflammasome stimulator	Inflammasome stimulator	Reference(s)
Bacteria	*K. pneumoniae*	(Willingham *et al.*, 2009)
	L. monocytogenes	(Mariathasan *et al.*, 2006)
	S. aureus	(Mariathasan *et al.*, 2006; Munoz-Planillo *et al.*, 2009)
	S. pyogenes	(Harder *et al.*, 2009)
Particulates	Aluminum salt crystals	(Eisenbarth *et al.*, 2008; Li *et al.*, 2008)
	Asbestos	(Dostert *et al.*, 2008)
	Silica crystals	(Dostert *et al.*, 2008)
	Uric acid crystals	(Martinon *et al.*, 2006)
Pore-forming agents	Adenosine triphosphate (ATP)	(Mariathasan *et al.*, 2006)
	Alpha hemolysin from *S. aureus*	(Craven *et al.*, 2009)
	Maitotoxin	(Mariathasan *et al.*, 2006)
	Nigericin	(Mariathasan *et al.*, 2006)
	Streptolysin O from *S. pyogenes*	(Harder *et al.*, 2009)
	Tetanolysin O from *C. tetani*	(Chu *et al.*, 2009)
Protein aggregates	Amyloid-β fibrils	(Halle *et al.*, 2008)
Viruses	Influenza	(Kanneganti *et al.*, 2006a; Allen *et al.*, 2009)
Yeasts	*C. albicans*	(Gross *et al.*, 2009)
Other	Nucleic acids	(Kanneganti *et al.*, 2006a; Kanneganti *et al.*, 2006b)
	Malarial hemozoin	(Tiemi Shio *et al.*, 2009)

Figure 3-1: NLRP3 inflammasome stimulators

Bacteria, particulates, pore-forming agents, protein aggregates, viruses, yeasts, nucleic acids, and malarial hemozoin stimulate the NLRP3 inflammasome. The studies where each inflammasome stimulator was identified are noted.

Aside from its role in pro-inflammatory cytokine secretion, NLRP3 has also been found to play a role in pathogen-induced cell death of monocytes and macrophages. *S. flexneri* (Willingham *et al.*, 2007) and *K. pneumoniae* (Willingham *et al.*, 2009) infection of monocytes or macrophages or exposure of these cells to *S. aureus* α-hemolysin (Craven *et al.*, 2009) results in NLRP3- and cathepsin B-dependent necrotic cell death termed as pyronecrosis. However, this pathway is independent of caspase-1 unlike a form of cell death known as pyroptosis that relies on caspase-1, but not cathepsin B (Bergsbaken *et al.*, 2009). This would suggest that NLRP3 is acting independently of its inflammasome function to bring about a program of cell death. Pyronecrosis is similar to necrosis in that a major hallmark is the loss of an intact plasma membrane that leads to the spilling of cellular contents that promote inflammation.

One such molecule known to be released during necrosis and pyronecrosis is high mobility group box 1 (HMGB1). HMGB1 is a nuclear protein, present in all nucleated cells, which was initially recognized for its role as a DNA binding protein that regulates transcription (Javaherian *et al.*, 1978; Singh & Dixon, 1990; Lange & Vasquez, 2009). More recently, HMGB1 has been shown to act as a cytokine after being passively released from necrotic cells (Scaffidi *et al.*, 2002) or actively released from activated monocytes or macrophages stimulated with LPS, TNF, IL-1β, or IFN-γ (Wang *et al.*, 1999; Rendon-Mitchell *et al.*, 2003). Following release, HMGB1 can bind to its receptor RAGE (receptor for advanced glycation-end products) to elicit additional pro-inflammatory cytokine release (e.g. IL-1β, TNF-α) (Andersson *et al.*, 2000; Kokkola *et al.*, 2005). Toll-like receptors (TLRs) 2 and 4 have also been suggested to be receptors for HMGB1, but these findings are controversial (Park *et al.*, 2004b; Kokkola *et al.*, 2005; van Zoelen *et al.*, 2009). HMGB1-mediated inflammation can be detrimental to the host

and contribute to lung and liver injury, gut epithelial-cell barrier leakage, sepsis, arthritis, and cancer (Dumitriu *et al.*, 2005; Lotze & Tracey, 2005).

The mechanism by which HMGB1 localizes from the nucleus to the extracellular space is not well understood. HMGB1 is a leaderless peptide that cannot translocate from the Golgi to the cell membrane after protein synthesis, much like IL-1β. It has been suggested (Gardella *et al.*, 2002) that upon 18h of LPS stimulation of monocytes, HMGB1 moves out of the nucleus into the cytoplasm, whereupon it enters cytoplasmic secretory vesicles before final exocytosis from the cells. Hyperacetylation seems to be required for HMGB1 to move out of the nucleus and this acetylation state prevents re-entry into the nucleus due to blocked interaction with the nuclear-importer complex (Bonaldi *et al.*, 2003). Contrary to active HMGB1 secretion, passive HMGB1 release results from the breakdown of cellular membranes during necrotic or pyronecrotic cell death. Since actively secreted HMGB1 requires acetylation while passively released HMGB1 does not, differences in post-translational modification of HMGB1 may result in differences in its downstream biological activities.

Our laboratory recently demonstrated that bacterial pore-forming toxin tetanolysin O (TLO), from the cholesterol-dependent cytolysin (CDC) family (Billington *et al.*, 2000; Palmer, 2001), rapidly activates caspase-1 and induces the secretion of IL-1β in a NLRP3- and cathepsin B-dependent manner from murine bone marrow-derived macrophages (BMDM) (Chu *et al.*, 2009). We observed these phenomena only with a sublytic dose of TLO, defined as a TLO concentration that perforates cells, but does not induce enough damage to make the cells immediately metabolically inactive. On the other hand, a lytic TLO dose induced rapid passive release of inactive pro-caspase-1, inactive pro-IL-1β (independently of NLRP3), and lactate dehydrogenase (LDH), a common marker of cell death. These studies were conducted in a

72

relatively short amount of time (30 min) and the ultimate fate (i.e. cell death) of TLO-exposed BMDM was not determined. It has been shown previously by Srivastava, *et al.* (Srivastava *et al.*, 2005) that high doses of purified CDC pneumolysin (PLY) cause apoptosis of macrophages via a TLR4-dependent mechanism. However, in the context of infection with CDC-secreting bacteria, macrophages undergo various types of cell death ranging from caspase-1-dependent pyroptosis (Cervantes *et al.*, 2008) and caspase-1-dependent apoptosis (Timmer *et al.*, 2009) to calpain-dependent oncosis (Goldmann *et al.*, 2009). The role of CDC in these bacterially induced cell death pathways is unclear.

Given that NLRP3 has been observed to play a role in pyronecrotic cell death initiated by other inflammasome-activating stimuli, we asked if TLO could also trigger NLRP3-dependent cell death in macrophages. We show here that low and high doses of TLO both cause cell death in BMDM, which is characterized by membrane permeability and plasma membrane breakdown that enables passive spilling of LDH and rapid HMGB1 release. At the low TLO dose, HMGB1 release is dependent on LPS priming, NLRP3, caspase-1, and cathepsin B, while these factors have no impact on HMGB1 release induced by the high TLO dose. After exposure of LPS-primed BMDM to the low TLO dose, NLRP3 appears to be required for the release of HMGB1 from cytoplasmic vesicles to the extracellular space and NLRP3-deficient BMDM are protected from plasma membrane damage, as evidenced by a lack of LDH release. These results suggest that the high TLO dose causes uncontrolled necrotic cell death in BMDM, while the low dose of TLO initiates a NLRP3 inflammasome-dependent necrotic cell death program. This is the first study to identify a NLRP3-dependent mode of cell death that relies both on cathepsin B and caspase-1 and to visualize the impact of NLRP3 on HMGB1 release.

3.3   MATERIALS AND METHODS

Reagents - Tetanolysin (TLO) was obtained from Biomol International (Plymouth Meeting, PA). Toxin was reduced with 10mM DTT (Sigma, St. Louis, MO) for 10min, 37°C before use unless indicated and untreated control samples were incubated in the same buffer lacking toxin. Adenosine triphosphate (ATP), nigericin, and lipopolysaccharide (LPS) were purchased from Sigma-Aldrich (St. Louis, MO), CA-074 Me/cathepsin B inhibitor IV from EMD Biosciences (Gibbstown, NJ), Ac-YVAD-cmk/caspase-1 inhibitor II from Axxora, LLC (San Diego, CA), triton X-100 from Fisher Scientific (Pittsburgh, PA), and glycerol from Invitrogen (Carlsbad, CA).

Bone marrow-derived macrophage preparation – The following protocol was adapted from (Davies & Gordon, 2005). Tibiae and femurs from wild type (gifts from Dr. Lisa Borghesi, University of Pittsburgh) and NLRP3$^{-/-}$ (gifts from Dr. Gabriel Nunez, University of Michigan) C57BL/6 mice were collected. Bone marrow cells were extracted using a 27 gauge needle and passed through a 21 gauge needle to obtain a homogenous mixture. Cells were plated in petri dishes (Day 1) in DMEM (Mediatech, Inc., Herndon, VA) supplemented with 20% Gemcell™ FBS (Gemini Bio-Products, West Sacramento, CA), 2mM L-glutamine, 500U Penicillin/500µg Streptomycin (Lonza Inc., Walkersville, MD), 1mM sodium pyruvate (MP Biomedicals, Solon, OH), and 30% L cell supernatant. L cell supernatant was generated by incubating L cell fibroblasts (CCL-1 from ATCC, Manassas, VA) in DMEM supplemented with 10% Gemcell™ FBS, 2mM L-glutamine, 500U Penicillin/500µg Streptomycin, 1X non-essential amino acids (Irvine Scientific, Santa Ana, CA), and 1mM sodium pyruvate until confluent. Supernatant was collected and filtered through a 0.22um filter. Differentiation media for BMDM was changed every 3-4 days and BMDM were used for experiments Days 8-22. For experiments, BMDM

were cultured in IMDM (Lonza, Inc.) containing 10% Gemcell™ FBS, 2mM L-glutamine, and 500U Penicillin/500μg Streptomycin.

Western blotting – $2x10^6$ BMDM (plated the day before in 6-well plates) were treated for 4 h with 1μg/ml LPS or were left untreated. BMDM were then washed with serum-free IMDM and incubated for 30 min in serum-free IMDM with DTT control buffer, 1.8nM TLO, 18.3nM TLO, 3mM ATP, 20μM nigericin, or sterile purified water. In some cases, BMDM were pre-treated with various inhibitors for 1 h in serum-free media after LPS priming. 1ml supernatants were collected and TCA/cholic acid-precipitated as described by Qu and colleagues (Qu *et al.*, 2007). Cells were lysed in wells with 1% triton X-100 lysis buffer (1% triton X-100, 10% glycerol, 50mM Hepes, 150mM NaCl, 1.5mM $MgCl_2$) containing a protease inhibitor cocktail (Sigma). Bradford assay (Bio-rad, Hercules, CA) was conducted to determine protein concentration of lysates and 20μg of protein lysate was run on SDS-PAGE gels along with concentrated supernatants. Proteins were transferred to PVDF membrane using Towbin buffer transfer or the iBlot™ system (Invitrogen) and probed for HMGB1 with mouse anti-HMGB1 primary antibody (Abcam, Cambridge, MA) and goat anti-mouse IgG-HRP secondary antibody (Santa Cruz Biotechnology, Santa Cruz, CA) using the SNAP i.d. system (Millipore, Billerica, MA). Western blotting luminol reagent (Santa Cruz Biotechnology) was applied and membranes were imaged with Kodak Image Station 4000MM (Molecular Imaging Systems, Carestream Health, Inc.).

LDH release assay – $4.5x10^5$ BMDM (plated the day before in 35mm petri dishes) were treated for 4 h with 1μg/ml LPS. Cells were then washed with PBS and incubated with DTT control buffer, 1.8nM TLO, or 18.3nM TLO in phenol red-free serum-free IMDM. TLO was incubated with cells for 5 min in this serum-free media (since serum contains cholesterol that can

inhibit TLO interaction with cells) followed by addition of 10% FBS and further incubation for 5 min – 6 h. 1% triton X-100 was used as a control of complete cell lysis and maximal LDH release. Supernatants were collected and assayed in duplicate for LDH content using the LDH Cytotoxicity Assay Kit from Cayman Chemical Company (Ann Arbor, MI). % cytotoxicity was calculated as follows: ((Mean OD value of experimental sample – Mean blank OD) / (Mean OD value of triton X-100 control sample – Mean blank OD)) * 100.

Live/dead flow cytometry assay – 4.5×10^5 BMDM (plated the day before in 35mm petri dishes) were treated for 4 h with 1μg/ml LPS. BMDM were then washed with serum-free IMDM and treated with DTT control buffer, 1.8nM TLO, or 18.3nM TLO in serum-free IMDM. TLO was incubated with cells for 5 min followed by addition of 10% FBS and cells were immediately harvested or further incubated for 30 min – 4 h. At each time point, cells from dishes and supernatants were harvested and stained using a calcein-AM and ethidium homodimer-1 LIVE/DEAD® Viability/Cytotoxicity Kit for mammalian cells according to the manufacturer's protocol (Invitrogen). Samples were analyzed on a BD™ LSR II flow cytometer (BD Biosciences) and FlowJo (Tree Star, Inc., Ashland, OR) was used for data analysis.

Fixed cell microscopy – 1.5×10^5 BMDM (plated overnight in 35mm glass bottom culture dishes (MatTek Corporation, Ashland, MA)) were primed with 1μg/ml LPS for 4 h. Cells were then washed with serum-free IMDM and immediately analyzed or incubated with 1.8nM TLO in serum-free IMDM. For the latter case, TLO was incubated with the cells for 5 min followed by addition of 10% FBS and cells were immediately harvested or further incubated for 15 – 30 min. At each time point, cells were washed with PBS and fixed with 2% PFA made in PBS for 10 minutes. Cells were washed with PBS, permeabilized for 15min with 0.1% Triton X-100 made in PBS, washed five times with 0.5% BSA, and blocked with 2% BSA for 45min. Cells were

again washed five times with 0.5% BSA, incubated with rabbit anti-mouse HMGB1 (generously provided by Michael T. Lotze, University of Pittsburgh) or rabbit IgG isotype control antibody (Jackson ImmunoResearch) in 0.5% BSA for 60min, washed five times with 0.5% BSA, and incubated with goat anti-rabbit Alexa Fluor® 488 (Invitrogen) in 0.5% BSA for 60min. Cells were washed five times with 0.5% BSA and five times with PBS followed by staining with Hoescht stain and rhodamine-phalloidin (Invitrogen) for 30s. Cells were washed twice with PBS, covered with gelvatol and dried in the dark at 4°C overnight. Fixed cell imaging was performed using an Olympus FluoView 1000 scanning confocal microscope (Olympus America Inc., Center Valley, PA). Images were viewed with Adobe® Photoshop® (Adobe Systems Inc., San Jose, CA).

Graphical and Statistical Analysis – All graphing analyses were completed using Microsoft Excel (Microsoft, Redmond, WA). Statistical analysis (Student's paired t-test) was conducted with GraphPad Prism (GraphPad Software, Inc., San Diego, CA). P-values were denoted as follows: p-value $\leq$ 0.05 = *, p-value $\leq$ 0.01 = **, and p-value > 0.05 was not significant (ns).

3.4   RESULTS

3.4.1 Low dose TLO causes plasma membrane permeability and breakdown that is NLRP3-dependent

Our previous study showed that a low TLO dose (1.8nM) induced NLRP3 inflammasome-dependent secretion of mature IL-1β, while a high dose (18.3nM) caused passive release of

inactive proteins from LPS-primed BMDM. Since that study was conducted over a relatively short time period (30 min), we wanted to further characterize the state of these LPS-primed BMDM over longer time points. To first assess membrane permeability, a two-color viability dye flow cytometry assay was employed. LPS-primed BMDM were control- or TLO-treated for various times and stained with calcein-AM, which is cleaved to a fluorescent form and retained only in viable cells, and ethidium homodimer-1 (EthD-1), which enters plasma membrane-compromised cells and fluorescently labels DNA. As shown in Figure 3-2A, control cells are predominantly intact up to 4h with the majority falling into the calcein-AM-positive cell gate. In comparison, 18.3nM TLO-treated BMDM are rapidly permeabilized up to 4h, allowing bright EthD-1 staining. Treatment with 1.8nM TLO also causes rapid permeabilization as evidenced by strong EthD-1 staining at 5min, but a percentage of this population recovered from plasma membrane damage as shown by a shift of cells to the calcein-AM-positive cell gate from the EthD-1-positive cell gate at 30min and onward. Lactate dehydrogenase (LDH) release was also used as a measure of membrane permeability and breakdown. Both 1.8nM and 18.3nM TLO induced LDH release with a higher percentage of LDH release for the high TLO dose compared to the low one (Figure 3-2B). Taken together, these results suggest that the high dose of TLO causes cell death of the entire cell population compared to the low dose of TLO that kills a percentage of the exposed cells, while a portion recover from initial cell damage.

Passive spilling of LDH suggests a necrotic cell death program. Since other second stimuli of the NLRP3 inflammasome have been shown to induce NLRP3-dependent necrotic cell death in monocytes and macrophages, we assessed if TLO-induced cell death was also dependent on NLRP3. Using LDH release as a readout, the magnitude of cell death was compared for wild type (WT) and NLRP3 knockout (KO) BMDM exposed to a low and a high dose of TLO. A

high dose (18.3nM) of TLO induced large amounts of LDH release with equivalent levels for WT and NLRP3 KO BMDM (Figure 3-2C). However, 1.8nM TLO only elicited LDH release from WT BMDM while BMDM lacking NLRP3 released levels of LDH that were comparable to control background levels. These data suggest that NLRP3 plays a role in the cell death program initiated in LPS-primed BMDM by the low dose of TLO.
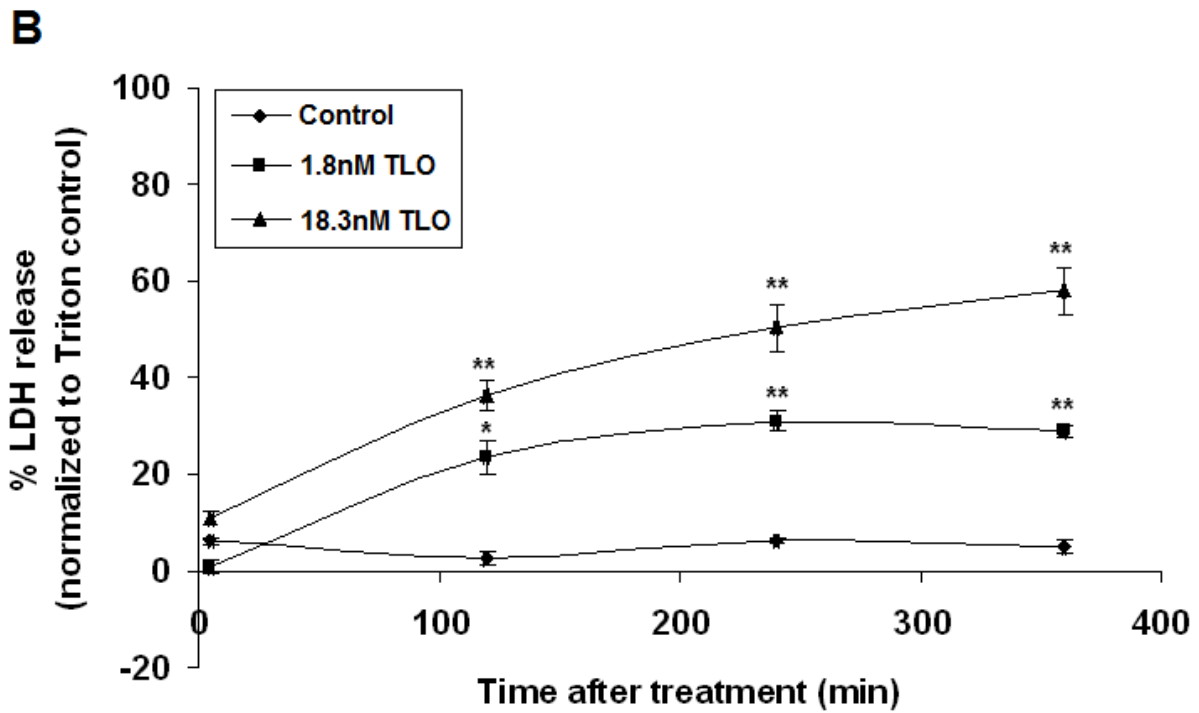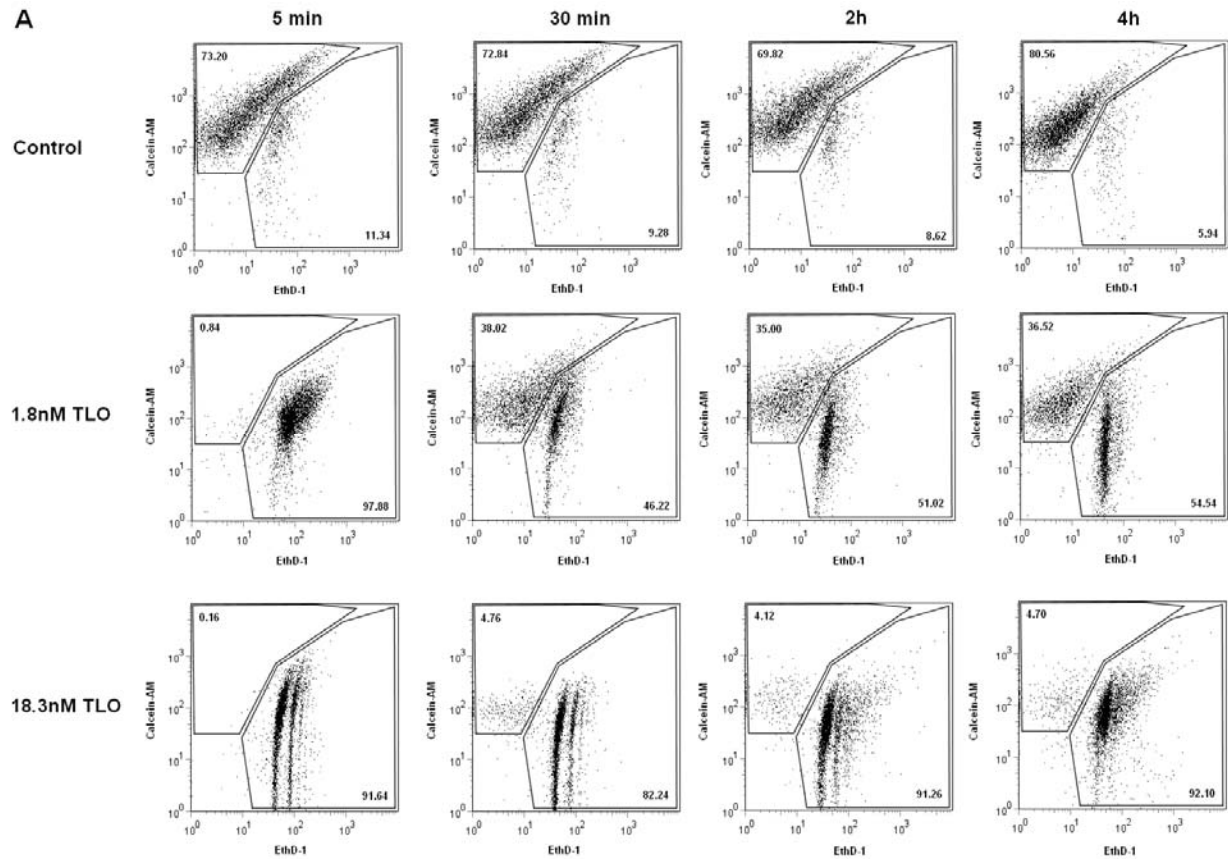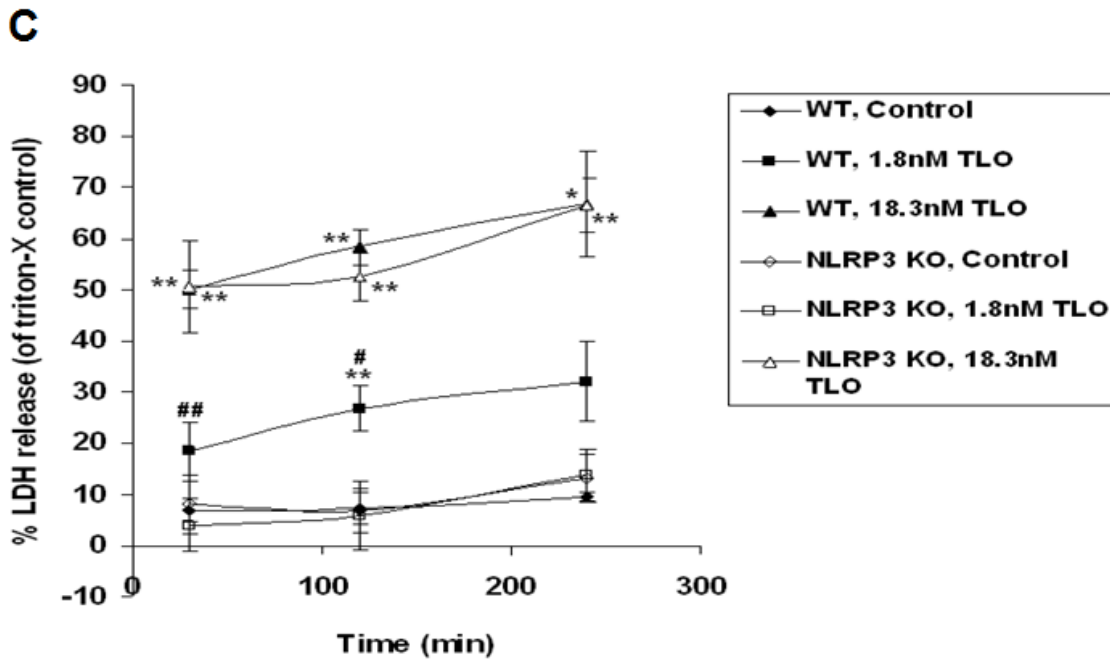
Figure 3-2: Low dose TLO induces membrane permeability and breakdown in LPS-primed BMDM that is NLRP3-dependent.

(A) Four-hour LPS-primed BMDM were treated with control buffer, 1.8nM TLO, or 18.3nM TLO for 5min – 4hr. Cells were then harvested and stained with calcein-AM and ethidium homodimer-2 (EthD-1) followed by flow cytometry analysis. Control-treated cells mostly fall into the calcein-AM (+) gate at all time points tested while 18.3nM TLO-treated cells fall mainly in the EthD-1(+) cell gate over time. 1.8nM TLO-treated BMDM initially stain EthD-1 (+) at 5min post-treatment, but a portion of the cells shift to the calcein-AM (+) gate at the later time points. This data is one representative example of three independent experiments. (B) Four-hour LPS-primed BMDM were treated with control buffer, 1.8nM TLO, or 18.3nM TLO up to 6hr. LDH release was assessed and normalized to the maximal amount of LDH released after 1% Triton X-100 treatment. TLO induced LDH release in a dose- and time-dependent manner. Data represents mean +/- SEM for 3 independent experiments. Student's paired t-test was applied for comparison of control versus TLO conditions; * = p≤ 0.05, ** = p≤ 0.01. (C) Four-hour LPS-primed WT or NLRP3 KO BMDM were treated with control buffer, 1.8nM TLO, or 18.3nM TLO up to 4hr. LDH release was assessed as in (B). TLO-induced LDH release was dependent on NLRP3 at the lower dose of TLO tested. Data represents mean +/- SEM for 3 independent experiments. Student's paired t-test was applied for

comparison of control versus TLO conditions (* = p≤ 0.05, ** = p≤ 0.01) or WT vs. NLRP3 KO BMDM (# = p≤ 0.05, ## = p≤ 0.01).

3.4.2 Low or high dose TLO induces the release of HMGB1 from BMDM

Several groups have recently shown that NLRP3-dependent necrotic cell death is characterized by the release of high mobility group box 1 (HMGB1) protein, which is a well known marker of necrotic cell death in general. Release of HMGB1 into supernatants of LPS-primed BMDM treated with a low and high dose of TLO was tested. Both the high and low dose of toxin caused the release of HMGB1, as did NLRP3 inflammasome stimulators nigericin and ATP (though to a lesser degree) (Figure 3-3). As a control, LPS-primed BMDM were treated with purified water to cause necrosis and, as expected, HMGB1 was released. These results confirm that TLO induces some form of necrotic cell death in LPS-primed BMDM.
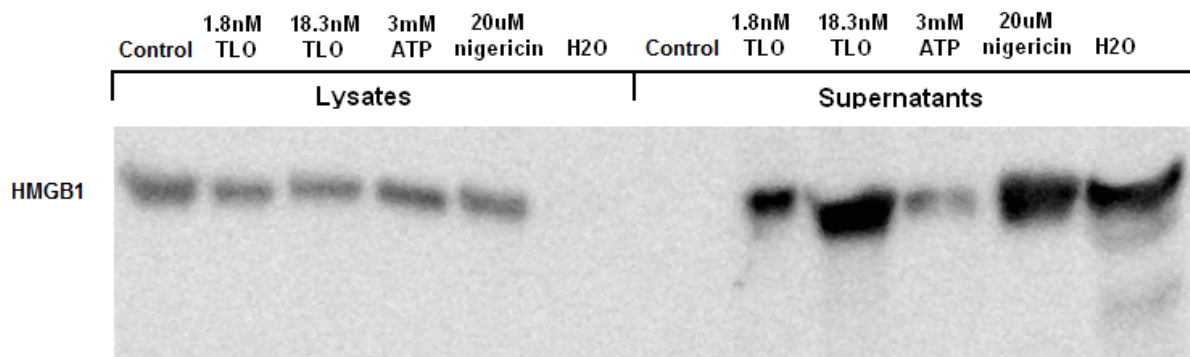
Figure 3-3: TLO induces HMGB1 release from LPS-primed BMDM.

Four-hour LPS-primed BMDM were treated with control buffer, 1.8nM TLO, 18.3nM TLO, 3mM ATP, 20μM nigericin, or purified water for 30min. 20μg of whole cell protein lysate or entire 1ml TCA/cholic acid precipitated supernatants were run on an SDS-PAGE gel and western blot conducted for HMGB1 (25kDa). All stimulators

except for the control induced HMGB1 release into cell supernatants. This data is a representative example of three independent experiments.

3.4.3 Low dose TLO-induced HMGB1 release is dependent on LPS priming and the activities of NLRP3, caspase-1, and cathepsin B

TLR priming of macrophages is a critical first step to license the NLRP3 inflammasome in terms of the upregulation of NLRP3 expression. It might be expected then that TLR stimulation (i.e. LPS priming) would be important for TLO-induced, NLRP3-dependent cell death. To test this, we stimulated BMDM that were either not primed or LPS primed with 1.8nM or 18.3nM TLO and probed for HMGB1 in supernatants. LPS priming was required for HMGB1 release induced by the low 1.8nM TLO dose, but not the high 18.3nM TLO dose (Figure 3-4A). It was also notable that LPS priming alone (LPS plus control buffer), did not result in any HMGB1 release. To visualize the localization of HMGB1 after 4 hours of LPS priming, fixed cell immunofluorescence microscopy was conducted. It can be seen in Figure 3-4B that cells exposed to media only retain HMGB1 in the nucleus. Interestingly, HMGB1 also localizes to the nucleus after 4 hours of LPS stimulation. This would suggest that a pathway initiated by TLO is responsible for the release of HMGB1 rather than LPS by itself.
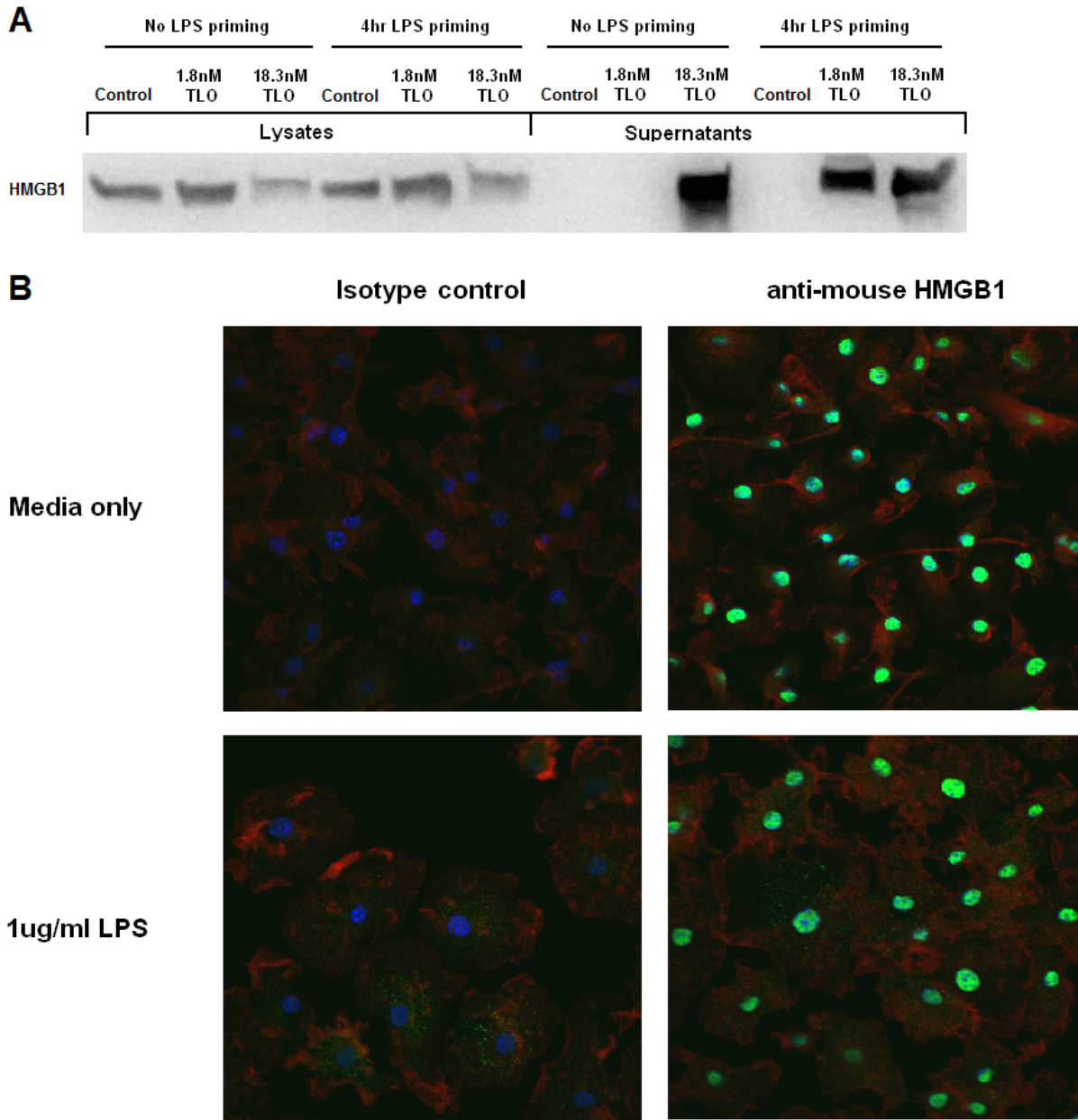
Figure 3-4: LPS priming is critical for low dose TLO-induced HMGB1 release.

(A) BMDM were left alone or LPS primed for 4 hours followed by treatment with control buffer, 1.8nM TLO, or 18.3nM TLO for 30min. 20μg of whole cell protein lysate or entire 1ml TCA/cholic acid precipitated supernatants were run on an SDS-PAGE gel and western blot conducted for HMGB1 (25kDa). LPS priming is required for the release of HMGB1 into supernatants after exposure to the low dose of TLO. This data is a representative example of multiple independent experiments. (B) BMDM were left alone or LPS primed for 4 hours. They were then fixed, permeabilized, and stained with rabbit anti-mouse HMGB1 or rabbit IgG isotype control and then goat anti-

rabbit Alexa Fluor® 488 (green), rhodamine-phalloidin (red) to label actin, and Hoescht stain (blue) to label the nucleus. Localization patterns were visualized with fixed cell fluorescence microscopy. HMGB1 co-localizes to the nucleus when exposed to media only or 1μg/ml LPS over 4 hours. Data are one representative example of two independent experiments.

To further characterize the role of NLRP3 and other inflammasome pathway components in TLO-induced cell death, we assessed HMGB1 release from WT BMDM in comparison to that released from NLRP3 KO BMDM or WT BMDM pre-treated with pharmacological inhibitors of caspase-1 (Ac-YVAD-cmk) or cathepsin B (CA-074-Me). HMGB1 release was abrogated in low dose TLO-exposed NLRP3 KO BMDM (Figure 3-5A), caspase-1-inhibited WT BMDM (Figure 3-5B), and cathepsin B-inhibited WT BMDM (Figure 3-5C). NLRP3 and caspase-1 only played a minimal role, if any, in HMGB1 induced by the high TLO dose. These results support a role for the NLRP3 inflammasome (NLRP3 and caspase-1) and cathepsin B in low dose TLO-induced HMGB1 release.
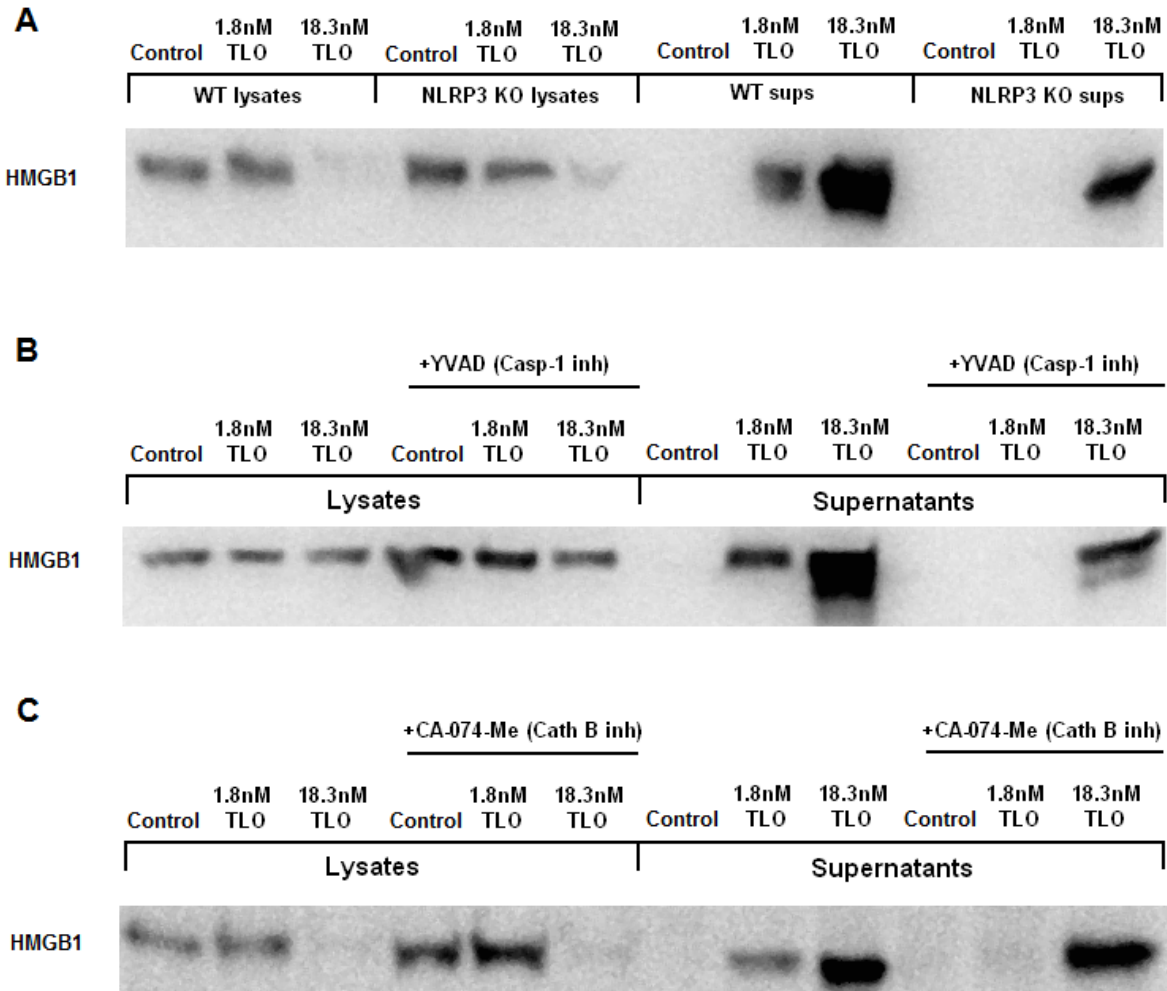
Figure 3-5: Low dose TLO-induced HMGB1 release is dependent on NLRP3, caspase-1, and cathepsin B. Four-hour LPS-primed BMDM were treated with control buffer, 1.8nM TLO, or 18.3nM TLO for 30min. 20μg of whole cell protein lysate or entire 1ml TCA/cholic acid precipitated supernatants were run on an SDS-PAGE gel and western blot conducted for HMGB1 (25kDa). HMGB1 release was compared for WT vs. NLRP3 KO BMDM (A), WT BMDM treated with no inhibitor vs. caspase-1 inhibitor Ac-YVAD-cmk (B), or WT BMDM treated with no inhibitor vs. cathepsin B inhibitor CA-074-Me (C). HMGB1 release into supernatants is dependent on NLRP3, caspase-1, and cathepsin B for the low dose of TLO. Data are single representative examples of multiple independent experiments.

3.4.4 HMGB1 translocates from the nucleus to the cytoplasm after exposure to low dose TLO and its release depends on NLRP3 activity

Since 4 hours of LPS priming did not cause HMGB1 to re-localize from the nucleus to the cytoplasm or to be released from the cell (Figure 3-4B), we wanted to explore the role that TLO had on the localization pattern of HMGB1 in the cell. Additionally, the role of NLRP3 in this localization process was assessed by comparing WT to NLRP3 KO BMDM. Since TLO-induced HMGB1 release is observed from BMDM by 30 min post-treatment with TLO, a shorter time course was conducted in order to track the localization of intracellular HMGB1. It can be observed at 0 min, before low dose TLO addition, that HMGB1 is localized to the nucleus both in WT and NLRP3 KO BMDM (Figure 3-6A). This pattern remains 5 min after TLO addition, but at 15 min the HMGB1 distribution pattern changes. Zoomed images of the 15 min time point (Figure 3-6B) show that HMGB1 translocates from the nucleus to the cytoplasm both in the WT and NLRP3 KO BMDM. Additionally, some of the HMGB1 staining appears punctate especially in the NLRP3 KO BMDM. By 30 min post-TLO treatment, some of the WT BMDM lack HMGB1 staining while the majority of the NLRP3 KO BMDM show HMGB1 localized to the nucleus again (Figure 3-6A). This data would suggest that NLRP3 plays a role in the release of HMGB1 from BMDM.

A

WT BMDM

NLRP3 KO BMDM

0 min

5 min

15 min

30 min

B

WT BMDM
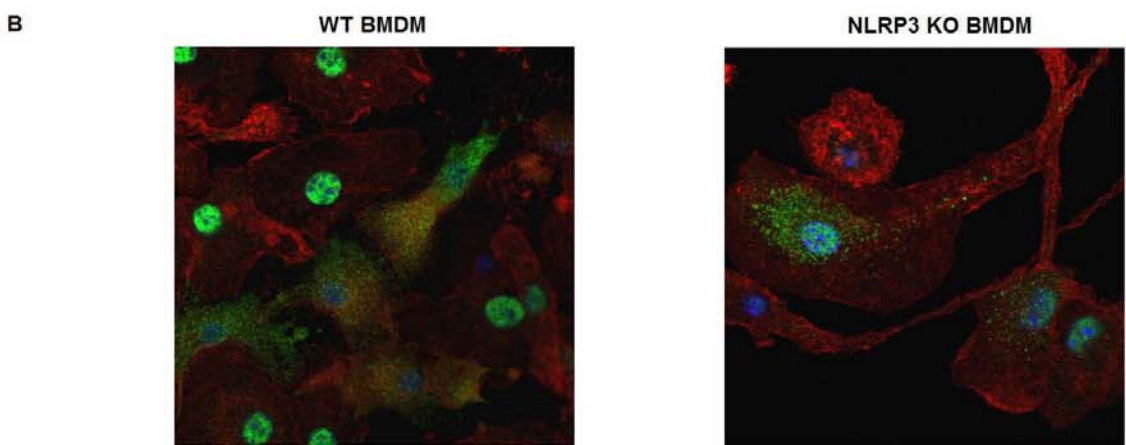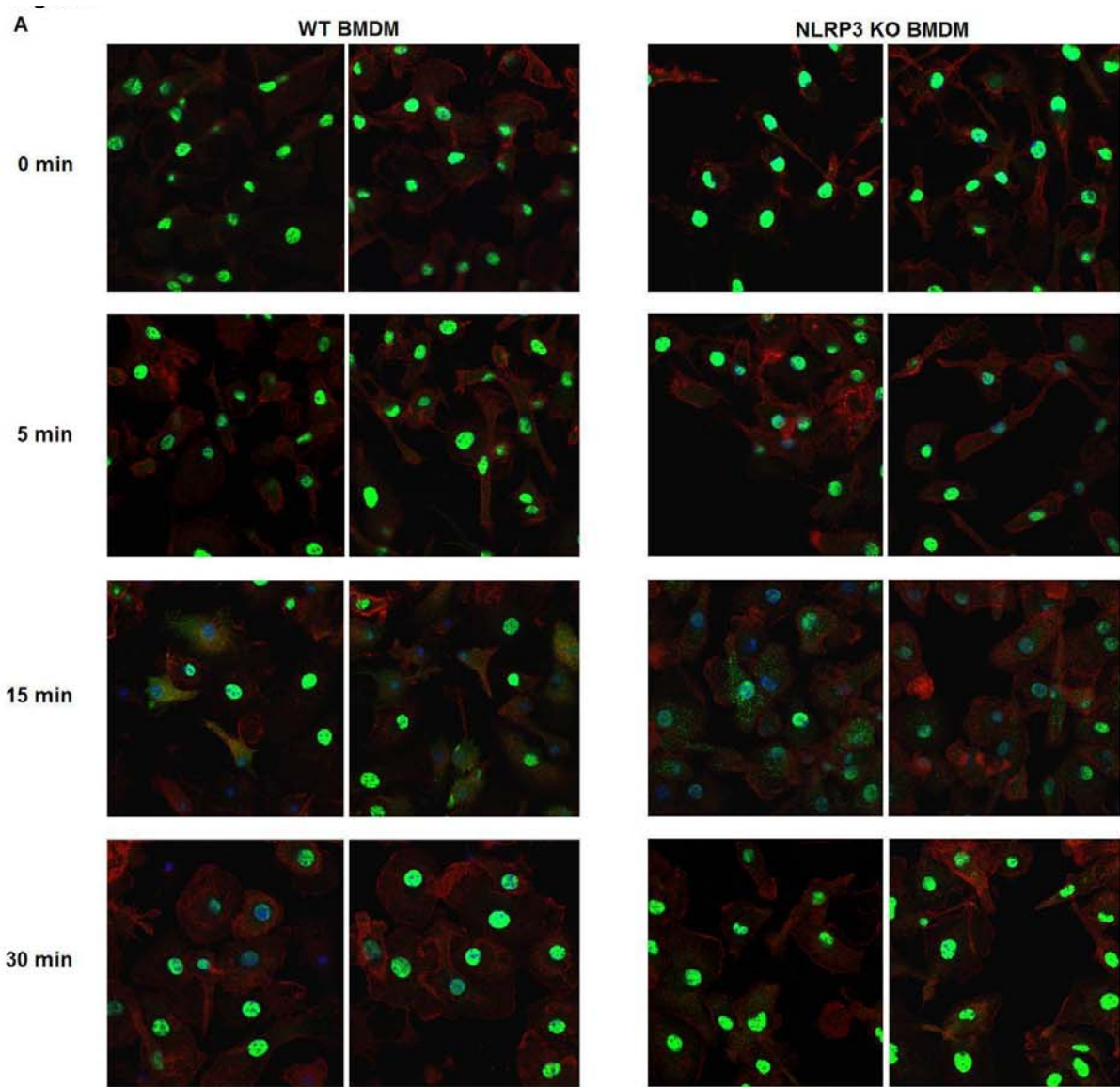
NLRP3 KO BMDM

Figure 3-6: HMGB1 translocates from the nucleus to the cytoplasm after low dose TLO stimulation.

(A) Four-hour LPS-primed WT or NLRP3 KO BMDM were left untreated (0min) or treated with 1.8nM TLO for 5-30min. Cells were then fixed, permeabilized, and stained with rabbit anti-mouse HMGB1 or rabbit IgG isotype control and then goat anti-rabbit Alexa Fluor® 488 (green), rhodamine-phalloidin (red) to label actin, and Hoescht stain (blue) to label the nucleus. Localization patterns were visualized with fixed cell fluorescence microscopy. Two fields of view are shown for each time point and cell type. At 0min and 5min, HMGB1 localizes to the nucleus in WT and NLRP3 KO BMDM. By 15min, HMGB1 localizes to the cytoplasm. Zoomed images show some punctate HMGB1 staining in both WT and NLRP3 KO BMDM (B). Finally, at 30min, some WT BMDM lack HMGB1 staining while others exhibit nuclear HMGB1. Most NLRP3 KO BMDM show nuclear HMGB1.

3.5   DISCUSSION

We have shown here that both low and high doses of TLO induce membrane permeabilization and membrane damage in LPS-primed BMDM, which is characterized by LDH and HMGB1 release. In particular, the low dose of TLO causes NLRP3-dependent LDH release and HMGB1 release. HMGB1 release is also dependent on LPS priming and the activities of caspase-1 and cathepsin B. Since HMGB1 is a common marker for necrotic cell death (Scaffidi *et al.*, 2002) and TLO induces HMGB1 from BMDM, this would suggest that these cells are undergoing some form of necrotic cell death. In the case of the high dose of TLO, BMDM passively release LDH and HMGB1 in a manner independent of NLRP3 inflammasome components, which would support a role for classical necrotic cell death rather than the specialized form of pyronecrotic cell death that relies on the activities of cathepsin B and NLRP3 (Willingham *et al.*, 2007; Willingham *et al.*, 2009). On the other hand, the low dose of TLO brings about a form of necrotic cell death that is dependent on cathepsin B and NLRP3. However, this cell death

program cannot be characterized as pyronecrosis either since caspase-1 activity plays a role. It should be noted that low dose TLO-induced cell death is also different from pyroptosis (Bergsbaken *et al.*, 2009), which relies on caspase-1 activity, but not cathepsin B activity and has not been linked to HMGB1 release. We believe that different NLRP3 inflammasome stimuli bring about distinct types of cell death that may share some, but not necessarily all of the same characteristics. Our data supports a model of necrotic cell death initiated by a low dose of TLO that is characterized by HMGB1 release that is dependent on the NLRP3 inflammasome (including NLRP3 and caspase-1) and cathepsin B activity. This is the first report to demonstrate a role for the caspase-1-containing NLRP3 inflammasome and cathepsin B in BMDM cell death caused by a pore-forming toxin.

As opposed to prior studies assessing cell death pathways using only purified CDC (Srivastava *et al.*, 2005), BMDM in our studies were first LPS primed before exposure to TLO. We found that LPS priming was essential for low dose TLO-induced release of HMGB1 from BMDM. TLR priming has been shown to license the NLRP3 inflammasome by causing the upregulation of NLRP3 expression (Bauernfeind *et al.*, 2009). Additionally, this priming step is required for the translocation of adaptor ASC from the nucleus to the cytoplasm where it can bridge NLRP3 and caspase-1 to form an inflammasome complex (Bryan *et al.*, 2009). This may explain our findings of the requirement for TLR priming since we also found a significant role for the NLRP3 inflammasome in low dose TLO-induced HMGB1 release. Many groups have previously found that LPS alone can induce HMGB1 secretion from monocytes and macrophages after 8-18 hours of stimulation (Wang *et al.*, 1999; Gardella *et al.*, 2002; Chen *et al.*, 2004). Moreover, LPS initiates the re-localization of HMGB1 from the nucleus to cytoplasmic vesicles (Gardella *et al.*, 2002; Liu *et al.*, 2006). In comparison, when we stimulate

murine macrophages with LPS, we do not see HMGB1 translocation from the nucleus nor do we observe HMGB1 externalization from the cells. However, these discrepancies may be explained by the kinetics of the experiments used in each study. In our experiments, the time of LPS stimulation is limited to 4 hours while previous studies have demonstrated HMGB1 localization and release after longer time points. According to Wang, *et al.* (Wang *et al.*, 1999), accumulated HMGB1 release from LPS-stimulated macrophage cultures is not detectable until 8 hours after stimulation. Additionally, they showed that in *in vivo* models of endotoxemia, where mice are administered LPS, serum HMGB1 levels do not increase until 12-18 hours post-LPS treatment, which is much later than other cytokines like TNF and IL-1 that reach peak levels by 2 hours and 4-6 hours, respectively. Thus, the lack of HMGB1 secretion after 4 hours of LPS stimulation may be explained by the short exposure period, but nevertheless is required for HMGB1 release induced by TLO.

It is well accepted that during necrotic cell death, membrane breakdown enables passive diffusion of HMGB1 from the nucleus to the external environment (Gauley & Pisetsky, 2009). However, the pathway(s) that govern HMGB1 translocation from the nucleus to the cytoplasm before active secretion are not well understood. First, the movement of HMGB1 from the nucleus to the cytoplasm is the hyperacetylation of HMGB1 on many of its 43 lysine residues (Bonaldi *et al.*, 2003). It is unknown what occurs downstream of cellular activation to bring about HMGB1 hyperacetylation. Second, once HMGB1 is out of the nucleus, it must enter the cytoplasm or compartments within the cytoplasm. After 18 hours of LPS stimulation, HMGB1 has been observed to re-localize from the nucleus to cytoplasmic Lamp-1+EEA-1-endolysosomes in primary human monocytes (Gardella *et al.*, 2002). In another study, a Caco-2 enterocyte cell line stimulated with a mix of IFN-γ, IL-1β, and TNF over 24h showed HMGB1

localization to multivesicular bodies (Liu *et al.*, 2006). Third and last, HMGB1 must be externalized to the extracellular environment. Data on mechanisms of HMGB1 secretion is limited, but one such mechanism has been suggested in the above Caco-2 study where HMGB1 was found to be associated with exosomes. It cannot be excluded that other mechanisms are also responsible for the active secretion of HMGB1.

In our study, we observe HMGB1 relocalization from the nucleus to the cytoplasm within 15 minutes post-treatment with the low dose of TLO. The punctate staining of HMGB1 in the cytoplasm suggests localization to vesicular compartments, but additional study will be required to test this hypothesis. Up to this point, the localization pattern of HMGB1 is similar in both the WT and NLRP3 KO BMDM. However, by 30 minutes post-TLO treatment, HMGB1 relocalizes to the nucleus for most of the NLRP3 KO BMDM and some of the WT BMDM. However, a portion of the WT BMDM lack strong HMGB1 staining in the nucleus or cytoplasm, suggesting HMGB1 release from the cells. These results are in line with the western blotting data showing that low dose TLO-induced HMGB1 release occurs for WT, but not NLRP3 KO BMDM. Furthermore, these findings implicate NLRP3 in the process for HMGB1 to exit the cell. It is possible that NLRP3 plays an active role in shuttling HMGB1 out of the cells once it is in the cytoplasm or cytoplasmic vesicles by some unknown mechanism. However, given that we found a role for NLRP3 in causing LDH release, it may be more likely that NLRP3 mediates a slower breakdown of cellular structures (compared to the NLRP3-independent rapid necrosis initiated by a high dose of TLO) such that LDH and HMGB1 can diffuse out. Further study is needed to determine the exact role that NLRP3 is playing to allow HMGB1 release after exposure to lower doses of TLO.

In summary, we have shown that TLO, a pore-forming toxin from the cholesterol-dependent cytolysin (CDC) family, initiates different cell death programs in LPS-primed murine macrophages based on dosage. A high dose of toxin leads to rapid necrotic cell death characterized by passive release of LDH and HMGB1. On the other hand, a low dose of toxin causes a necrotic cell death program characterized by NLRP3-dependent LDH release and HMGB1 release that is regulated by NLRP3, caspase-1, and cathepsin B activities. This is the first study to find a role for both caspase-1 and cathepsin B in BMDM cell death initiated by a NLRP3 inflammasome stimulator, to visualize HMGB1 localization in cells expressing or lacking NLRP3, and to identify a member of the CDC family as an inducer of HMGB1 release and a novel cell death pathway. The findings of these studies contribute to the understanding of how HMGB1 release is regulated, which could be useful for the development of therapeutics aimed to control HMGB1 release into the extracellular environment. This would be important given that HMGB1 contributes to many inflammatory diseases. Additionally, understanding how innate immune cells sense and respond to bacterial virulence factors such as CDC could be useful in understanding both bacterial pathogenesis as well as subsequent host responses.

3.6   ACKNOWLEDGEMENTS

4.0 EXPLORING THE ROLE OF P2X7 ACTIVATION IN THE POTENTIATION OF CHOLESTEROL-DEPENDENT CYTOLYSIN-INDUCED PORE FORMATION

4.1 HYPOTHESIS

We generated a toxin-resistant variant of a myeloid cell line that while able to bind toxin, was inefficiently perforated, with reduced adenosine triphosphate (ATP) release. Diminished sensitivity to exogenous ATP was also observed in the variant and was associated with decreased expression of purinergic receptor $P2X_7$, known to initiate pannexin-1-mediated pore formation. Pharmacologic inhibition of ATP or $P2X_7$ reduced toxin-induced functional pore formation in the parental cell line. These data implicate ATP release and $P2X_7$ activation as important components in the response of myeloid cells to CDC toxins, with potential roles in the potentiation of toxicity during Gram-positive bacterial infection. We hypothesize that CDC-induced pore formation is potentiated by the activities of ATP and $P2X_7$.

4.2 INTRODUCTION

The cholesterol-dependent cytolysin (CDC) family of exotoxins plays an important role in bacterial pathogenesis. Expressed by more than twenty species of gram-positive bacteria (Billington *et al.*, 2000; Palmer, 2001), CDC confer virulence to the bacteria that secrete them.

Such examples are *Bacillus anthracis* anthrolysin O (ALO) (Shannon *et al.*, 2003), *Clostridium tetani* tetanolysin O (TLO) (Mitsui *et al.*, 1982), *Streptococcus pyogenes* streptolysin O (SLO) (Herbert & Todd, 1941; Bernheimer, 1948), and *Streptococcus pneumoniae* pneumolysin (PLY) (Shumway & Klebanoff, 1971; Johnson *et al.*, 1980). In mice infected with bacteria expressing non-active forms of CDC toxins, survival is enhanced relative to mice infected with bacteria expressing wild type toxin. Direct toxicity of several CDC family members has been shown *in vivo* (Berry *et al.*, 1989; Paton *et al.*, 1993; Benton *et al.*, 1995; Berry *et al.*, 1995; Paton, 1996), and intravenous injection of 100 pmol of purified forms of several different CDC into mice was shown to cause almost immediate death (Watanabe *et al.*, 2006).

How CDC toxins bind to cells is generally well understood. Interaction with cholesterol typically mediates attachment to the plasma membrane (Billington *et al.*, 2000; Palmer, 2001), although the CDC family member intermedilysin (ILY) binds exclusively to human CD59 (Giddings *et al.*, 2004; Polekhina *et al.*, 2005; Soltani *et al.*, 2007), a late stage complement inhibitor on mammalian cells. After binding to cholesterol in a lipid bilayer, CDC monomers undergo a conformational change from a soluble to hydrophobic form followed by oligomerization of monomers into a pre-pore complex and then membrane insertion for final pore conversion (Tweten, 2005; Cocklin *et al.*, 2006). Between 40 and 80 monomers assemble to form a full-sized pore up to 30nm in size, but in some cases incomplete pores or arcs are formed particularly at low concentrations of toxin monomers (Billington *et al.*, 2000). Each monomer contains four domains that mediate assembly and pore formation. Domain four, which contains a conserved undecapeptide sequence, is important for binding to cholesterol, while regions of other domains participate in oligomerization. It should be noted that ALO and several other CDC have also been shown to stimulate rapid IκBα degradation and p38 MAPK

phosphorylation in mouse macrophages, which was associated with increased transcription of IL-1β, IL-6, and TNF-α genes and later apoptotic death (Malley *et al.*, 2003; Park *et al.*, 2004a; Ito *et al.*, 2005). The signaling pathway was shown to involve a TLR4-dependent pathway that was independent of toxin lytic activity. In fact, CDC have been shown to bind directly to TLR4 (Srivastava *et al.*, 2005).

Formation of pores in the plasma membrane leads to disruption in osmotic balance and if left unrepaired, ultimately cell death. The lethal effects of CDC on cells can be demonstrated using assays measuring uptake of fluorescent or colorimetric dyes by exposed cells (Mosser & Rest, 2006). This has revealed large differences in susceptibility of different cells to these toxins that cannot be readily explained by minor differences in cellular cholesterol content, which is relatively constant between cell types. Since CDC-perforated cells are capable of resealing their pores (Walev *et al.*, 2001b; Husmann *et al.*, 2006; Idone *et al.*, 2008), it is possible that differences in pore-resealing machinery are responsible for resistance or susceptibility of cells to these toxins. This has not yet been demonstrated however. It is also possible that pores formed by CDC might cause release of soluble factors that could act in an autocrine or paracrine fashion to trigger cellular responses, leading to death.

Using a previously described cell line (FSDC) (Girolomoni *et al.*, 1995) derived from fetal mouse skin with myeloid dendritic cell properties, we generated a toxin-resistant cell line by selection with increasing concentrations of CDC family member TLO. We used this variant cell line to identify a potential role for ATP and its purinergic receptor $P2X_7$ in CDC-induced pore formation. CDC may utilize this endogenous $P2X_7$ pathway in order to bring about rapid cell death at the site of bacterial infection. Studies were also conducted with primary cells or cell lines manipulated to express or lack $P2X_7$ in order to define its role in CDC-induced perforation.

97

4.3   MATERIALS AND METHODS

Toxins – Anthrolysin O (ALO) was generated as described (Shannon *et al.*, 2003). Tetanolysin (TLO) was obtained from Biomol International (Plymouth Meeting, PA). Toxins were reduced with 10mM DTT (Sigma, St. Louis, MO) for 10min, 37°C before use unless indicated. Untreated control samples were incubated in the same buffer lacking toxin. For reference, TLO has a molecular weight of 55kDa, so 1000ng/ml is equivalent to 18.3nM.

Cell culture – The mouse fetal skin-derived dendritic cell line (FSDC) (from Dr. Paola Ricciardi-Castagnoli, Milan) (Girolomoni *et al.*, 1995) was cultured in IMDM (Lonza Inc, Walkersville, MD) supplemented with 10% Gemcell™ FBS (Gemini Bio-Products, West Sacramento, CA), 2mM L-glutamine, and 500U Penicillin/500μg Streptomycin (Lonza Inc.). FSDC were harvested from flasks using CellStripper™ (Mediatech, Inc, Herndon, VA). Bone marrow-derived macrophages were created from femurs and tibiae from wild type (gifts from Lisa Borghesi) and $P2X_7$-/- (gifts from George Dubyak, Case Western Reserve University) C57BL/6 mice using the protocol discussed in section 2.4.

TLO-resistant and ATP-resistant variant selection process – Wild type FSDC were washed with HBSS plus Ca^{2+}/Mg^{2+} (Mediatech, Inc), treated with TLO for 1-2hr, 37°C in HBSS, washed, and cultured in fresh IMDM. Cells were selected at bi-weekly intervals in 18.3nM, 36.4nM, 72.7nM, and 109.1nM TLO successively. After the final selection, limiting dilution cloning was performed and single colonies tested for resistance to TLO-induced dye uptake. Clone 4 was selected from several resistant clones for subsequent use and thereafter called TLO-resistant FSDC (TLO-r). A similar protocol was conducted for the generation of ATP-resistant D2SC-1 (abbreviated D2) cells except that cells were treated with increasing concentrations of ATP (3mM, 6mM, 6mM, 12mM, 15mM, 15mM, and 20mM) over time. Each treatment was

98

administered for 1hr, 37°C in DMEM media supplemented with 10% Gemcell™ FBS, 2mM L-glutamine, and 500U Penicillin/500μg Streptomycin (Lonza Inc.). Cells were then washed, cultured in fresh DMEM, and grown to confluency before the next selection. After the final selection, limiting dilution cloning was performed and single colonies tested for P2X$_7$ expression via western blot and flow cytometry. A final clone called D2-C1 was selected and used for experiments.

Cloning and construction of cDNA encoding the mouse P2X$_7$ receptor and mouse pannexin-1 – Total RNA was extracted and purified from FSDC cells using an RNeasy Mini Kit and RNase-Free DNase Set, as recommended by the manufacturer (QIAGEN, Valencia, CA). MuLV Reverse Transcriptase (Applied Biosystems, Foster City, CA) was used to synthesize first strand cDNA with an oligo-dT$_{16-18}$ primer (Invitrogen, Carlsbad, CA) from 1μg of the purified total RNA at 42°C for 60 min. For mouse P2X$_7$, a pair of the sequence specific primers with XhoI or EcoRI sites, respectively, were designed based on the published mouse P2X$_7$ cDNA sequence (GenBank accession number NM_011027) to amplify the entire coding sequence of the mouse P2X7 subunit by PCR. The primers were as follows: forward primer, 5'-AGCCTCGAGCCATGCCGGCTTGCTGCAGCT-3'; reverse primer, 5'-CAGCGAATTCATCAGTAGGGATACTTGAAGCCACT-3'. AmpliTaq® DNA polymerase was used for amplification as described by the manufacturer (Applied Biosystems, Foster City, CA). The cycling reaction was modified as 1cycle of 95°C for 2 min, 35 cycles of 95°C for 1 min, 62.6°C for 1min, 72°C for 3 min, with a final extension at 72°C for 10 min. PCR products were separated in a 1% agarose gel containing 1ug/ml ethidium bromide (Sigma, Saint Louis, MO) and purified with the Wizard® SV Gel and PCR Clean-Up System (Promega, Madison, WI). The purified PCR products were then cloned into the pGEM®-T vector (Promega, Madison,

99

WI). The screened clones were identified by XhoI and EcoRI. The resulting clones were finally sequenced and analyzed using DNAStar software. The mouse $P2X_7$ fragment from the positive clones was fused with double flag epitopes at the N-terminals using semi-nested PCR and cloned into a p2CI vector or retroviral pFB/H$^+$ vector. The p2CI vector was derived from PCR2.1 by insertion of a cytomegalovirus promoter, PCR-amplified IRES-neomycin-resistant sequences from the pFB-Neo-LacZ vector, and poly(A) signal sequences from pcDNA3.1. The pFB/H$^+$ vector was modified from a retroviral pFB/neo vector by replacement of a neomycin-resistant gene with a hygromycin-resistant gene. Primers with sequences of the flag epitope were designed based on the corresponding sequences from the pCMV-Tag 1 vector (Stratagene, La Jolla, CA). The Expand high fidelity PCR system (Roche Applied Science, Indianapolis, IN, USA) was used for all the PCR reactions. The final PCR amplicons were cloned into the p2CI vector or pFB/H$^+$ vector using the appropriate restriction enzymes and the Rapid DNA ligation Kit (Roche Applied Science, Indianapolis, IN, USA).

For mouse pannexin-1, a pair of the sequence specific primers with NotI or EcoRI sites, respectively, were designed based on the published mouse pannexin-1 cDNA sequence (GenBank accession number NM_019482) to amplify the entire coding sequence of mouse pannexin-1 by PCR. The primers were as follows: forward primer, 5'- TTAATT<u>GCGGCCGC</u>CTTGACCATGGCCATCGCCCACTTGG -3'; reverse primer, 5'- TGTGG<u>GAATTC</u>GTGGGATCCTCATTAGCAGGACGGATTCAG -3'. The above AmpliTaq$^®$ DNA polymerase was used for amplification. The cycling reaction was modified as 1 cycle of 95°C for 2 min, 35 cycles of 95°C for 1 min, 64.4^{o}C for 1min, 72°C for 3 min, with a final extension at 72°C for 10 min. The PCR-amplified pannexin-1 fragment was cloned into a retroviral pFB/neo vector with NotI and EcoRI. Pannexin-1 fused with an HA tag at its C-

terminals was generated by semi-nested PCR and cloned into the pFB/neo vector. Detailed plasmid maps and sequences of primers are available upon request. All of the mutants and corresponding sequences subcloned into vectors were verified by DNA sequencing.

Transfection and transduction – HEK-293, gp293, D2SC-1 (abbreviated D2), and NRK cells were grown in complete (DMEM). For transfection, HEK-293 cells were plated in six-well plates and transfected with mouse $P2X_7$ expression constructs using Lipofectamine™ LTX Reagent, as recommended by the manufacturer (Invitrogen, Carlsbad, CA). 2.5μg of DNA, 2.5μl of Plus™ reagent, and 6.25μl of Lipofectamine™ LTX Reagent in 500μl of Opti-MEM® I Reduced Serum Medium were used per well. The cells were selected with 1 mg/ml G418 for 3-5 weeks to generate stably transfected cell lines and maintained in 500μg/ml G418.

For making retroviruses, retrovirus-packaging gp293 cells were plated in 6-well plates for 1 day before co-transfection with retroviral constructs containing $P2X_7$ or Pannexin-1 and VSV-G vector using Lipofectamine™ LTX Reagent. 4μg of retroviral constructs, 2μg of VSV-G vector, 5μl of Plus™ reagent, and 10μl of Lipofectamine™ LTX Reagent in 500μl of Opti-MEM® I Reduced Serum Medium were used per well with 2 ml media. Then the plates were incubated at 37^oC for 4 hour, media replaced with 3ml of fresh media, and again incubated for 2-3 days. The media containing retroviruses was harvested, filtered, aliquoted, and stored at - 80^oC prior to transduction. For transduction, 3-4x10^5 D2SC-1 or NRK cells were plated in 12-well plates for a day before infection. Media was replaced with 1ml of retroviral preparation containing 3μg polybrene and cells were incubated for 1 day. Then, media was replaced with media containing selection drugs; hygromycin for mouse $P2X_7$ and G418 for mouse pannexin-1 to make stable cell lines. Expression of $P2X_7$ was assessed using surface staining with a monoclonal rat anti-mouse $P2X_7$ antibody (Axxora) and goat anti-rat-Cy5 secondary antibody

(Jackson ImmunoResearch Laboratories, Inc., West Grove, PA) followed by flow cytometry analysis, by permeabilization and staining for the HA tag followed by flow cytometry, or by western blotting analysis as described below (P2X$_7$ Western Blot section).

Cholesterol assay – Cells were washed with PBS (Ca^{2+}, Mg^{2+}-free), lysed with 1X reaction buffer, and 50µg of protein equivalent (determined by Bio-Rad Bradford assay) run for each of two replicates using the Amplex Red Cholesterol Assay Kit (Invitrogen). Samples were read at 570nm.

ATP bioluminescence assay – 6x10^5 FSDC/well were adhered to 12-well plates for 2hr, 37°C, PBS washed, and PBS control or TLO treated for 5min. 300µl supernatants were collected, cells were lysed with 300µl lysis buffer (Dojindo ATP kit, Gaithersburg, MD), and both were centrifuged 10000rpm, 10min, 4°C and assayed in duplicate using the ATP Determination Kit (Invitrogen). Each well was read immediately after D-luciferin injection using the Berthold Orion microplate luminometer and Simplicity 2.1 software.

Cell surface phenotyping – Cells were incubated with FITC –labeled anti-mouse I-A^b, I-A^d, CD40, CD11c, or CD86 (BD Biosciences Pharmingen). Flow cytometry analysis was conducted on a BD LSR II system with FACSDiva software (BD Biosciences) and Flow Jo (Tree Star, Inc., Ashland, OR).

Bacterial phagocytosis assay – E. Coli GFP (Salter *et al.*, 2004), grown in 100µg/ml ampicillin (Sigma) LB broth, was added to 2.5x10^5 FSDC/well for 1hr, 37°C. Bacterial uptake by cells was analyzed with flow cytometry. Plating dilutions were used to determine bacterial cell counts.

LDH release assay – 4.5x10^5 cells were plated/well of 12-well plates overnight. The next day, spent media was removed and cells were washed with PBS and incubated for 30 min with

DTT control buffer, various TLO concentrations, various doses of ATP, or 20μM nigericin in phenol red-free IMDM. TLO was pre-bound to cells for 5 min before addition of 10% FBS to all wells. 1% triton X-100 was used as a control of complete cell lysis and maximal LDH release. Supernatants were collected and assayed in duplicate for LDH content using the LDH Cytotoxicity Assay Kit from Cayman Chemical Company (Ann Arbor, MI). % cytotoxicity was calculated as a percentage of LDH release from experimental samples over total Triton X-100 LDH release, which was set to 100%.

Dye uptake pore assays – Flow cytometry: Cells were washed with PBS containing Ca^{2+} and Mg^{2+} (Lonza Inc.), an equivalent volume of cells (62.5μl, $2.5x10^5$) was incubated with toxin or ATP dilution in filtered 0.1% BSA (Sigma) (62.5μl), for indicated times at 37^oC. Cells were washed in PBS, stained with 5μM propidium iodide (Sigma), 5μM ethidium bromide (Sigma), 5μM YO-PRO-1 (Invitrogen), or 5μM DAPI and analyzed by flow cytometry. *Trypan blue staining on plates*: Cells plated at $3.0-4.0x10^5$/well of 12-well plates were PBS washed and exposed to 350μl toxin or ATP dilutions made in filtered 0.05% BSA for 2hr, 37^oC. Supernatants were removed, cells were stained with 5% trypan blue (Sigma), and >100 cells/well counted. For inhibition experiments: 15mM methyl-β-cyclodextrin (MβCD, Sigma) in serum-free IMDM was pre-incubated with cells for 30min; 0.6mM oxidized ATP (oATP, Sigma) was pre-incubated with cells for 2hr; and 24U/ml apyrase (Sigma) was added simultaneously with toxin or ATP.

P2X$_7$ Western Blot – Protein concentration of lysates was normalized with Bradford assay and lysates loaded onto SDS-PAGE. Following electrophoretic transfer, membranes were probed with 1:200 primary rabbit anti-mouse P2X$_7$ (Sigma), 1:5000 secondary donkey anti-

rabbit Ig-HRP (Biolegend), and proteins detected with ECL substrate (PerkinElmer Life Sciences). Blots were imaged with the KODAK Image Station 2000R.

Preparation of ELISA supernatants and IL-1β ELISA – See section 2.4.

Toxin-binding assays – Adsorption assay: This assay was adapted from (Duncan & Buckingham, 1978). 2.5×10^5 FSDC/well of a 12-well plate adhered for 2hr, 37°C were treated with serum-free IMDM or 15mM MβCD for 30min, 37°C. A TLO pore assay was carried out and supernatants were collected, centrifuged 10min, 1200xg, 4°C, and tested on THP-1 in a separate pore assay. As a control, cell-free wells were treated with toxin before application on THP-1 and this represents maximum toxin carryover. *TLO-Cy5 labeling and direct binding assay*: A monofunctional NHS-Ester Cy5 (GE Healthcare) vial was resuspended in 20μl DMSO and diluted 1:100. 10μg TLO (10μl) or 10μg BSA control (10μl) was labeled with 2μl of PBS (control) or 2μl of 1:100 Cy5 for 10min, RT, in the dark. To quench the reactions, 10μg of BSA was added and incubated 10min, RT, in the dark. Labeling reactions were used in flow cytometry binding and pore assays where Cy5 signal and YO-PRO-1 uptake were measured.

Live cell imaging of toxin-cell interactions – Live cell imaging was performed using a Nikon 2000E inverted microscope with a 60X 1.45 NA oil immersion optic, an ASI (Eugene, OR) Piezo driven XYZ stage, a Yogagawa spinning disk confocal head and Prairie Technology (Madison WI) laser bench. Images were collected using a Cascade II backthinned 512B camera (Photometrics, Tucson AZ). Cells were maintained at 37°C in the microscope with a PDMI2 stage (Harvard Scientific, Holliston MA). Software control of the microscope was with Metamorph 7.0, (Molecular Devices, Downingtown, PA). Cells were grown overnight in collagen-coated glass-bottomed #1.5 MatTek culture dishes (MatTek, Ashland, MA). Images

were collected every 10 sec both before and after addition of Cy5-labeled toxin. Data analysis was performed using Metamorph software.

Immunofluorescent staining of fixed cells – Cells were allowed to adhere on collagen-coated glass-bottomed MatTek culture dishes before washing with PBS and fixation using 2% paraformaldehyde, followed by permeabilization with 0.1% triton x-100 in PBS. Samples were then incubated with phalloidin-texas red (actin stain), Hoescht 33258 (nuclear stain), and anti-$P2X_7$ monoclonal antibody (HANO43, Axxora, San Diego, CA) followed by Alexa488-labeled anti-rat IgG. Confocal z-sections at the mid-plane of cells were collected using an Olympus Fluoview 1000 microscope.

Graphical and Statistical Analysis – All graphing analyses were completed using Microsoft Excel (Microsoft, Redmond, WA), GraphPad Prism (GraphPad Software, Inc., San Diego, CA), and FlowJo (Tree Star, Inc.). Statistical analysis (student's paired t-test) was conducted with GraphPad Prism. P-values $\leq 0.05 = *$, p-values $\leq 0.01 = **$, and p-values > 0.05 = not significant (ns).

4.4   RESULTS

4.4.1 Isolation of a toxin-resistant dendritic cell line variant

A toxin-resistant cell line was generated from wild type FSDC as described in Experimental Procedures and Figure 4-1. One of the clones selected (TLO-r) was highly resistant to TLO compared to wild type cells, as shown by PI uptake in Figure 4-2A. TLO-r was approximately four-fold more resistant to toxin-induced dye uptake, suggesting that this phenotype allowed the

cell to avoid lysis during the selection process. TLO-r was also less susceptible to pore formation induced by ALO (Figure 4-2A), demonstrating that the resistance phenotype was not TLO-specific. Moreover, inhibiting the pore-forming activity of these toxins with free cholesterol prevented dye uptake presumably because the toxins could no longer interact with the cell surface cholesterol (Figure 4-2A). To test whether exposure to CDC might result in pores too small to admit PI into TLO-r, ethidium bromide (394Da) and YO-PRO-1 (629Da) were tested in addition to PI (668.4Da) (Figure 4-2B). Similar results were obtained, suggesting that differences in pore size relative to the wild type cells are unlikely to explain TLO-r resistance to CDC. To visualize toxin-induced responses in wild type and variant cells, live cell imaging was used (Figure 4-2C). We observed that WT FSDC underwent extensive blebbing and loosened attachment from culture dishes within minutes of exposure to TLO, while TLO-r cells appeared unaffected. These results demonstrate that responses of variant TLO-r cells to CDC are profoundly different from that of the wild type parental FSDC.
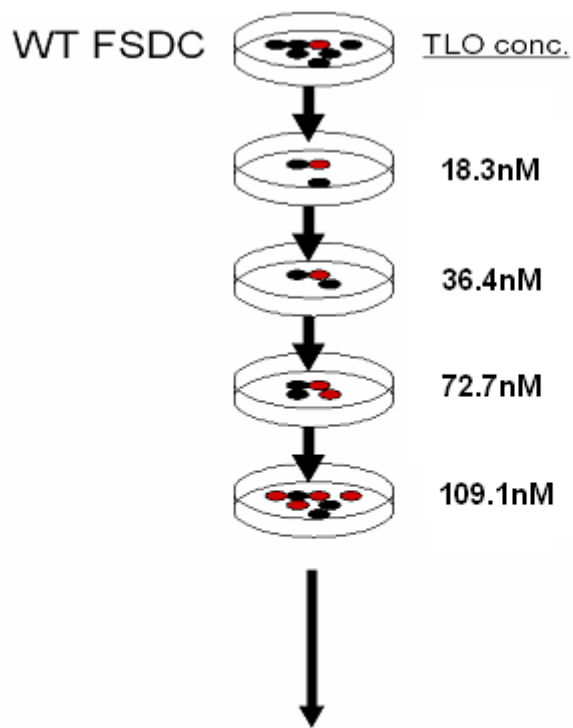
Figure 4-1: Schematic diagram of the selection process.

Wild type FSDC cells were first subjected to a toxic dose of 18.3nM TLO. Surviving cells were cultured and subjected to further rounds of selection with increasing concentrations of TLO over a period of several months. Following limiting dilution cloning, isolates were screened for sensitivity to toxins by measuring propidium iodide (PI) uptake.
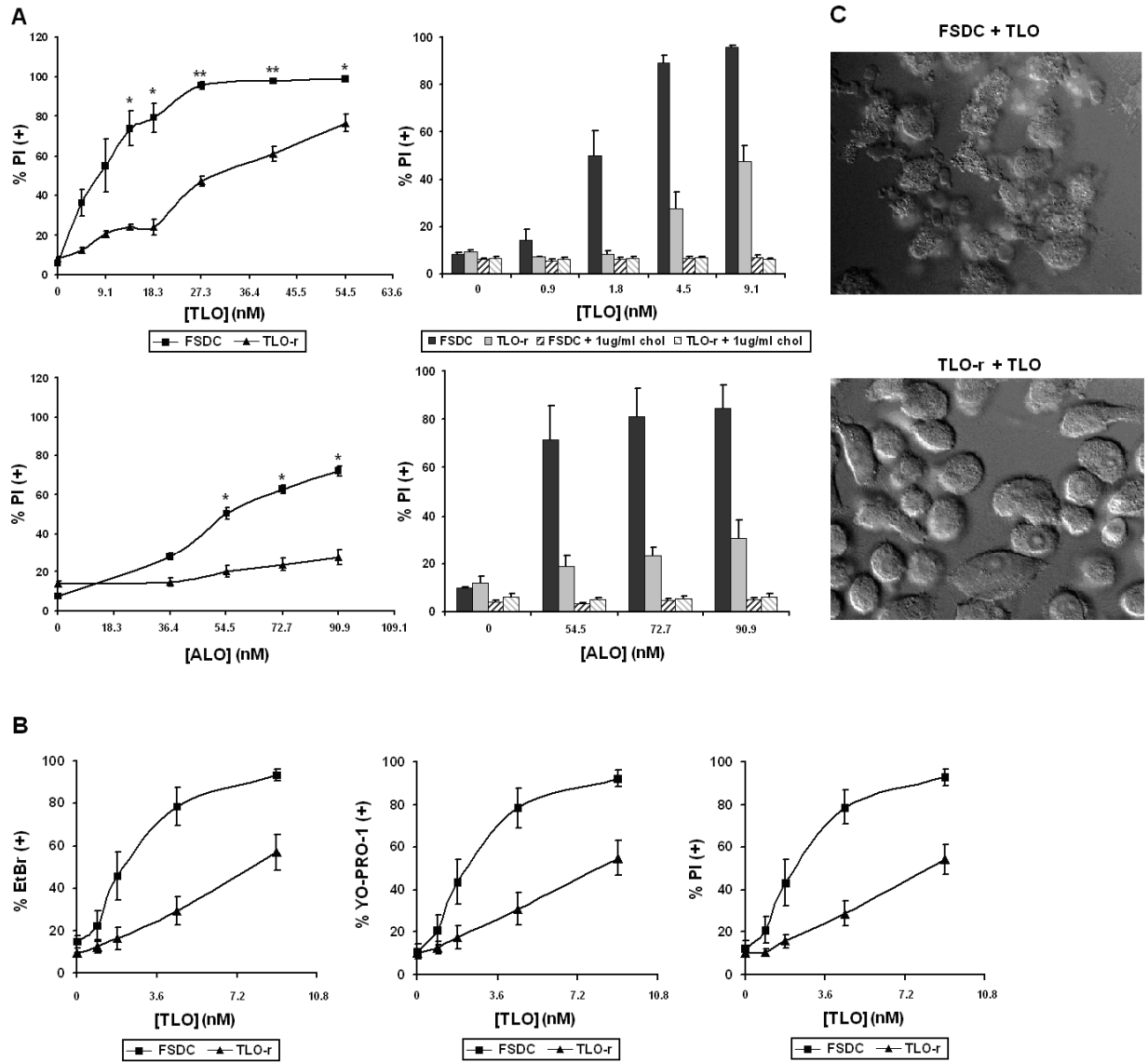
Figure 4-2: Generation of a toxin-resistant dendritic cell line variant.

(A) Cells were exposed to TLO (upper panels) or ALO (lower panels), with or without pre-exposure to 1ug/ml free cholesterol (right panels), for 30 min at the indicated concentrations followed by PI staining and flow cytometry analysis, with the percentage of PI$^+$ cells indicated. TLO-r are insensitive to TLO and ALO amounts that induce pore formation in wild type FSDC. Data represents mean +/- SEM for 3 independent experiments each for TLO and ALO; student's paired t-test comparing FSDC and TLO-r for TLO or ALO treatment; * = p≤0.05, ** = p≤0.01. (B) Cells were exposed to TLO for 30 min at the indicated concentrations followed by staining with ethidium bromide (EtBr), YO-PRO-1, or propidium iodide (PI) and flow cytometry analysis with the percentage of % dye-positive

108

cells indicated. There was no difference in dye uptake for all three dyes tested, which represents a range of different sized molecules capable of entering through toxin-induced pores. Again, TLO-r are more resistant to dye uptake compared to FSDC regardless of dye type. Data represents mean +/- SEM for 3 independent experiments for each of the three dyes. (C) Live cell microscopy of FSDC and TLO-r treated with 54.5nM TLO (non-reduced). Differential Interference Contrast (DIC) imaging was performed every 5s with the images shown collected 5 min after toxin addition. FSDC parental cells show blebbing and eventual detachment from the substrate while TLO-r maintain normal morphology and attachment to the dish. Data are representative of multiple experiments.

4.4.2 TLO-r does not differ from wild type cells in cholesterol content or ability to bind TLO

Since cholesterol is the major cell surface receptor for CDC, we hypothesized that lower levels of cholesterol in TLO-r could explain their apparent defect in pore formation after CDC treatment. Whole cell lysates of WT and TLO-r cells were tested for cholesterol content using a standard colorimetric assay. When normalized to total protein (Figure 4-3A) no significant differences in cholesterol content were observed. This suggests that wild type and variant cells do not differ significantly in the major cell surface receptor for CDC. To directly test CDC binding to cells, two different assays were used. In the first, the ability of wild type or variant cells to deplete toxin in solution by adsorption was determined. WT and TLO-r cells were exposed to TLO for 30 min to allow binding, and supernatants were harvested and subsequently incubated with a reporter cell line highly sensitive to CDC toxicity. Pore formation was then measured in the reporter cell line. Figure 4-3B shows that WT and TLO-r were equally able to adsorb TLO at all concentrations tested. In this assay, ability of cells to adsorb TLO was dependent on cholesterol, since it could be inhibited using the cholesterol chelating compound methyl-β-cyclodextrin (MβCD). The second method used to test binding was to label TLO with

the fluorescent dye Cy5 followed by incubation with cells and flow cytometry or fluorescence microscopy to measure cell-associated fluorescence. TLO-Cy5 bound to both WT and TLO-r cells similarly, above levels seen with a control protein BSA that was Cy5-labeled using the same protocol (Figure 4-3C). Preparations of Cy5-labeled TLO induced pore formation at similar concentrations as unlabeled TLO, suggesting that dye conjugation did not affect the pore forming ability of the protein. Binding was inhibited by MβCD, establishing cholesterol dependence (Figure 4-3C). Interaction of Cy5-TLO with the cell surface was determined using live cell microscopy (Figure 4-3D). Punctate staining of the plasma membrane was observed for both WT and TLO-r within 30 sec of Cy5-TLO addition, with subsequent internalization seen primarily in TLO-r, suggestive of pinocytosis. In summary, these data show that variant TLO-r cells do not have reduced levels of cholesterol, the major receptor for CDC, and exhibit no apparent defects in toxin binding.
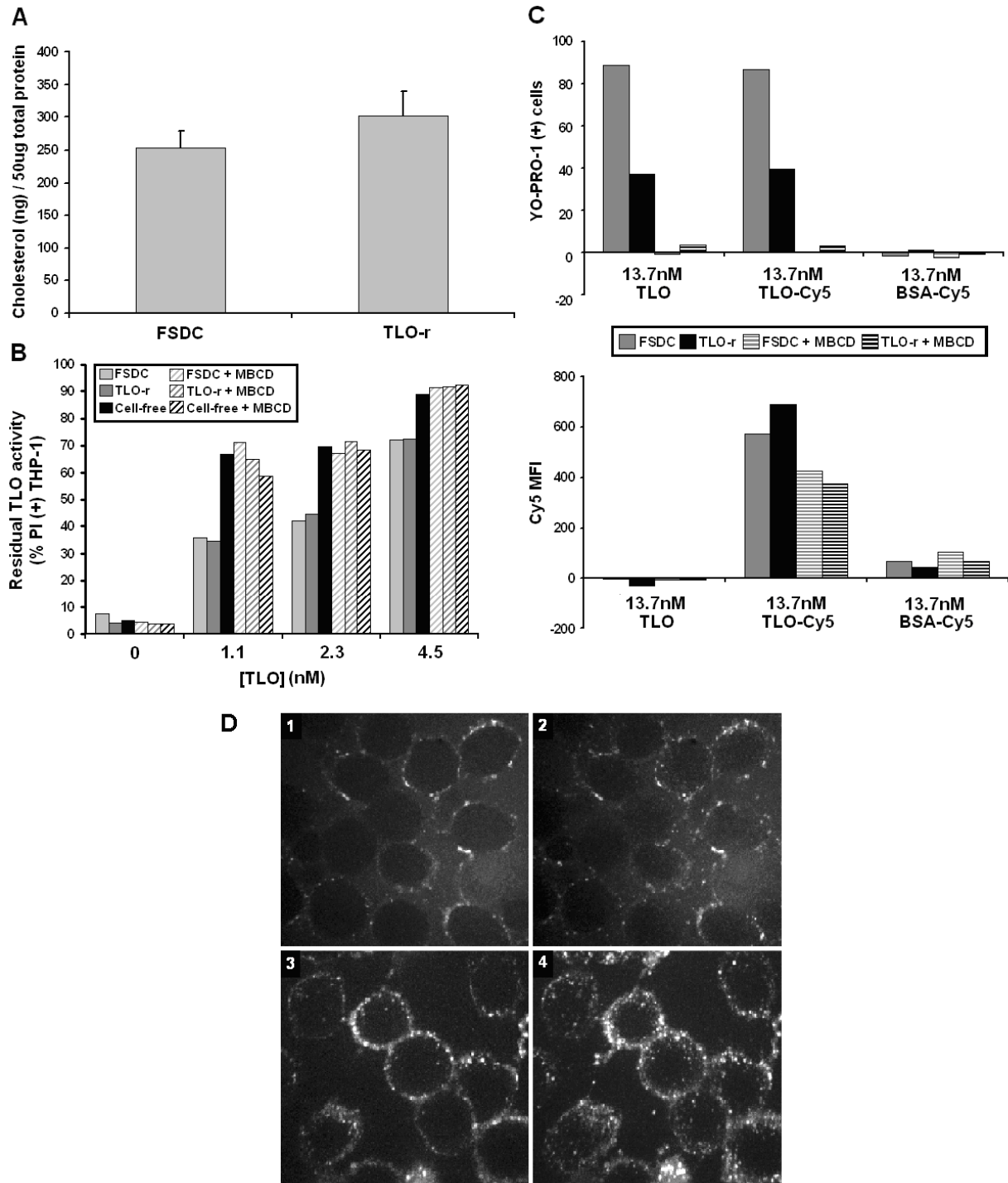
Figure 4-3: Total cholesterol levels and TLO binding levels are unaltered in TLO-r mutant cells.

(A) Total cholesterol content was measured using an Amplex Red assay and results normalized to total protein content. Cholesterol levels do not differ significantly between FSDC and TLO-r (mean +/- SEM, n = 6, student's paired t-test where p = 0.0551). (B) FSDC and TLO-r have a similar capacity to adsorb TLO from supernatants.

FSDC or TLO-r were incubated 30 min with TLO concentrations indicated on the x-axis or left untreated. As a control for maximum carryover of TLO in supernatants, TLO was incubated in wells containing no cells (cell-free). Where indicated, 15mM MβCD was incubated in wells containing FSDC, TLO-r, or no cells 30min prior to TLO treatment. Supernatants were collected from wells, centrifuged, and added to reporter THP-1 cells for 30 min. THP-1 were PI-stained and analyzed by flow cytometry. These results represent data obtained in 2 independent experiments. (C) TLO binds both FSDC and TLO-r at similar levels. TLO was labeled with Cy5 and incubated 30 min with cells before analysis of binding (Cy5) and pore formation (YO-PRO-1) by flow cytometry. TLO does not lose activity as a consequence of labeling as indicated by comparable pore formation relative to unlabeled TLO. BSA was also labeled with Cy5 and incubated with cells in parallel to show that the labeling reaction does not generate non-specific products toxic to cells. TLO-Cy5 binding to cells and subsequent pore formation are both inhibited by pre-incubation of cells with 15mM MβCD, confirming cholesterol-dependence. These results represent data obtained in 2 independent experiments. (D) Visualization of Cy5-labeled TLO binding to FSDC (panels 1 and 3) and TLO-r (panels 2 and 4) by live cell imaging. Cells were imaged continuously before and after addition of 54.5nM TLO-Cy5 (non-reduced), with confocal z-stacks collected at approximately 10s intervals over 15 min. Images shown were collected 5 min after addition of labeled toxin, and represent mid-plane z-sections (panels 1 and 2) and maximal projections (panels 3 and 4). Binding to both cell types is similar in intensity, consistent with (C) above, but internalization of the toxin is evident for TLO-r (panel 2) and absent in FSDC (panel 1). Data are representative of multiple experiments.

4.4.3 Phenotypic characterization of TLO-r cells relative to wild type

The results described above demonstrate that the pore forming ability of CDC can be dissociated from their ability to bind to cells. This was unexpected and prompted us to further explore phenotypic changes that might be associated with the toxin-resistant phenotype of TLO-r. A panel of monoclonal antibodies reactive against surface markers was tested for reactivity with both variant and wild type, and expression of MHC class II (I-A^b, I-A^d), CD40, CD11c, and CD86 were unchanged in TLO-r (Figure 4-4A). Phagocytosis of bacteria, a characteristic of

myeloid lineage cells such as FSDC (Figure 4-4B) was also unchanged as shown by measuring uptake of EGFP-expressing *E. coli*. These data combined with the similar morphology observed for the wild type and TLO-r cells before toxin exposure suggest that the variant has not undergone any gross changes in phenotype that can readily explain toxin resistance.
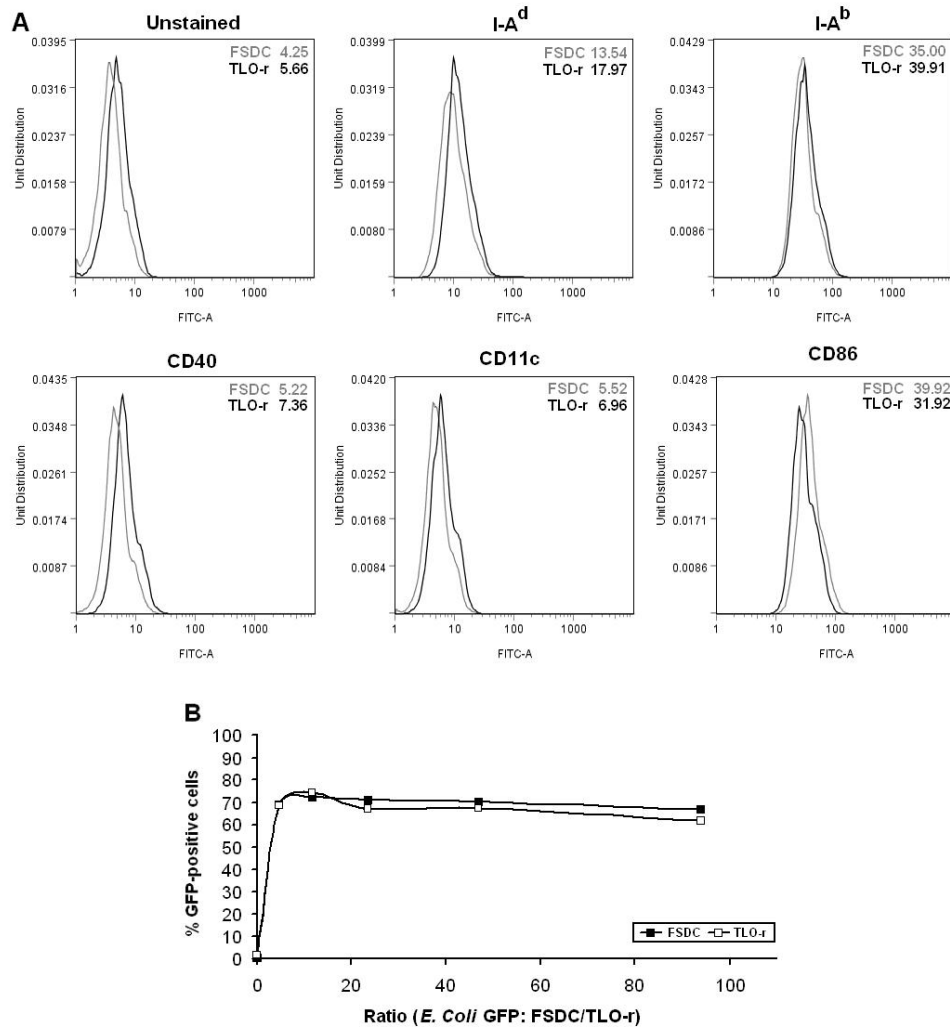
Figure 4-4: TLO-r retain the surface phenotype and phagocytic function of the FSDC parental cell line.

(A) FSDC and TLO-r were left unstained or stained with antibodies against MHC class II (I-A^b, I-A^d), CD40, CD11c, and CD86 followed by flow cytometry analysis. Profiles are similar for FSDC and TLO-r. These results are representative of 2 independent experiments. (B) FSDC and TLO-r were incubated with *E. coli*-expressing GFP at various doses for 1hr to allow phagocytosis followed by flow cytometry analysis. *E. coli*-GFP amounts were determined by plating in order to calculate a ratio of *E. coli*-GFP to cells. A similar percentage of FSDC and TLO-r phagocytose bacteria at all ratios tested.

4.4.4 TLO induces higher levels of ATP release from wild type cells compared to TLO-r

Since toxin-exposed TLO-r cells are perforated less than wild type cells as determined by dye uptake assays, we considered it likely that release of cytosolic contents from the variant cells into the extracellular environment might also be reduced. To test this, we measured ATP levels, a commonly used marker of cell viability (Petty *et al.*, 1995; Walev *et al.*, 2001b) in cell fractions and supernatants of both wild type and variant cells exposed to TLO. As shown in Figure 4-5, TLO treatment induced higher levels of ATP release from WT cells as compared to the variant. Inversely, variant cells retained more of their cellular ATP compared to wild type cells.
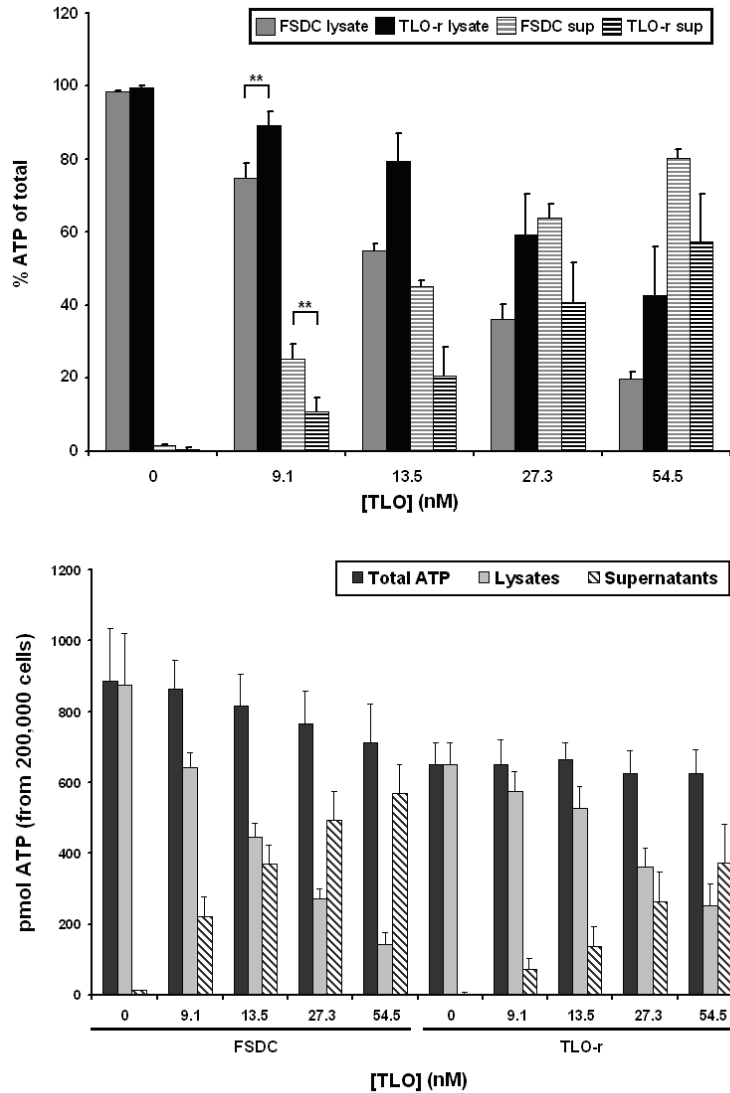
Figure 4-5: TLO induces ATP release from FSDC, a process impaired in TLO-r.

TLO induces more ATP release from FSDC compared to TLO-r. FSDC and TLO-r were treated for 5min with various concentrations of TLO as indicated. 300μl supernatants were collected from wells and cells were lysed with 300μl of lysis buffer. ATP in equivalent volumes of supernatants and cell lysates was measured by an ATP bioluminescence assay. Actual amounts of ATP (pmol) in supernatants or lysates are shown in the bottom panel while the percentage of ATP in supernatants or lysates was calculated based on total ATP, which is the combined amount of ATP in supernatants and lysates (top panel). With increasing TLO dose, the cells release ATP and this is mirrored in the decreased percentage ATP inside cells. FSDC show greater ATP release and greater loss of cellular ATP compared to TLO-r (mean +/- SEM, n = 3, student's paired t-test; ** = p≤0.01).

116

4.4.5 TLO-initiated pore formation in FSDC is potentiated by extracellular ATP and may require P2X$_7$ activity

Release of ATP from cells can be considered a marker of viability, but it is also known that ATP in the extracellular environment can have profound effects on cells expressing purinergic receptors. This includes myeloid lineage cells, which express multiple members of this family (Di Virgilio *et al.*, 2001; Bours *et al.*, 2006) including the P2X$_7$ receptor that can form pores in cells after prolonged exposure to millimolar concentrations of ATP (Chessell *et al.*, 2001; Aga *et al.*, 2002). Recently, pannexin-1 has been identified as a protein that binds to P2X$_7$ in membranes as part of the pore forming complex (Pelegrin & Surprenant, 2006; Kanneganti *et al.*, 2007; Locovei *et al.*, 2007). We hypothesized that CDC might exert their effects on myeloid cells such as FSDC through the release of ATP, which could then act in an autocrine or paracrine fashion to stimulate P2X$_7$-dependent pore formation. This suggests that exogenous dye influx and ATP efflux from intracellular stores would be maximal when pores generated both by assembled toxin subunits and by activated P2X$_7$ receptors were present on cells. To address this question, we used the enzyme apyrase to degrade ATP (Cohn & Meek, 1957) in extracellular medium during exposure of FSDC cells to TLO, and measured subsequent pore formation. As shown in Figure 4-6, apyrase treatment reduced TLO-induced dye uptake by cells, consistent with a role for ATP in toxin-induced pore formation. Additionally, we used irreversible P2X$_7$ inhibitor oxidized ATP (oATP) and measured pore formation via trypan blue dye uptake. Though not statistically significant, a trend was observed where TLO-induced dye uptake was decreased in the presence of oATP, especially at lower TLO doses, whereas no difference was observed at higher TLO doses (Figure 4-7). These data suggest a possible role for P2X$_7$ in CDC-induced pore formation.
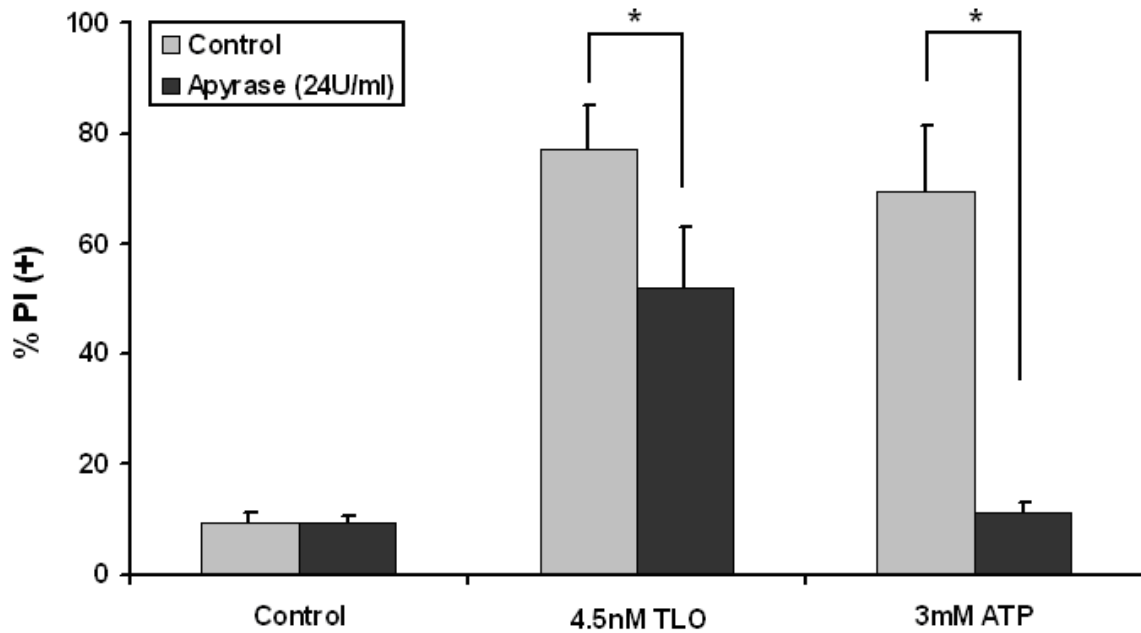
Figure 4-6: Apyrase inhibits TLO-induced pore formation in FSDC.

Pore formation in FSDC caused by TLO can be reduced by ATP-degrading enzyme apyrase. Wild type parental FSDC were treated with TLO or ATP (control) in the presence or absence of 24U/ml apyrase for 30min. Cells were then incubated with PI and analyzed by flow cytometry for PI uptake. Apyrase inhibited PI uptake by FSDC treated with both TLO and ATP (mean +/- SEM, n = 4, student's paired t-test; * = p$\leq$0.05).
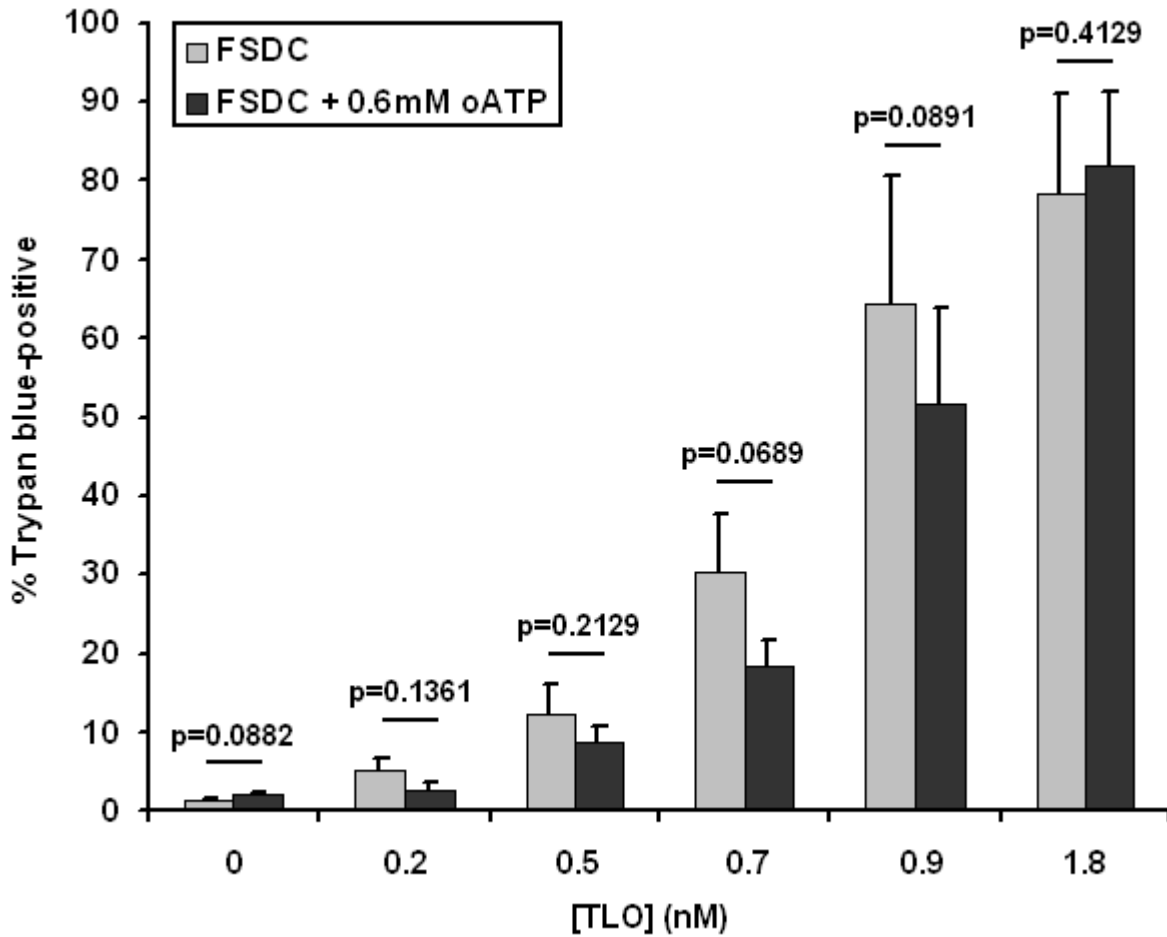
Figure 4-7: oATP inhibits TLO-induced trypan blue uptake by FSDC.

Pore formation in FSDC caused by TLO can be reduced by irreversible $P2X_7$ inhibitor oATP. Wild type parental FSDC were treated with TLO in the presence or absence of 0.6mM oATP for 30min. Cells were then incubated with trypan blue and at least 100 cells counted to calculate percentage of trypan blue-positive cells. oATP inhibited trypan blue uptake by FSDC treated with low doses of TLO (mean +/- SEM, n = 5, student's paired t-test).

4.4.6 TLO-r variant cells have reduced levels of P2X$_7$ receptor and reduced responsiveness to ATP

A role for both ATP and P2X$_7$ in toxin-induced pore formation is suggested by the previous data showing that toxin-induced dye uptake was decreased in the presence of inhibitors of ATP and P2X$_7$. Moreover, the data above also suggested that the defect in ATP release observed in the toxin-resistant variant might result from loss of P2X$_7$ expression, since activation of this receptor by ATP can induce further ATP release (Anderson *et al.*, 2004; Suadicani *et al.*, 2006). Western blot analysis showed that TLO-r cells expressed 10-15% of wild type P2X$_7$ levels and reduced levels were also observed by fluorescence microscopy of fixed and permeabilized cells stained with anti-P2X$_7$ antibody (Figure 4-8A). P2X$_7$ deficiency would be expected to impair ATP-induced pore formation and as shown in Figure 4-8B, TLO-r cells treated with 3mM ATP were indeed less susceptible to ATP-induced pore formation than wild type cells.

Taking all of the data together, a model (Figure 4-9) can be suggested whereby CDC form pores in cell membranes, which allows the release of ATP that can act in an autocrine or paracrine fashion on P2X$_7$-expressing cells. P2X$_7$ activation leads to recruitment of pannexin 1, which has been implicated in large pore formation (Pelegrin & Surprenant, 2006; Locovei *et al.*, 2007) and has also been linked to the activation of the inflammasome (Pelegrin & Surprenant, 2006; Kanneganti *et al.*, 2007), which is responsible for the maturation of pro-IL-1β to its mature 17kDa form.
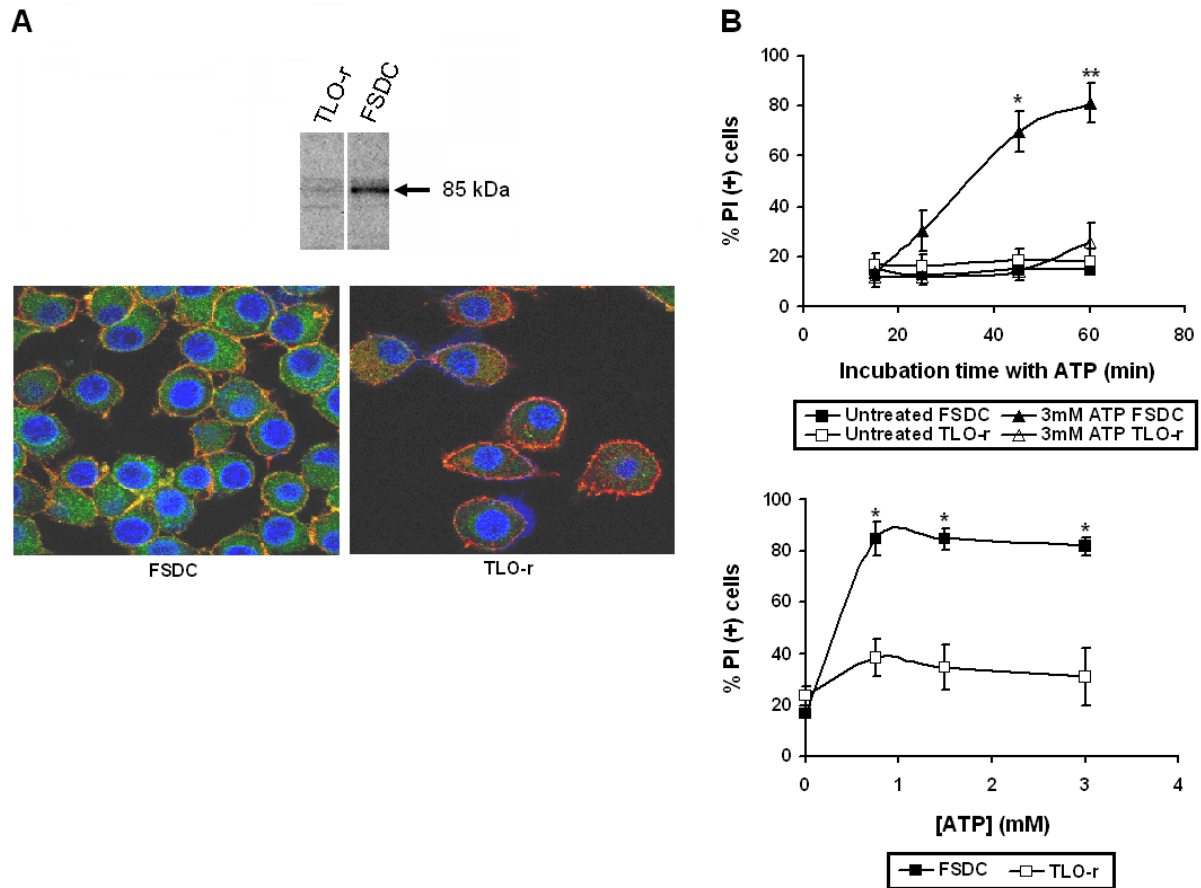
Figure 4-8: TLO-r express less purinergic receptor P2X$_7$ compared to FSDC, which affects downstream ATP-mediated pore formation.

(A) Total P2X$_7$ expression is decreased in TLO-r compared to FSDC. For western blotting (top panel), equivalent amounts of total protein (20µg) for FSDC and TLO-r were probed for P2X$_7$, which is approximately 85kDa in size. The 85kDa band is much reduced in intensity for TLO-r compared to FSDC. It should be noted that TLO-r and FSDC lysates were run on two different parts of the same gel. For fluorescence microscopy, FSDC and TLO-r were fixed, permeabilized, and stained with phalloidin-texas red actin stain (red), Hoescht 33258 nuclear stain (blue), and anti-P2X$_7$ monoclonal antibody followed by Alexa488-labeled anti-rat IgG (green). These confocal z-sections at the mid-plane of cells show brighter P2X$_7$ staining in FSDC as opposed to the dim staining seen in TLO-r. (B) The pore formation response of TLO-r to ATP treatment is decreased compared to FSDC. FSDC or TLO-r were left untreated or treated with 3mM ATP over various time points (top panel) or with varying ATP doses for 30min (bottom panel). Cells were incubated with PI and analyzed by flow cytometry. PI uptake increases for FSDC with

time and at all doses tested whereas dye uptake by TLO-r is closer to background levels. Data was analyzed with the student's paired t-test comparing ATP-treated FSDC versus ATP-treated TLO-r at each time point or each dose for 3 independent experiments. Data represented as mean +/- SEM. Student's paired t-test; * = $p \leq 0.05$, ** = $p \leq 0.01$.
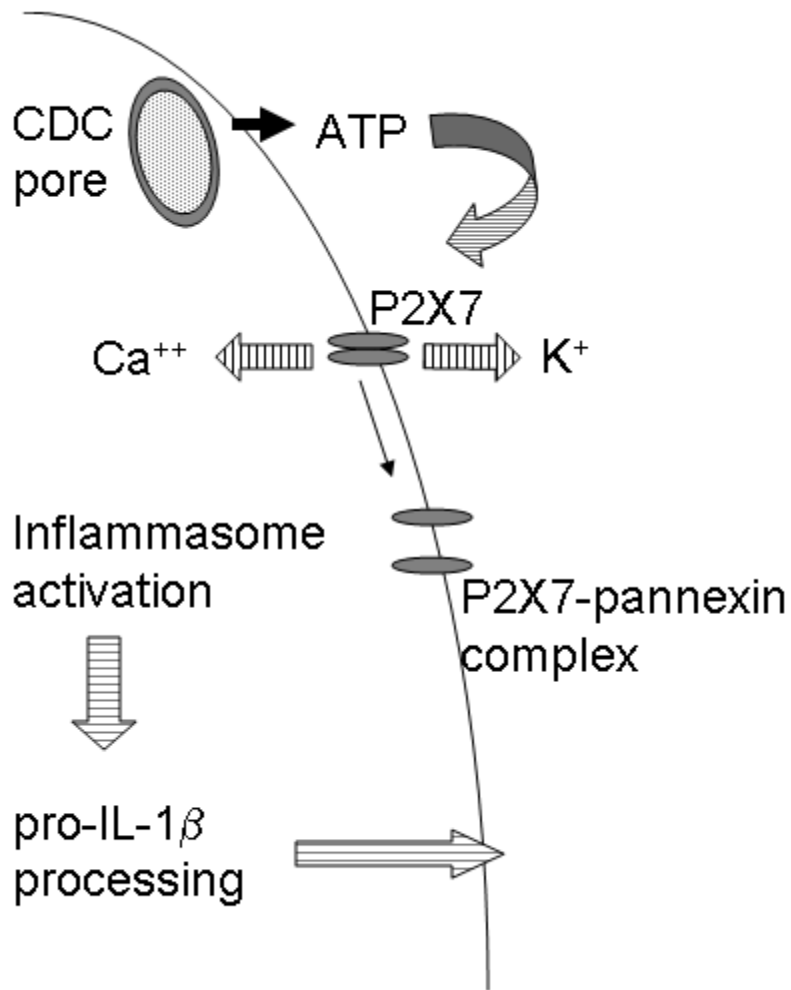
Figure 4-9: Model of CDC-initiated, P2X7-potentiated pore formation.

Gram-positive bacteria secrete CDC that bind cholesterol on eukaryotic cells, leading to pore formation and subsequent intracellular ATP release. Extracellular ATP then binds (in an autocrine or paracrine manner) to purinergic receptor P2X7, causing pannexin-1-mediated pore formation that allows a feedback loop of ATP release through these pores. $P2X_7$ activation has also been coupled to the activation of the inflammasome, a molecular platform for the processing of pre-formed stores of cytokines such as IL-1β.

4.4.7 Determination of the role of $P2X_7$ in CDC-induced pore formation using $P2X_7$-deficient or $P2X_7$-expressing cell lines

Aside from the ATP and $P2X_7$-related variations in TLO-r already discussed, we also observe defects in pro-IL-1β, TNF-α, and IL-6 production and/or secretion after LPS stimulation compared to FSDC (Figure 4-10). As a result of the defect in pro-IL-1β production, TLO-r also lack the ability to secrete processed IL-1β (data not shown). Due to the many identified and potentially unidentified defects in TLO-r, it is difficult to solely attribute the perforation-resistance phenotype to $P2X_7$ expression and function. Therefore, we engineered several $P2X_7$-deficient or $P2X_7^{lo}$-expressing cell lines to express or overexpress, respectively, $P2X_7$ and assessed pore formation via dye uptake as measured by flow cytometry or LDH release. Expression of $P2X_7$ was verified using immunostaining and flow cytometry (Figure 4-11).
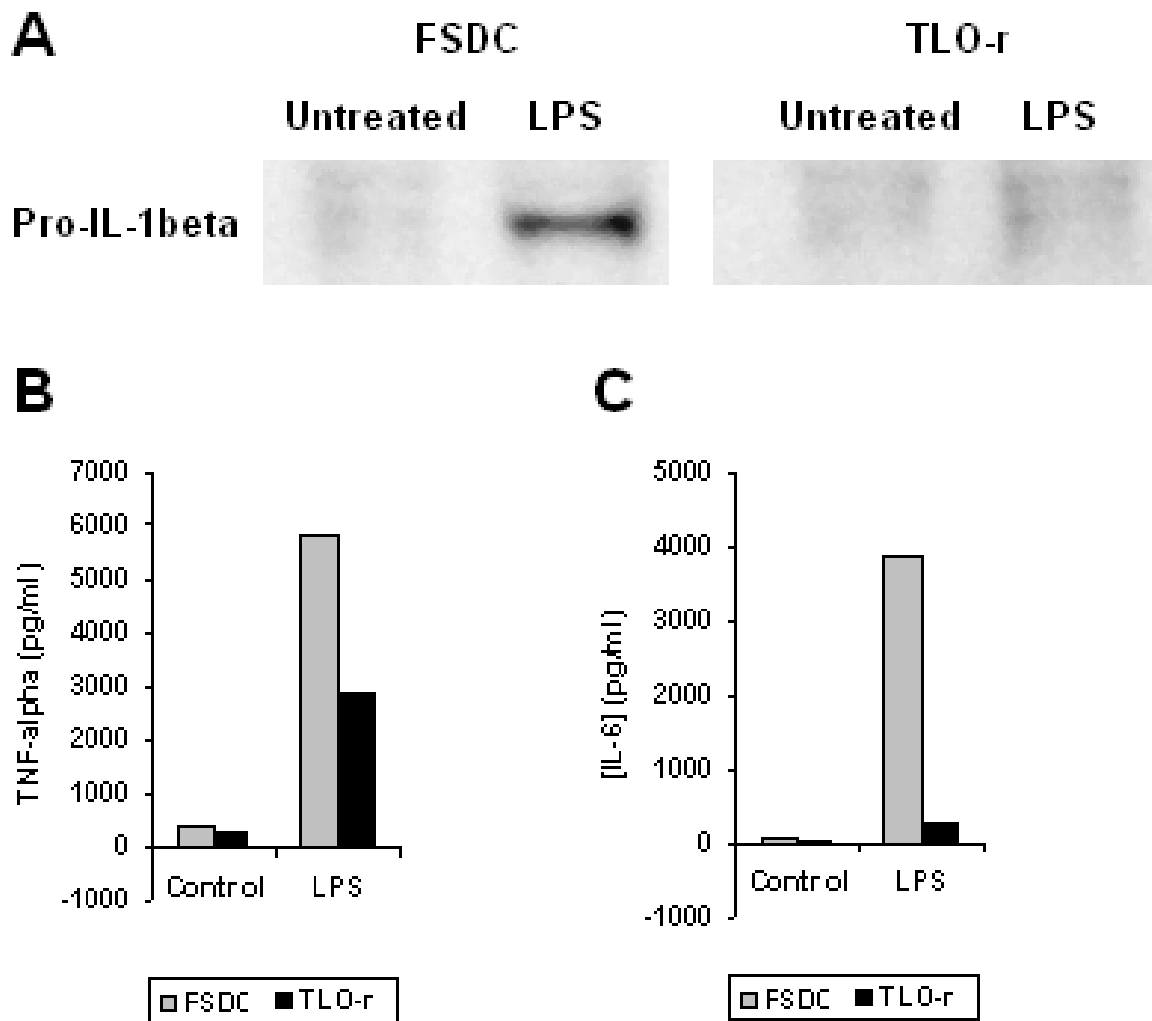
Figure 4-10: TLO-r have defects in pro-inflammatory cytokine production.

(A) FSDC and TLO-r were left untreated or treated with 1μg/ml LPS for 24hr in complete media, lysed, and 20μg of protein sample immunoblotted for pro-IL-1β content. LPS-treated FSDC, but not LPS- treated TLO-r produce pro-IL-1β. (B-C) FSDC and TLO-r were left untreated or treated with 1μg/ml LPS for 24hr in complete media and supernatants were collected analyzed by ELISA for (B) TNF-α or (C) IL-6. TLO-r produce less of both cytokines compared to FSDC.

A D2SC-1
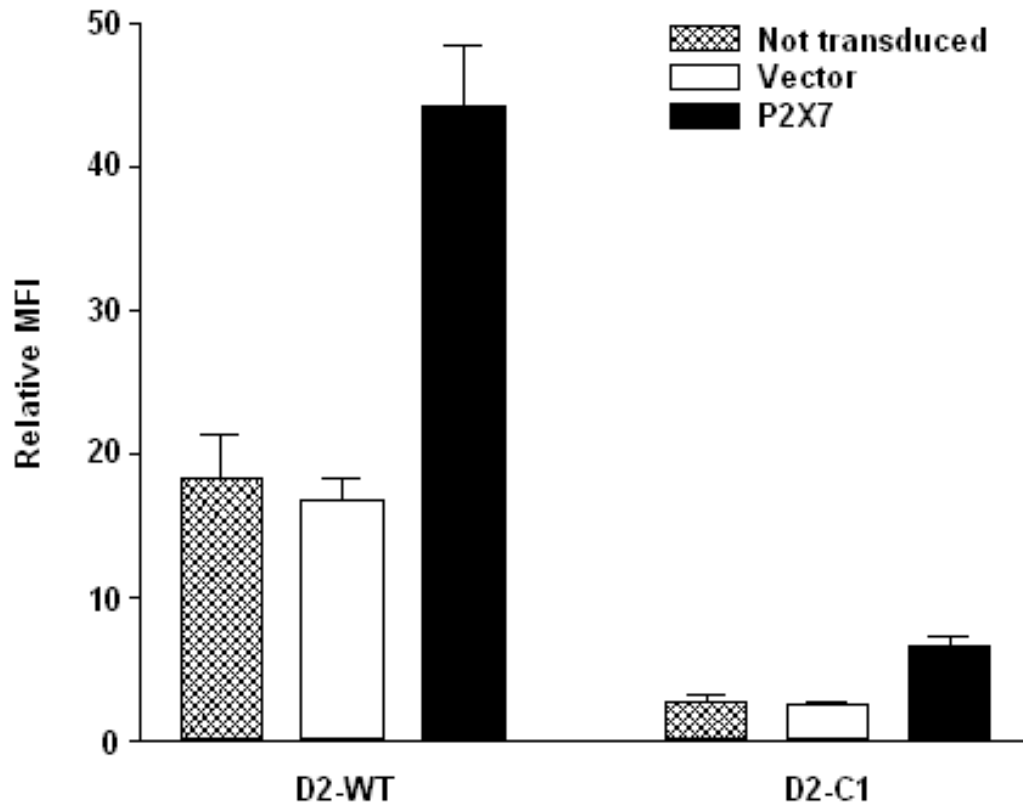
B HEK 293
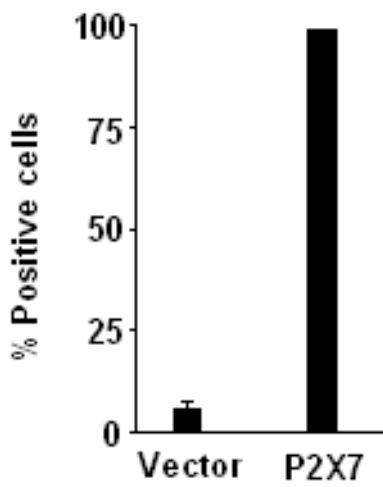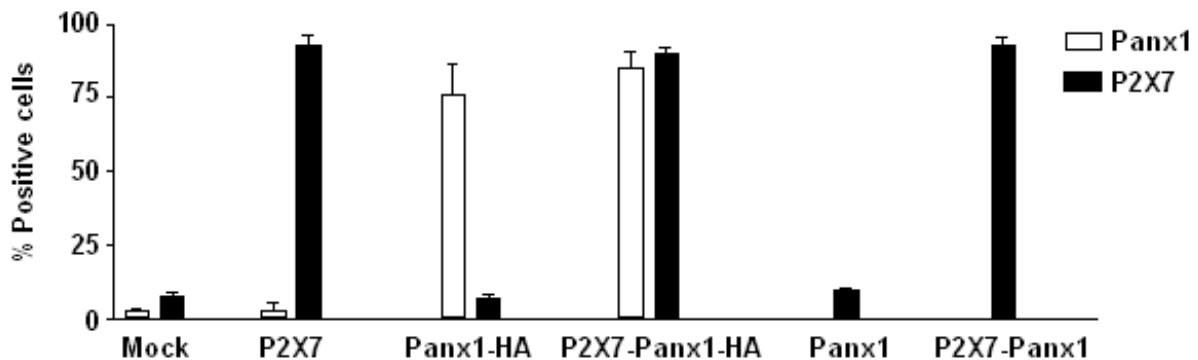
Figure 4-11: P2X7 expression on transfected or transduced cell lines

(A) P2X7 expression on WT or C1 (ATP-resistant) D2SC-1 (D2) cells that were not transduced or transduced with vector only or a $P2X_7$-expressing retrovirus. Cells were left unstained or stained with a $P2X_7$ antibody followed by addition of a goat anti-rat-Cy5 secondary antibody and analysis via flow cytometry. Relative MFI represents the ratio of MFI ($P2X_7$ antibody staining) to MFI (No antibody). (B) $P2X_7$ expression, represented as % positive cells, on HEK 293 cells transfected with vector only or a $P2X_7$ construct. Staining and analysis were conducted as in part A. (C) $P2X_7$ and pannexin-1 expression, represented as % positive cells, on NRK cells transduced with mock, $P2X_7$, pannexin-1-HA (panx1-HA), $P2X_7$-pannexin-1-HA ($P2X_7$-panx1-HA), pannexin-1 (panx1), or $P2X_7$-pannexin-1 ($P2X_7$-panx-1) retrovirus. $P2X_7$ staining and analysis were conducted as in part A. Pannexin-1 expression was assessed through permeabilization and staining for the HA tag, followed by flow cytometry. Reliable reagents to directly test the expression of pannexin-1 are not currently available, so only $P2X_7$ expression could be assessed for NRK expressing panx1 or $P2X_7$-panx1.

We observed no difference in PI uptake by the D2 dendritic cell line transduced with control vector or $P2X_7$ for any of the TLO concentrations tested (Figure 4-12A). As expected, ATP induced more PI uptake by $P2X_7$-overexpressing D2 compared to vector only control. Similar amounts of PI uptake were observed with wild type D2 cells and D2-C1 treated with various TLO doses (Figure 4-12B). D2-C1 cells represent an ATP-resistant cell line selected using a similar scheme as shown in Figure 4-1, except that ATP was used as the selection agent. These cells take up little PI compared to wild type D2 after exposure to ATP. Similarly, $P2X_7$-negative HEK 293 cells were transfected with control vector or $P2X_7$ and PI uptake (Figure 4-12C) or LDH release (Figure 4-12D) was assessed. BzATP and ATP induce modestly more PI uptake and LDH release, respectively, in HEK293-$P2X_7$ compared to HEK293-vector. However, no differences in PI uptake or LDH release were observed with various doses of TLO. Lastly, the roles of both $P2X_7$ and pannexin-1 in TLO-induced pore formation were tested using $P2X_7$- and pannexin-1-negative NRK cells transduced with vector alone, $P2X_7$ alone, pannexin-1 alone, or $P2X_7$ and pannexin-1 together. No major differences in PI (Figure 4-12E, upper panel) or DAPI (Figure 4-12F, upper panel) uptake were observed between all cell lines treated with various doses of TLO. On the other hand, $P2X_7$-expressing NRK took up DAPI, but not PI, after ATP treatment (Figure 4-12E-F, bottom panels). Unexpectedly, pannexin-1 appeared to play no role in dye uptake. Together, these data suggest that $P2X_7$ does not play a role in TLO-induced pore formation.
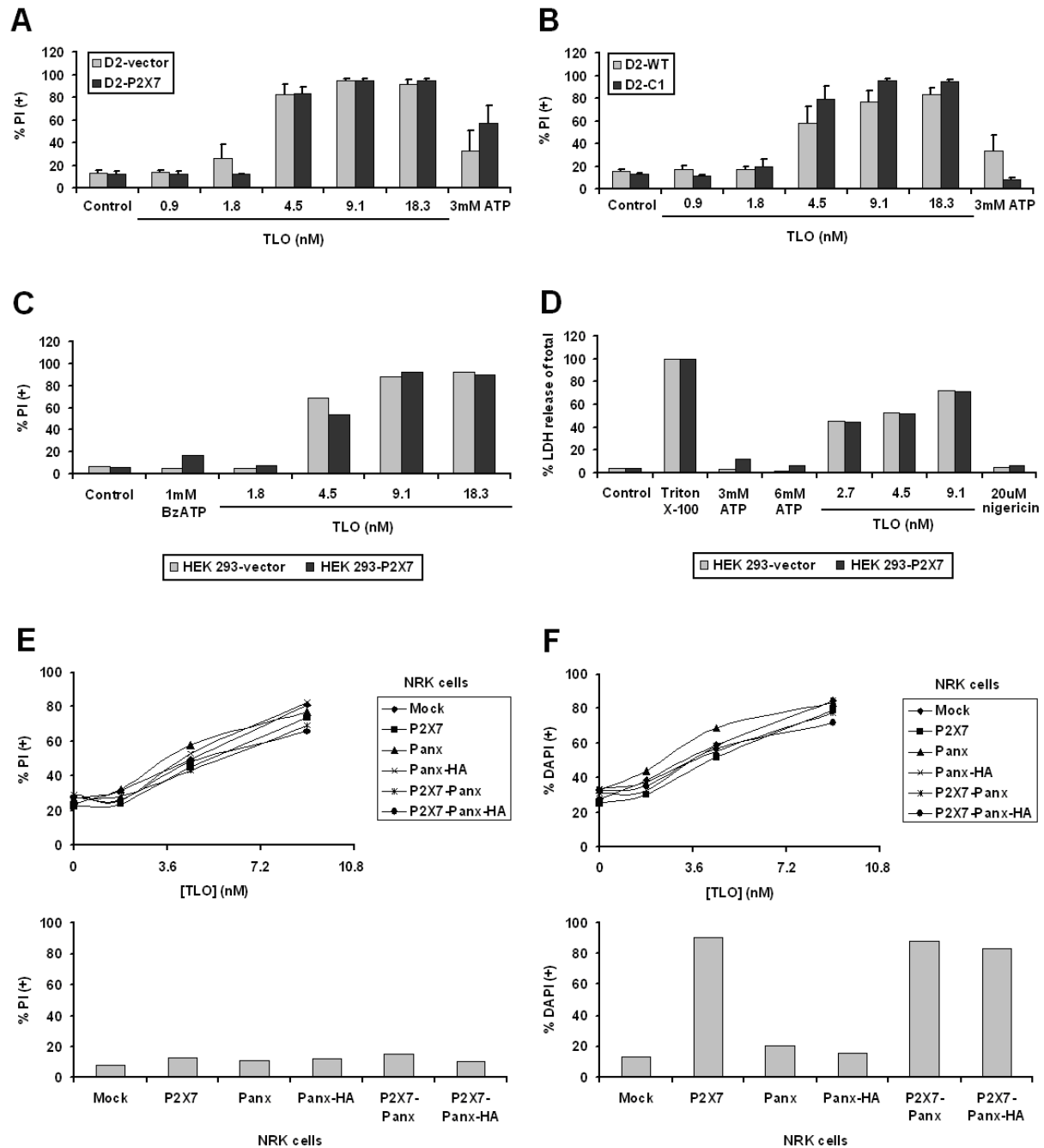
Figure 4-12: No difference in CDC-induced pore formation for P2X$_7$-expressing versus P2X$_7$-deficient cell lines.

(A-B) Dendritic cell line D2 (D2-WT) were retrovirally transduced to express P2X$_7$ (D2-P2X$_7$) or control vector (D2-vector) or were selected for resistance to ATP-induced pore formation (D2-C1). Each cell type was treated with DTT control buffer, various concentrations of TLO, or 3mM ATP and analyzed for PI uptake via flow

cytometry. D2-P2X$_7$ and D2-WT were more sensitive to ATP-induced dye uptake compared to D2-vector and D2-C1, respectively. There was no difference in TLO-induced dye uptake for either pair of cells. Data represents mean +/- SEM for three independent experiments. (C-D) HEK 293 cells were stably transfected to express P2X$_7$ (HEK 293-P2X$_7$) or control vector (HEK 293-vector) and treated with DTT control and various concentrations of TLO, BzATP, ATP, or nigericin. Cells were analyzed for PI uptake via flow cytometry (C) or LDH release as compared to total after Triton X-100 treatment (D). BzATP and ATP induce somewhat more PI uptake and LDH release, respectively, from HEK293-P2X$_7$ while no difference is observed for all TLO concentrations tested. (E-F) NRK cells were retrovirally transduced to express control vector (mock), P2X$_7$, pannexin-1 (panx), HA-tagged pannexin-1 (panx-HA), P2X$_7$ + pannexin-1 (P2X7-Panx), or P2X$_7$ + HA-tagged pannexin-1 (P2X7-Panx-HA) and treated with various doses of TLO (top panels) or 3mM ATP (bottom panels). PI (left panels) or DAPI (right panels) dye uptake was assessed via flow cytometry. Little difference in PI or DAPI uptake was observed after TLO treatment for all cell lines while DAPI uptake was evident for P2X$_7$-expressing NRK treated with ATP.

4.4.8 Determination of the role of P2X$_7$ in CDC-induced IL-1β release using P2X$_7$-deficient primary macrophages

We next explored the role of P2X$_7$ in another downstream effect of TLO: IL-1β release (see section 1.2 for a review and chapter 2). To test this, we used primary macrophages, which have the capacity to generate large stores of pro-IL-1β after TLR priming, that normally express P2X$_7$ or ones that were deficient in this receptor. As shown in Figure 4-13, ATP, nigericin, and TLO induce the secretion of IL-1β from LPS-primed BMDM, but only ATP-induced IL-1β secretion is dependent on P2X$_7$. These data serve as further evidence that P2X$_7$ does not play a role in TLO-induced effects.
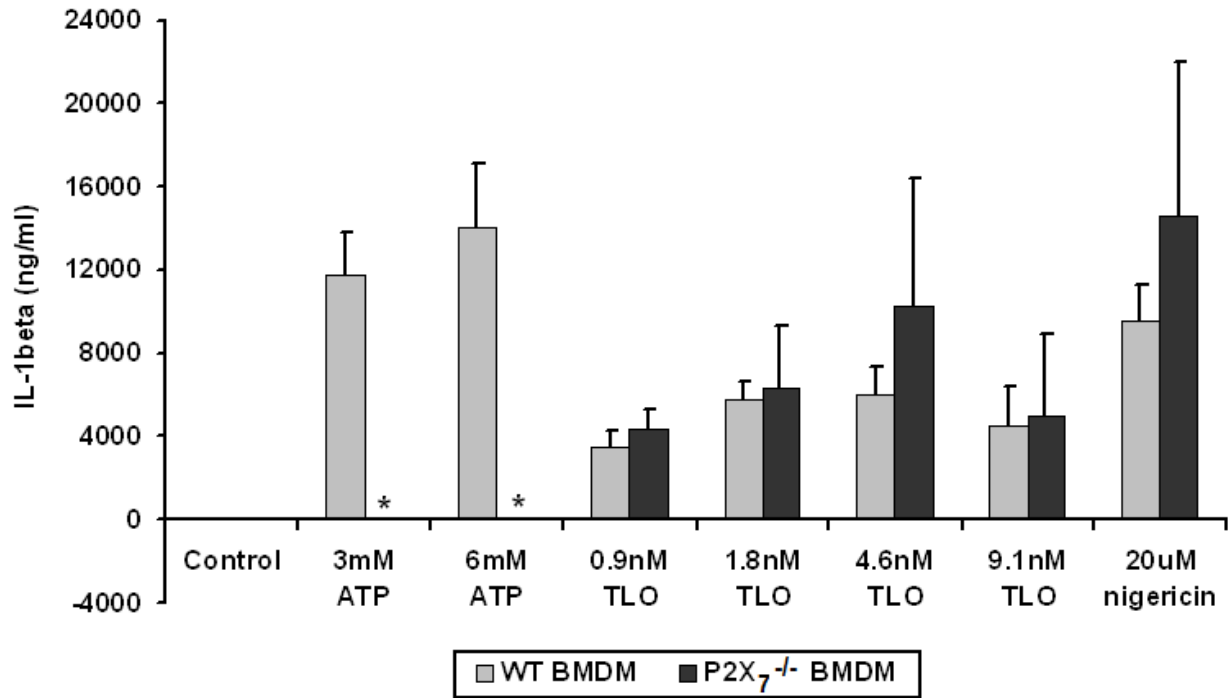
Figure 4-13: TLO-induced IL-1β release from BMDM is P2X$_7$-independent.

BMDM generated from wild type (WT) or P2X$_7^{-/-}$ mice were primed with LPS for 4 h and then treated with control (DTT-containing buffer), ATP, TLO, or nigericin for 30 min. Supernatants were collected and assayed by ELISA for IL-1β. As expected, P2X$_7^{-/-}$ BMDM treated with ATP did not produce IL-1β, but when treated with nigericin they produced similar amounts of IL-1β to WT BMDM. TLO also induced equivalents amounts of IL-1β from WT compared to P2X$_7^{-/-}$ BMDM, showing that it does not depend on P2X$_7$ activity. Data represents mean +/- SEM for 3 independent experiments. Student's paired t-test was applied for comparison of WT versus P2X$_7^{-/-}$ conditions. * = p ≤ 0.05.

4.5   DISCUSSION

It has been observed that the lethal concentration of a single CDC family member varies depending on the cell type being exposed to it (Mosser & Rest, 2006). Pore formation largely contributes to this cell death, but the pathways that are involved after pore formation but before final cell death are not well understood. In order to identify critical pathways or molecules that contribute to CDC-induced pore formation, we generated a dendritic cell line resistant to CDC TLO (TLO-r). We observed that these variant cells were more resistant to TLO-induced pore formation and maintained a healthy morphology, as opposed to the parental cell line (FSDC) that underwent cell death. It was ruled out that differences in pore size, cholesterol content, CDC binding to the plasma membrane, or changes in phenotype (surface markers, phagocytosis of bacteria) were responsible for the pore resistance phenotype of the variant. Instead, we identified ATP and its receptor $P2X_7$ as potential candidates using the following observations: (1) TLO induces ATP release from FSDC, (2) TLO-induced ATP release is greatly reduced in TLO-r, (3) TLO-induced dye uptake in FSDC is partially inhibited by apyrase (degrades ATP) and oATP (inhibits $P2X_7$), (4) TLO-r express less $P2X_7$ than FSDC, and (5) TLO-r are more resistant to ATP-induced dye uptake. From these data, we proposed the model shown in Figure 4-9. However, we identified other defects in TLO-r, which prompted us to study the role of $P2X_7$ in TLO-induced pore formation and IL-1β release using more straightforward cell systems ($P2X_7$-expressing or –deficient cell lines or primary macrophages). Using these latter systems, we have concluded that $P2X_7$ does not play a role in TLO-induced pore formation or IL-1β secretion.

The generation of the ATP-resistance phenotype may have occurred in a parallel, but unrelated way during the generation of the TLO-resistance phenotype. ATP is present inside cells at a concentration of 5-10mM and can be released upon membrane damage (Di Virgilio, 2005; Bours *et al.*, 2006). We show with our data that high doses of CDC perforate cells and allow the release of ATP. If this were to occur during the TLO selection process, high concentrations of ATP would be locally present around the cells and would be capable of binding to and activating $P2X_7$, which would ultimately lead to cell death. Thus, ATP itself would apply its own selective pressures (as shown in the ability to create ATP-resistant D2 cells) so that cells with low levels of $P2X_7$ and therefore, less responsiveness to ATP would be favored. This phenomenon would explain the phenotype observed in TLO-r and would suggest that another factor or pathway is responsible for the TLO-induced pore resistance phenotype.

The factor or pathway responsible for the pore formation resistance phenotype is currently unknown. It could be speculated that pore resealing machinery may be more active in TLO-r than FSDC such that TLO-r can deal with membrane attack much more rapidly than FSDC. It was originally demonstrated by Walev, *et al.* that CDC pores can be repaired or resealed (Walev *et al.*, 2001b; Husmann *et al.*, 2006) and it was later suggested that these resealing processes may involve calcium- or calmodulin-mediated signaling pathways (Aroian & van der Goot, 2007). Recent work by Idone, *et al.* supports the role of calcium signaling in pore resealing and further shows that endocytosis is responsible for the removal of pores from the cell surface (Idone *et al.*, 2008). Though there are no noticeable differences in phagocytic activity between FSDC and TLO-r, it is possible that TLO-r have enhanced endocytic machinery expression and/or activity.

Interestingly, we also observed that TLO-r had defects in proinflammatory cytokine secretion (Figure 4-10). This phenotype could be a reflection of the selection for TLR4 low to negative cells since TLR4 has been reported to act as a CDC receptor (Malley *et al.*, 2003; Park *et al.*, 2004a; Ito *et al.*, 2005; Srivastava *et al.*, 2005) and its activation results in proinflammatory cytokine secretion from myeloid cells. However, the expression levels of TLR4 on TLO-r have not been assessed. Another explanation for this phenotype is that there is a defect on the transcription factor level. Such transcription factors known to play a role in cytokine secretion are p38 MAPK and NF-κB. Both transcription factors have been shown to participate in an osmotic stress response to CDC that results in cytokine secretion (Walev *et al.*, 2001b; Husmann *et al.*, 2006; Ratner *et al.*, 2006; Kloft *et al.*, 2009). Thus, TLO-r may have a defect in p38 MAPK or NF-κB activation, which would result in secretion of lower cytokine levels. This has yet to be determined.

In general, TLO-r could be a useful tool to initially identify potential candidates involved in CDC-induced pore formation and possibly other pathways induced by CDC that have yet to be discovered. Many candidates could be simultaneously identified using a proteomic approach to compare the differential protein expression between FSDC and TLO-r. Similarly, differential expression of mRNA or protein levels could be determined by using RT-PCR or proteomics, respectively, for untreated versus CDC-treated cells. Once candidate factors were identified, it would be essential to test their contribution, if any, to the host cellular response to CDC. As demonstrated by the work in this chapter, it would also be critical to use primary cells or engineered cells that lack or express the proteins of interest. Identifying new pathways initiated by CDC will help us to better understand their interactions with host cells and generate specific therapies to supplement antibiotic treatments in bacterially infected patients.

4.6   ACKNOWLEDGEMENTS

5.0   SUMMARY & INTERPRETATIONS

5.1   PROPOSED MODEL AND THERAPEUTIC IMPLICATIONS

The work contained herein implicates CDC in triggering distinct pathways regulated by the NLRP3 inflammasome in murine macrophages. One pathway is characterized by ion fluxes and the activation of iPLA2, the NLRP3 inflammasome, and cathepsin B for the maturation of pro-IL-1β and subsequent secretion. The other pathway results in necrotic cell death, marked by LDH and HMGB1 release, that is dependent on the NLRP3 inflammasome and cathepsin B activity. These NLRP3 inflammasome-dependent events only occur after exposure to lower toxin doses whereas higher toxin doses induce passive spilling of contents such as LDH, HMGB1, pro-caspase-1, and pro-IL-1β.

A model (Figure 5-1) can be postulated where invading bacteria secrete many CDC monomers that exist at a high concentration closest to the bacterial source, but as the toxin diffuses outwards, its concentration decreases. These higher doses would be expected to perforate nearby cells and bring about necrotic cell death characterized by LDH and HMGB1 release. These cells would also lose contents such as pro-caspase-1 and pro-IL-1β before activation and processing, respectively, could occur. This environment would most likely be advantageous to the pathogen since innate immune cells would be killed before having a chance to notify the rest of the immune system of a pathogenic threat. Moreover, extracellular HMGB1

could lead to uncontrolled inflammation, which occurs in the case of sepsis (Wang *et al.*, 1999; Wang *et al.*, 2004). On the other hand, lower CDC doses would activate the NLRP3 inflammasome for mature IL-1β secretion and regulated HMGB1 release. Though these cells would ultimately succumb to cell death, IL-1β and HMGB1 could still serve to recruit other innate inflammatory immune cells for the initiation of an immune response. However, this is purely speculative and it is difficult to predict if extracellular IL-1β and HMGB1 would play more of a detrimental or beneficial role. Additional work must be conducted *in vivo* to determine the contribution of the NLRP3 inflammasome, IL-1β, and HMGB1 in the host response to infection with CDC-secreting gram-positive bacteria. The NLRP3 inflammasome, IL-1β, and HMGB1 could be potential therapeutic targets if they did significantly contribute to disease in the context of gram-positive bacterial infection.
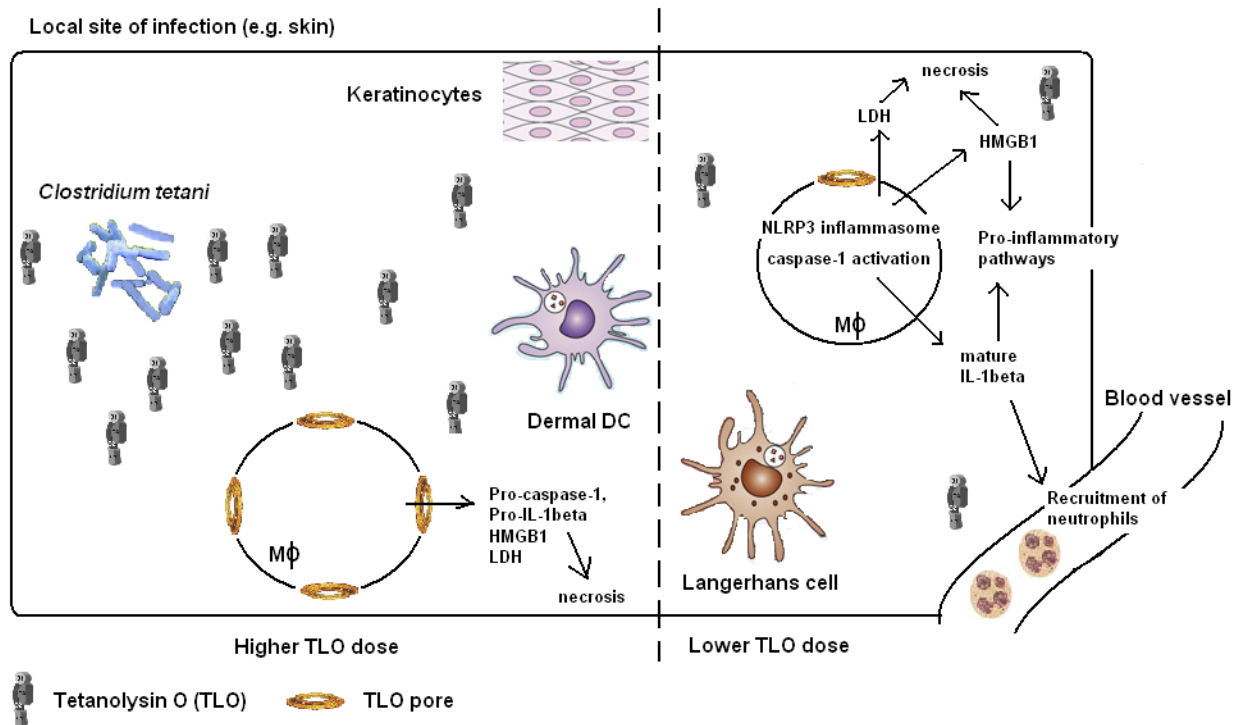
Figure 5-1: Model for TLO-induced IL-1β and HMGB1 release in the context of bacterial infection.

Bacterial infection by TLO-producing *C. tetani* might occur at a local site such as the skin where various cells such as keratinocytes, dermal dendritic cells (DC), Langerhans cells, and macrophages are present. Macrophages closest to the bacterial source would be exposed to the high concentrations of TLO, leading to necrotic cell death characterized by the release of HMGB1, LDH, inactive pro-caspase-1, and inactive pro-IL-1β. On the other hand, macrophages further from the bacterial source would encounter lower concentrations of TLO, which would enable NLRP3 inflammasome activation. This would then lead to HMGB1 release and mature IL-1β secretion, two factors that could enhance inflammation through the generation of additional pro-inflammatory molecules and recruitment of other innate immune cells such as neutrophils. This might be a last effort for these cells to stimulate immunity before also undergoing necrotic cell death.

Not only can this work enable a better understanding of the role of CDC in bacterial pathogenesis and the host response, but it is clear that CDC can serve as a useful tool to identify new intracellular pathways linked to NLRP3 and the inflammasome complex. Already, IL-1β and HMGB1 release have been identified as factors linked to the NLRP3 inflammasome that can contribute to disease. IL-1β has been shown to initiate inflammation for the generation of robust immune responses, but uncontrolled release can contribute to autoinflammatory disease. Disease can arise when mutations in the NLRP3 inflammasome lead to overactivation and subsequent constitutive IL-1β secretion (Masters *et al.*, 2009). Treatments such as anakinra (IL-1Ra) have been useful in controlling IL-1β levels in patients with autoinflammatory syndromes (Leslie *et al.*, 2006; Maksimovic *et al.*, 2008). Similarly, HMGB1 has been implicated in contributing to disease states such as sepsis and arthritis and neutralizing antibodies to HMGB1 help to lessen the severity of disease (Wang *et al.*, 1999; Andersson & Erlandsson-Harris, 2004; Andersson & Tracey, 2004; Wang *et al.*, 2004; Lotze & Tracey, 2005). Another disease thought to be impacted by HMGB1-induced inflammation is systemic lupus erythematosus (SLE) (Ardoin & Pisetsky, 2008). SLE is characterized by the formation of immune complexes, activation of

autoreactive B cells, generation of autoantibodies to nuclear factors, and production of high

levels of interferon-α (IFN-α). Increased cell death in the setting of autoimmune disease would

lead to increased release of HMGB1, which has been shown to participate in immune complexes

that induce IFN-α secretion and B cell activation. This would suggest that HMGB1 plays a

potential role in the pathogenesis of SLE. HMGB1 may also contribute to cancer where necrotic

tumor cells would be expected to release HMGB1 for the mediation of tumor cell invasion,

migration, growth, and spread via RAGE signaling (Ellerman *et al.*, 2007). Thus, identifying

new targets using CDC could lead to the development of new treatments for patients with

overactive inflammation, autoimmune diseases, and cancer.

Lastly, we have isolated a CDC-resistant dendritic cell line that may serve as a useful tool

in the future to identify factors and pathways involved in CDC-induced pore formation and cell

damage. These pathways could be specific to CDC and other pore-forming toxins or could

extend to general mechanisms for defense against cell stress. Targeting these pathways would be

useful not only in combating bacterial infections, but also under circumstances of exposure to

environmental insults, oxidative stress, and hypoxia/ischemia.

5.2   COMPARISON OF TLO TO OTHER CDC FAMILY MEMBERS

CDC share 30-60% homology in primary amino acid sequence (Billington *et al.*, 2000), so while

they share many similarities there could also be differences in function. Most CDC share

complete homology in the domain 4 undecapeptide sequence (consensus sequence:

ECTGLAWEWWR), which is important for CDC membrane insertion, the prepore to pore

transition, and sensitivity to reducing agents (Billington *et al.*, 2000; Soltani *et al.*, 2007).

However, vaginolysin (VLY; EKTGLVWEPWR), intermedilysin (ILY; GATGLAWEPWR), and pyolysin (PLO; EATGLAWDPWW) all lack the cysteine residue in the undecapeptide sequence, making them insensitive to reducing agents (Gelber *et al.*, 2008). Differences in overall amino acid sequence can also lead to unique functions for CDC. VLY and ILY both require binding to human CD59 for cytolytic activity (Soltani *et al.*, 2007; Gelber *et al.*, 2008) and listeriolysin O (LLO) is highly active at acidic pH (Beauregard *et al.*, 1997). TLO contains the consensus undecapeptide sequence (Genbank accession number YP_001921918) and therefore, would be expected to form pores in cell membranes and be sensitive to reducing agents. We believe that TLO binds cholesterol, since free cholesterol can block its actions, and we observe dye uptake by cells after exposure to TLO, which would suggest that TLO also induces pore formation. Additionally, cells have increased sensitivity to dye uptake after exposure to TLO that has been reduced with dithiothreitol (DTT). Thus, TLO is similar to most other CDC in its ability to bind cholesterol, form pores in the plasma membrane, and become more active in a reduced state.

General downstream pathways of cell surface pore formation might be expected to occur for all CDC that bind cholesterol and form pores. These pathways include pore sensing (calcium fluxes, transcription factor activation, cytokine release) and membrane resealing (Walev *et al.*, 2001a; Walev *et al.*, 2001b; Uhlik *et al.*, 2003; Husmann *et al.*, 2006; Ratner *et al.*, 2006; Idone *et al.*, 2008; Kloft *et al.*, 2009). We have observed TLO-induced calcium fluxes as measured with calcium-sensitive dyes (data not shown), but fail to observe transcription factor activation (NF-κB, p38 MAPK) and cytokine release (data not shown), other than IL-1β. Transcription factor activation and cytokine release can occur both at high toxin doses where pores are formed and at low toxin doses where minimal membrane damage is evident. The latter effect is thought

to be caused by TLR4 activation, which has been shown for a few other CDC like ALO (Malley *et al.*, 2003; Park *et al.*, 2004a; Ito *et al.*, 2005; Srivastava *et al.*, 2005). In our hands, ALO does not induce transcription factor activation or cytokine release when applied in the presence of free cholesterol (data not shown), suggesting that CDC do not act as TLR4 agonists. This disparity may be explained by contamination of CDC with well accepted TLR agonists such as endotoxin. In the former case, it is unclear why TLO does not elicit these cellular responses. It is possible that a more careful titration must be conducted to identify a high enough toxin dose where pores are formed, but cells still retain their functions. Lastly, we have not yet fully assessed membrane resealing processes after TLO exposure, but have observed viability dye exclusion from a population of TLO-treated cells after an initial time point of complete viability dye staining. These results would suggest that a portion of TLO-treated cells recover from initial membrane damage. Taken together, many processes related to pore formation observed for other CDC (e.g. calcium flux, IL-1β release, membrane repair) seem to hold for TLO. Differences observed between TLO and other CDC could be explained by mere technical challenges or may in fact be due to slight differences in amino acid sequence. Thus, it is important to test each CDC for a specific function (pore-dependent or pore-independent) before making conclusions about the CDC family as a whole.

5.3   APPLICATION OF FINDINGS TO OTHER CELL SYSTEMS AND DOWNSTREAM PRO-INFLAMMATORY PATHWAYS

Though our work focused on the response of the macrophage to CDC, it would be expected that other TLR-primed, NLRP3 inflammasome-containing cells would also be capable of making IL-

1 after toxin exposure. NLRP3 inflammasome-dependent release of IL-1β has been demonstrated for murine DC exposed to *Candida albicans* (Gross *et al.*, 2009; Kumar *et al.*, 2009b) and particulate adjuvants (Sharp *et al.*, 2009), human THP-1 monocytes exposed to α-hemolysin from *S. aureus* (Craven *et al.*, 2009), and human keratinocytes treated with contact sensitizers like trinitro-chlorobenzene (Watanabe *et al.*, 2007). Epithelial cells also appear to have the potential for NLRP3-dependent IL-1β release as supported by two studies. First, human airway epithelial cells upregulate Nlrp3 mRNA and secrete IL-1β after exposure to Influenza A Virus (Allen *et al.*, 2009). This would suggest that NLRP3 plays a role in IL-1β secretion during influenza infection, but this was not directly tested. Second, human cervical epithelial cells (HeLa 229) contain a functional NLRP3 inflammasome that becomes activated during infection with *Chlamydia trachomatis* (Abdul-Sater *et al.*, 2009), but IL-1β secretion was not assessed. It might also be expected that other cell types containing a functional NLRP3 inflammasome could mediate HMGB1 release after low dose CDC exposure. However, there is an added level of complexity in that any stimulator of necrosis (e.g. high dose CDC) could also cause HMGB1 release in a manner independent of the NLRP3 inflammasome. Since HMGB1 is present in all nucleated cells, most cells are capable of releasing HMGB1. Thus, release of mature IL-1β is more selective than HMGB1 release, since the former event only occurs in NLRP3 inflammasome-containing cells.

Aside from IL-1β and HMGB1, we have also observed that TLO induces the secretion of IL-1α from macrophages. It is likely that TLO causes NLRP3-dependent IL-18 release, but this has yet to be tested. In contrast, we have no evidence that TLO can induce other pro-inflammatory cytokines such as TNF-α and IL-6. This difference may be explained by the mechanisms of cytokine processing and release required for leaderless peptides such as IL-1α,

IL-1β, IL-18, and HMGB1. Ligation of IL-1RI, which is highly expressed on many cell types, with IL-1α and IL-1β, would lead to the secretion of additional pro-inflammatory factors such as COX-2, iNOS, chemokines, cytokines, and matrix metalloproteinases (Apte & Voronov, 2008) to create a positive feedback loop of inflammatory responses. IL-1 also causes the upregulation of adhesion molecules on endothelial cells, stromal cells, and leukocytes, enabling the recruitment of inflammatory cells (e.g. neutrophils) from the blood into the tissues (Apte & Voronov, 2008). In terms of adaptive immunity, IL-1 contributes to Th2 polarization (Nakae *et al.*, 2003), antibody production (Nakae *et al.*, 2001), and Th17 responses (Sutton *et al.*, 2006; Acosta-Rodriguez *et al.*, 2007). Similarly to IL-1, IL-18 also amplifies the inflammatory response by inducing pro-inflammatory cytokines and chemokines like GM-CSF, TNF-α, IL-1β, IL-6, and IL-8 and upregulating adhesion molecules (Puren *et al.*, 1998; Arend *et al.*, 2008). IL-18 stimulates the activity of innate immune cells like neutrophils and NK cells and adaptive immune cells such as CD8$^+$ effector T cells, Th1 cells, Th2 cells, and Th17 cells (Arend *et al.*, 2008). These T helper responses depend on other cytokines that act in concert with IL-18, namely IL-12 for Th1 responses (Robinson *et al.*, 1997), IL-2 for Th2 responses (Hoshino *et al.*, 1999), and IL-23 for IL-17 responses (Weaver *et al.*, 2006). Well known for its IFN-γ-promoting ability, IL-18 synergizes with IL-12 to induce IFN-γ from Th1 cells (Robinson *et al.*, 1997), CD8$^+$ T cells (Okamoto *et al.*, 1999), and activated B cells (Yoshimoto *et al.*, 1997). IL-1 and IL-18 impact so many cell types and inflammatory processes that overexpression often leads to disease. The list of these diseases includes, but is not limited to: (1) For IL-1 – autoinflammation (Masters *et al.*, 2009), sepsis (Dinarello, 1991), rheumatoid arthritis (RA) (Gabay, 2000), type 2 diabetes (Maedler *et al.*, 2009), cancer (Apte & Voronov, 2008), cardiovascular disease (Kleemann *et al.*, 2008; Vicenova *et al.*, 2009), and neurodegeneration

(Simi *et al.*, 2007), (2) For IL-18 – multiple sclerosis (Karni *et al.*, 2002), RA (Matsui *et al.*, 2003), inflammatory bowel diseases (Lochner & Forster, 2002; Reuter & Pizarro, 2004), psoriasis (Companjen *et al.*, 2004), atherosclerosis (Kleemann *et al.*, 2008), and cancer (Park *et al.*, 2007). Understanding the mechanisms that regulate the release of pro-inflammatory molecules, identifying the cell types that release these factors and determining their impact on other cells will be invaluable in identifying multiple therapeutic targets to treat many of these diseases.

5.4 TRANSLATING *IN VITRO* RESULTS TO *IN VIVO* MODELS

Precise amounts of CDC needed to induce pathways such as cytokine secretion or cell death are most likely different *in vitro* versus *in vivo*, but this is difficult to measure. Differences may arise due to several factors such as cell number, homogeneity vs. heterogeneity of cell populations, and amount of exogenous cholesterol present. *In vitro* settings allow for a controlled environment where cell number is fixed and exogenous cholesterol can be excluded to allow for more efficient toxin interaction with cells. Moreover, only one cell type is present so there is no impact of other cell types that would normally be present *in vivo*. Obtaining an accurate quantitative measurement of CDC concentrations at exact time points and locations *in vivo* would be difficult since the act of collecting the measurement could change the measurement. Only qualitative assumptions can be made, where toxin dose is highest at the bacterial source and lower as toxin diffuses away from the source. Due to this limitation, known *in vitro* doses cannot be compared to unknown amounts of CDC present *in vivo*.

Even more complicated is the comparison of different *in vivo* scenarios where the CDC dose required to bring about a specific effect could vary due to the site of bacterial infection. 100pmol of various CDC administered i.v. can bring about the death of a mouse within seconds (Watanabe *et al.*, 2006), but this could differ if CDC were administered through a non-systemic route. A more likely site of initial infection might be the lungs or skin and probably more toxin would be required to kill an organism if administered through these entry ways. Additionally, these locations would be expected to have more innate immune cells than the bloodstream such that immune responses might be more robust than if CDC-producing bacteria were only in the bloodstream.

Though CDC and host cell interactions *in vivo* are complex and exact CDC concentrations cannot be compared between *in vitro* and *in vivo* situations, our *in vitro* data provides qualitative information that can be used as a starting point for studying the role of CDC *in vivo*. Based on our *in vitro* data, we show that CDC at some concentration can induce mature IL-1β and HMGB1 release from murine macrophages. This *in vitro* finding could be applied to an *in vivo* model where mice are infected with CDC-producing bacteria at various MOIs or directly injected with different toxin doses through a route such as the skin. The contribution of CDC could be separated from that of whole bacteria by also infecting with a mutant CDC-secreting strain or a strain that does not secrete CDC. Tissue samples and serum samples could be collected and analyzed for mature IL-1β and HMGB1 content. It might be expected that at some time point and concentration of bacteria or purified CDC, both of these pro-inflammatory cytokines would be produced. To further test the role of the NLRP3 inflammasome, these experiments could be carried out in NLRP3$^{-/-}$, caspase-1$^{-/-}$, and ASC$^{-/-}$ mice. These studies could be supplemented with additional experiments to assess bacterial titer, the degree of tissue

144

inflammation, other markers of inflammation, the cells producing these inflammatory molecules, and the cellular composition of the tissue samples. Depending on these results, further studies on the generation of adaptive immune responses (e.g. antibody titers, antigen-specific T cells and their responses) would be warranted. Ultimately, it would be important to assess the survival outcome after infection with CDC-producing bacteria in order to determine if subsequent NLRP3-dependent responses are beneficial or detrimental to the host. Results of these studies would be the basis for generating novel anti-bacterial therapies.

BIBLIOGRAPHY

Abdul-Sater AA, Koo E, Hacker G & Ojcius DM. (2009). Inflammasome-dependent caspase-1 activation in cervical epithelial cells stimulates growth of the intracellular pathogen Chlamydia trachomatis. *J Biol Chem* **284,** 26789-26796.

Acosta-Rodriguez EV, Napolitani G, Lanzavecchia A & Sallusto F. (2007). Interleukins 1beta and 6 but not transforming growth factor-beta are essential for the differentiation of interleukin 17-producing human T helper cells. *Nat Immunol* **8,** 942-949.

Aga M, Johnson CJ, Hart AP, Guadarrama AG, Suresh M, Svaren J, Bertics PJ & Darien BJ. (2002). Modulation of monocyte signaling and pore formation in response to agonists of the nucleotide receptor P2X7. *J Leukoc Biol* **72,** 222-232.

Akhter A, Gavrilin MA, Frantz L, Washington S, Ditty C, Limoli D, Day C, Sarkar A, Newland C, Butchar J, Marsh CB, Wewers MD, Tridandapani S, Kanneganti TD & Amer AO. (2009). Caspase-7 activation by the Nlrc4/Ipaf inflammasome restricts Legionella pneumophila infection. *PLoS Pathog* **5,** e1000361.

Akira S, Takeda K & Kaisho T. (2001). Toll-like receptors: critical proteins linking innate and acquired immunity. *Nat Immunol* **2,** 675-680.

Aksentijevich I, Nowak M, Mallah M, Chae JJ, Watford WT, Hofmann SR, Stein L, Russo R, Goldsmith D, Dent P, Rosenberg HF, Austin F, Remmers EF, Balow JE, Jr., Rosenzweig S, Komarow H, Shoham NG, Wood G, Jones J, Mangra N, Carrero H, Adams BS, Moore TL, Schikler K, Hoffman H, Lovell DJ, Lipnick R, Barron K, O'Shea JJ, Kastner DL & Goldbach-Mansky R. (2002). De novo CIAS1 mutations, cytokine activation, and evidence for genetic heterogeneity in patients with neonatal-onset multisystem inflammatory disease (NOMID): a new member of the expanding family of pyrin-associated autoinflammatory diseases. *Arthritis Rheum* **46,** 3340-3348.

Allen IC, Scull MA, Moore CB, Holl EK, McElvania-TeKippe E, Taxman DJ, Guthrie EH, Pickles RJ & Ting JP. (2009). The NLRP3 inflammasome mediates in vivo innate immunity to influenza A virus through recognition of viral RNA. *Immunity* **30,** 556-565.

Amer A, Franchi L, Kanneganti TD, Body-Malapel M, Ozoren N, Brady G, Meshinchi S, Jagirdar R, Gewirtz A, Akira S & Nunez G. (2006). Regulation of Legionella phagosome maturation and infection through flagellin and host Ipaf. *J Biol Chem* **281,** 35217-35223.

Anderson CM, Bergher JP & Swanson RA. (2004). ATP-induced ATP release from astrocytes. *Journal of Neurochemistry* **88,** 246-256.

Andersson U & Erlandsson-Harris H. (2004). HMGB1 is a potent trigger of arthritis. *J Intern Med* **255,** 344-350.

Andersson U & Tracey KJ. (2004). HMGB1 as a mediator of necrosis-induced inflammation and a therapeutic target in arthritis. *Rheum Dis Clin North Am* **30,** 627-637, xi.

Andersson U, Wang H, Palmblad K, Aveberger AC, Bloom O, Erlandsson-Harris H, Janson A, Kokkola R, Zhang M, Yang H & Tracey KJ. (2000). High mobility group 1 protein (HMG-1) stimulates proinflammatory cytokine synthesis in human monocytes. *J Exp Med* **192,** 565-570.

Andrei C, Margiocco P, Poggi A, Lotti LV, Torrisi MR & Rubartelli A. (2004). Phospholipases C and A2 control lysosome-mediated IL-1 beta secretion: Implications for inflammatory processes. *Proc Natl Acad Sci U S A* **101,** 9745-9750.

Apte RN & Voronov E. (2008). Is interleukin-1 a good or bad 'guy' in tumor immunobiology and immunotherapy? *Immunol Rev* **222,** 222-241.

Ardoin SP & Pisetsky DS. (2008). The role of cell death in the pathogenesis of autoimmune disease: HMGB1 and microparticles as intercellular mediators of inflammation. *Mod Rheumatol* **18,** 319-326.

Arend WP. (1990). Interleukin-1 receptor antagonist: discovery, structure and properties. *Prog Growth Factor Res* **2,** 193-205.

Arend WP, Palmer G & Gabay C. (2008). IL-1, IL-18, and IL-33 families of cytokines. *Immunol Rev* **223,** 20-38.

Aroian R & van der Goot FG. (2007). Pore-forming toxins and cellular non-immune defenses (CNIDs). *Current Opinion in Microbiology* **10,** 57-61.

Averette KM, Pratt MR, Yang Y, Bassilian S, Whitelegge JP, Loo JA, Muir TW & Bradley KA. (2009). Anthrax lethal toxin induced lysosomal membrane permeabilization and cytosolic cathepsin release is Nlrp1b/Nalp1b-dependent. *PLoS One* **4,** e7913.

Bauernfeind FG, Horvath G, Stutz A, Alnemri ES, MacDonald K, Speert D, Fernandes-Alnemri T, Wu J, Monks BG, Fitzgerald KA, Hornung V & Latz E. (2009). Cutting edge: NF-kappaB activating pattern recognition and cytokine receptors license NLRP3 inflammasome activation by regulating NLRP3 expression. *J Immunol* **183,** 787-791.

Bavdek A, Gekara NO, Priselac D, Gutierrez Aguirre I, Darji A, Chakraborty T, Macek P, Lakey JH, Weiss S & Anderluh G. (2007). Sterol and pH interdependence in the binding, oligomerization, and pore formation of Listeriolysin O. *Biochemistry* **46,** 4425-4437.

Beauregard KE, Lee KD, Collier RJ & Swanson JA. (1997). pH-dependent perforation of macrophage phagosomes by listeriolysin O from Listeria monocytogenes. *J Exp Med* **186,** 1159-1163.

Benton KA, Everson MP & Briles DE. (1995). A pneumolysin-negative mutant of Streptococcus pneumoniae causes chronic bacteremia rather than acute sepsis in mice. *Infect Immun* **63,** 448-455.

Bergsbaken T, Fink SL & Cookson BT. (2009). Pyroptosis: host cell death and inflammation. *Nat Rev Microbiol* **7,** 99-109.

Bernheimer AW. (1948). Properties of certain rapidly acting bacterial toxins as illustrated by streptolysins O and S. *Microbiol Mol Biol Rev* **12,** 195-202.

Berry AM, Alexander JE, Mitchell TJ, Andrew PW, Hansman D & Paton JC. (1995). Effect of defined point mutations in the pneumolysin gene on the virulence of Streptococcus pneumoniae. *Infect Immun* **63,** 1969-1974.

Berry AM, Yother J, Briles DE, Hansman D & Paton JC. (1989). Reduced virulence of a defined pneumolysin-negative mutant of Streptococcus pneumoniae. *Infect Immun* **57,** 2037-2042.

Bhakdi S, Bayley H, Valeva A, Walev I, Walker B, Kehoe M & Palmer M. (1996). Staphylococcal alpha-toxin, streptolysin-O, and Escherichia coli hemolysin: prototypes of pore-forming bacterial cytolysins. *Arch Microbiol* **165,** 73-79.

Bhakdi S, Muhly M, Korom S & Hugo F. (1989). Release of interleukin-1 beta associated with potent cytocidal action of staphylococcal alpha-toxin on human monocytes. *Infect Immun* **57,** 3512-3519.

Bhakdi S, Tranum-Jensen J & Sziegoleit A. (1985). Mechanism of membrane damage by streptolysin-O. *Infect Immun* **47,** 52-60.

Billington SJ, Jost BH & Songer JG. (2000). Thiol-activated cytolysins: structure, function and role in pathogenesis. *FEMS Microbiology Letters* **182,** 197-205.

Bonaldi T, Talamo F, Scaffidi P, Ferrera D, Porto A, Bachi A, Rubartelli A, Agresti A & Bianchi ME. (2003). Monocytic cells hyperacetylate chromatin protein HMGB1 to redirect it towards secretion. *EMBO J* **22,** 5551-5560.

Boraschi D & Tagliabue A. (2006). The interleukin-1 receptor family. *Vitam Horm* **74,** 229-254.

Bours MJL, Swennen ELR, Di Virgilio F, Cronstein BN & Dagnelie PC. (2006). Adenosine 5'-triphosphate and adenosine as endogenous signaling molecules in immunity and inflammation. *Pharmacology & Therapeutics* **112,** 358-404.

Boyden ED & Dietrich WF. (2006). Nalp1b controls mouse macrophage susceptibility to anthrax lethal toxin. *Nat Genet* **38,** 240-244.

Brough D, Le Feuvre RA, Wheeler RD, Solovyova N, Hilfiker S, Rothwell NJ & Verkhratsky A. (2003). Ca2+ stores and Ca2+ entry differentially contribute to the release of IL-1 beta and IL-1 alpha from murine macrophages. *J Immunol* **170,** 3029-3036.

Bryan NB, Dorfleutner A, Rojanasakul Y & Stehlik C. (2009). Activation of inflammasomes requires intracellular redistribution of the apoptotic speck-like protein containing a caspase recruitment domain. *J Immunol* **182,** 3173-3182.

Bussolino F, Breviario F, Tetta C, Aglietta M, Mantovani A & Dejana E. (1986). Interleukin 1 stimulates platelet-activating factor production in cultured human endothelial cells. *J Clin Invest* **77,** 2027-2033.

Case CL, Shin S & Roy CR. (2009). Asc and Ipaf Inflammasomes direct distinct pathways for caspase-1 activation in response to Legionella pneumophila. *Infect Immun* **77,** 1981-1991.

Cassel SL, Joly S & Sutterwala FS. (2009). The NLRP3 inflammasome: a sensor of immune danger signals. *Semin Immunol* **21,** 194-198.

Cervantes J, Nagata T, Uchijima M, Shibata K & Koide Y. (2008). Intracytosolic Listeria monocytogenes induces cell death through caspase-1 activation in murine macrophages. *Cell Microbiol* **10,** 41-52.

Chakraborty T, Schmid A, Notermans S & Benz R. (1990). Aerolysin of Aeromonas sobria: evidence for formation of ion-permeable channels and comparison with alpha-toxin of Staphylococcus aureus. *Infect Immun* **58,** 2127-2132.

Chen G, Li J, Ochani M, Rendon-Mitchell B, Qiang X, Susarla S, Ulloa L, Yang H, Fan S, Goyert SM, Wang P, Tracey KJ, Sama AE & Wang H. (2004). Bacterial endotoxin stimulates macrophages to release HMGB1 partly through CD14- and TNF-dependent mechanisms. *J Leukoc Biol* **76,** 994-1001.

Chessell IP, Grahames CBA, Michel AD & Humphrey PPA. (2001). Dynamics of P2X7 receptor pore dilation: Pharmacological and functional consequences. *Drug Development Research* **53,** 60-65.

Chu J, Thomas LM, Watkins SC, Franchi L, Nunez G & Salter RD. (2009). Cholesterol-dependent cytolysins induce rapid release of mature IL-1beta from murine macrophages

in a NLRP3 inflammasome and cathepsin B-dependent manner. *J Leukoc Biol* **86,** 1227-1238.

Cocklin S, Jost M, Robertson NM, Weeks SD, Weber H-W, Young E, Seal S, Zhang C, Mosser E, Loll PJ, Saunders AJ, Rest RF & Chaiken IM. (2006). Real-time monitoring of the membrane-binding and insertion properties of the cholesterol-dependent cytolysin anthrolysin O from Bacillus anthracis. *Journal of Molecular Recognition* **19,** 354-362.

Coers J, Vance RE, Fontana MF & Dietrich WF. (2007). Restriction of Legionella pneumophila growth in macrophages requires the concerted action of cytokine and Naip5/Ipaf signalling pathways. *Cell Microbiol* **9,** 2344-2357.

Cohn M & Meek GA. (1957). The mechanism of hydrolysis of adenosine di- and tri-phosphate catalysed by potato apyrase. *Biochem J* **66,** 128-130.

Companjen A, van der Wel L, van der Fits L, Laman J & Prens E. (2004). Elevated interleukin-18 protein expression in early active and progressive plaque-type psoriatic lesions. *Eur Cytokine Netw* **15,** 210-216.

Cowan GJ, Atkins HS, Johnson LK, Titball RW & Mitchell TJ. (2007). Immunisation with anthrolysin O or a genetic toxoid protects against challenge with the toxin but not against Bacillus anthracis. *Vaccine* **25,** 7197-7205.

Craven RR, Gao X, Allen IC, Gris D, Bubeck Wardenburg J, McElvania-Tekippe E, Ting JP & Duncan JA. (2009). Staphylococcus aureus alpha-hemolysin activates the NLRP3-inflammasome in human and mouse monocytic cells. *PLoS One* **4,** e7446.

Davies JQ & Gordon S. (2005). Isolation and culture of murine macrophages. *Methods Mol Biol* **290,** 91-103.

Di Virgilio F. (2005). Purinergic mechanism in the immune system: A signal of danger for dendritic cells. *Purinergic Signalling* **1,** 205-209.

Di Virgilio F, Chiozzi P, Ferrari D, Falzoni S, Sanz JM, Morelli A, Torboli M, Bolognesi G & Baricordi OR. (2001). Nucleotide receptors: an emerging family of regulatory molecules in blood cells. *Blood* **97,** 587-600.

Dinarello CA. (1991). The proinflammatory cytokines interleukin-1 and tumor necrosis factor and treatment of the septic shock syndrome. *J Infect Dis* **163,** 1177-1184.

Dinarello CA. (2009). Immunological and inflammatory functions of the interleukin-1 family. *Annu Rev Immunol* **27,** 519-550.

Dostert C, Petrilli V, Van Bruggen R, Steele C, Mossman BT & Tschopp J. (2008). Innate immune activation through Nalp3 inflammasome sensing of asbestos and silica. *Science* **320,** 674-677.

Dumitriu IE, Baruah P, Manfredi AA, Bianchi ME & Rovere-Querini P. (2005). HMGB1: guiding immunity from within. *Trends Immunol* **26,** 381-387.

Duncan JL & Buckingham L. (1978). Increased resistance to streptolysin O in mammalian cells treated with oxygenated derivatives of cholesterol. *Infect Immun* **22,** 94-100.

Dunne A & O'Neill LA. (2003). The interleukin-1 receptor/Toll-like receptor superfamily: signal transduction during inflammation and host defense. *Sci STKE* **2003,** re3.

Eisenbarth SC, Colegio OR, O'Connor W, Sutterwala FS & Flavell RA. (2008). Crucial role for the Nalp3 inflammasome in the immunostimulatory properties of aluminium adjuvants. *Nature* **453,** 1122-1126.

Ellerman JE, Brown CK, de Vera M, Zeh HJ, Billiar T, Rubartelli A & Lotze MT. (2007). Masquerader: high mobility group box-1 and cancer. *Clin Cancer Res* **13,** 2836-2848.

Faustin B, Lartigue L, Bruey JM, Luciano F, Sergienko E, Bailly-Maitre B, Volkmann N, Hanein D, Rouiller I & Reed JC. (2007). Reconstituted NALP1 inflammasome reveals two-step mechanism of caspase-1 activation. *Mol Cell* **25,** 713-724.

Ferrari D, Pizzirani C, Adinolfi E, Lemoli RM, Curti A, Idzko M, Panther E & Di Virgilio F. (2006). The P2X7 Receptor: A Key Player in IL-1 Processing and Release. *J Immunol* **176,** 3877-3883.

Fink SL & Cookson BT. (2005). Apoptosis, pyroptosis, and necrosis: mechanistic description of dead and dying eukaryotic cells. *Infect Immun* **73,** 1907-1916.

Franchi L, Amer A, Body-Malapel M, Kanneganti TD, Ozoren N, Jagirdar R, Inohara N, Vandenabeele P, Bertin J, Coyle A, Grant EP & Nunez G. (2006). Cytosolic flagellin requires Ipaf for activation of caspase-1 and interleukin 1beta in salmonella-infected macrophages. *Nat Immunol* **7,** 576-582.

Franchi L, Eigenbrod T, Munoz-Planillo R & Nunez G. (2009). The inflammasome: a caspase-1-activation platform that regulates immune responses and disease pathogenesis. *Nat Immunol* **10,** 241-247.

Gabay C. (2000). IL-1 inhibitors: novel agents in the treatment of rheumatoid arthritis. *Expert Opin Investig Drugs* **9,** 113-127.

Gardella S, Andrei C, Ferrera D, Lotti LV, Torrisi MR, Bianchi ME & Rubartelli A. (2002). The nuclear protein HMGB1 is secreted by monocytes via a non-classical, vesicle-mediated secretory pathway. *EMBO Rep* **3,** 995-1001.

Gauley J & Pisetsky DS. (2009). The translocation of HMGB1 during cell activation and cell death. *Autoimmunity* **42,** 299-301.

Gekara NO, Jacobs T, Chakraborty T & Weiss S. (2005). The cholesterol-dependent cytolysin listeriolysin O aggregates rafts via oligomerization. *Cell Microbiol* **7,** 1345-1356.

Gekara NO & Weiss S. (2004). Lipid rafts clustering and signalling by listeriolysin O. *Biochem Soc Trans* **32,** 712-714.

Gekara NO, Westphal K, Ma B, Rohde M, Groebe L & Weiss S. (2007). The multiple mechanisms of Ca2+ signalling by listeriolysin O, the cholesterol-dependent cytolysin of Listeria monocytogenes. *Cell Microbiol* **9,** 2008-2021.

Gelber SE, Aguilar JL, Lewis KL & Ratner AJ. (2008). Functional and phylogenetic characterization of Vaginolysin, the human-specific cytolysin from Gardnerella vaginalis. *J Bacteriol* **190,** 3896-3903.

Geoffroy C, Gaillard JL, Alouf JE & Berche P. (1987). Purification, characterization, and toxicity of the sulfhydryl-activated hemolysin listeriolysin O from Listeria monocytogenes. *Infect Immun* **55,** 1641-1646.

Giddings KS, Zhao J, Sims PJ & Tweten RK. (2004). Human CD59 is a receptor for the cholesterol-dependent cytolysin intermedilysin. *Nat Struct Mol Biol* **11,** 1173-1178.

Girardin SE, Sansonetti PJ & Philpott DJ. (2002). Intracellular vs extracellular recognition of pathogens--common concepts in mammals and flies. *Trends Microbiol* **10,** 193-199.

Girolomoni G, Lutz MB, Pastore S, Assmann CU, Cavani A & Ricciardi-Castagnoli P. (1995). Establishment of a cell line with features of early dendritic cell precursors from fetal mouse skin. *European Journal of Immunology* **25,** 2163-2169.

Goldmann O, Sastalla I, Wos-Oxley M, Rohde M & Medina E. (2009). Streptococcus pyogenes induces oncosis in macrophages through the activation of an inflammatory programmed cell death pathway. *Cell Microbiol* **11,** 138-155.

Gonzalez MR, Bischofberger M, Pernot L, van der Goot FG & Freche B. (2008). Bacterial pore-forming toxins: the (w)hole story? *Cell Mol Life Sci* **65,** 493-507.

Grandel U & Grimminger F. (2003). Endothelial responses to bacterial toxins in sepsis. *Crit Rev Immunol* **23,** 267-299.

Gross O, Poeck H, Bscheider M, Dostert C, Hannesschlager N, Endres S, Hartmann G, Tardivel A, Schweighoffer E, Tybulewicz V, Mocsai A, Tschopp J & Ruland J. (2009). Syk kinase signalling couples to the Nlrp3 inflammasome for anti-fungal host defence. *Nature* **459,** 433-436.

Gurcel L, Abrami L, Girardin S, Tschopp J & van der Goot FG. (2006). Caspase-1 activation of lipid metabolic pathways in response to bacterial pore-forming toxins promotes cell survival. *Cell* **126,** 1135-1145.

Hackett SP & Stevens DL. (1992). Streptococcal toxic shock syndrome: synthesis of tumor necrosis factor and interleukin-1 by monocytes stimulated with pyrogenic exotoxin A and streptolysin O. *J Infect Dis* **165,** 879-885.

Halle A, Hornung V, Petzold GC, Stewart CR, Monks BG, Reinheckel T, Fitzgerald KA, Latz E, Moore KJ & Golenbock DT. (2008). The NALP3 inflammasome is involved in the innate immune response to amyloid-beta. *Nat Immunol* **9,** 857-865.

Hamon MA, Batsche E, Regnault B, Tham TN, Seveau S, Muchardt C & Cossart P. (2007). Histone modifications induced by a family of bacterial toxins. *Proc Natl Acad Sci U S A* **104,** 13467-13472.

Harder J, Franchi L, Munoz-Planillo R, Park JH, Reimer T & Nunez G. (2009). Activation of the Nlrp3 inflammasome by Streptococcus pyogenes requires streptolysin O and NF-kappaB activation but proceeds independently of TLR signaling and P2X7 receptor. *J Immunol* **183,** 5823-5829.

Henderson B, Wilson M & Wren B. (1997). Are bacterial exotoxins cytokine network regulators? *Trends in Microbiology* **5,** 454-458.

Herbert D & Todd EW. (1941). Purification and properties of a haemolysin produced by group A haemolytic streptococci (streptolysin O). *Biochem J* **35,** 1124–1139.

Hewinson J, Moore SF, Glover C, Watts AG & MacKenzie AB. (2008). A key role for redox signaling in rapid P2X7 receptor-induced IL-1 beta processing in human monocytes. *J Immunol* **180,** 8410-8420.

Hoffman HM, Mueller JL, Broide DH, Wanderer AA & Kolodner RD. (2001). Mutation of a new gene encoding a putative pyrin-like protein causes familial cold autoinflammatory syndrome and Muckle-Wells syndrome. *Nat Genet* **29,** 301-305.

Hornung V, Bauernfeind F, Halle A, Samstad EO, Kono H, Rock KL, Fitzgerald KA & Latz E. (2008). Silica crystals and aluminum salts activate the NALP3 inflammasome through phagosomal destabilization. *Nat Immunol* **9,** 847-856.

Hoshino T, Kawase Y, Okamoto M, Yokota K, Yoshino K, Yamamura K, Miyazaki J, Young HA & Oizumi K. (2001). Cutting edge: IL-18-transgenic mice: in vivo evidence of a broad role for IL-18 in modulating immune function. *J Immunol* **166,** 7014-7018.

Hoshino T, Wiltrout RH & Young HA. (1999). IL-18 is a potent coinducer of IL-13 in NK and T cells: a new potential role for IL-18 in modulating the immune response. *J Immunol* **162,** 5070-5077.

Houldsworth S, Andrew PW & Mitchell TJ. (1994). Pneumolysin stimulates production of tumor necrosis factor alpha and interleukin-1 beta by human mononuclear phagocytes. *Infect Immun* **62,** 1501-1503.

Hsu LC, Ali SR, McGillivray S, Tseng PH, Mariathasan S, Humke EW, Eckmann L, Powell JJ, Nizet V, Dixit VM & Karin M. (2008). A NOD2-NALP1 complex mediates caspase-1-dependent IL-1beta secretion in response to Bacillus anthracis infection and muramyl dipeptide. *Proc Natl Acad Sci U S A* **105,** 7803-7808.

Husmann M, Dersch K, Bobkiewicz W, Beckmann E, Veerachato G & Bhakdi S. (2006). Differential role of p38 mitogen activated protein kinase for cellular recovery from attack by pore-forming S. aureus alpha-toxin or streptolysin O. *Biochem Biophys Res Commun* **344,** 1128-1134.

Idone V, Tam C, Goss JW, Toomre D, Pypaert M & Andrews NW. (2008). Repair of injured plasma membrane by rapid Ca2+-dependent endocytosis. *J Cell Biol* **180,** 905-914.

Iliev AI, Djannatian JR, Nau R, Mitchell TJ & Wouters FS. (2007). Cholesterol-dependent actin remodeling via RhoA and Rac1 activation by the Streptococcus pneumoniae toxin pneumolysin. *Proc Natl Acad Sci U S A* **104,** 2897-2902.

Iliev AI, Djannatian JR, Opazo F, Gerber J, Nau R, Mitchell TJ & Wouters FS. (2009). Rapid microtubule bundling and stabilization by the Streptococcus pneumoniae neurotoxin pneumolysin in a cholesterol-dependent, non-lytic and Src-kinase dependent manner inhibits intracellular trafficking. *Mol Microbiol* **71,** 461-477.

Inohara N & Nunez G. (2003). NODs: intracellular proteins involved in inflammation and apoptosis. *Nat Rev Immunol* **3,** 371-382.

Inohara N, Ogura Y & Nunez G. (2002). Nods: a family of cytosolic proteins that regulate the host response to pathogens. *Curr Opin Microbiol* **5,** 76-80.

Ito Y, Kawamura I, Kohda C, Tsuchiya K, Nomura T & Mitsuyama M. (2005). Seeligeriolysin O, a protein toxin of Listeria seeligeri, stimulates macrophage cytokine production via Toll-like receptors in a profile different from that induced by other bacterial ligands. *Int Immunol* **17,** 1597-1606.

Javaherian K, Liu JF & Wang JC. (1978). Nonhistone proteins HMG1 and HMG2 change the DNA helical structure. *Science* **199,** 1345-1346.

Johnson MK, Geoffroy C & Alouf JE. (1980). Binding of cholesterol by sulfhydryl-activated cytolysins. *Infect Immun* **27,** 97-101.

Jones MR, Simms BT, Lupa MM, Kogan MS & Mizgerd JP. (2005). Lung NF-kappaB activation and neutrophil recruitment require IL-1 and TNF receptor signaling during pneumococcal pneumonia. *J Immunol* **175,** 7530-7535.

Jost BH, Songer JG & Billington SJ. (1999). An Arcanobacterium (Actinomyces) pyogenes mutant deficient in production of the pore-forming cytolysin pyolysin has reduced virulence. *Infect Immun* **67,** 1723-1728.

Kahlenberg JM, Lundberg KC, Kertesy SB, Qu Y & Dubyak GR. (2005). Potentiation of caspase-1 activation by the P2X7 receptor is dependent on TLR signals and requires NF-kappaB-driven protein synthesis. *J Immunol* **175,** 7611-7622.

Kanneganti T-D, Lamkanfi M, Kim Y-G, Chen G, Park J-H, Franchi L, Vandenabeele P & Nunez G. (2007). Pannexin-1-Mediated Recognition of Bacterial Molecules Activates the Cryopyrin Inflammasome Independent of Toll-like Receptor Signaling. *Immunity* **26,** 433-443.

Kanneganti TD, Body-Malapel M, Amer A, Park JH, Whitfield J, Franchi L, Taraporewala ZF, Miller D, Patton JT, Inohara N & Nunez G. (2006a). Critical role for Cryopyrin/Nalp3 in activation of caspase-1 in response to viral infection and double-stranded RNA. *J Biol Chem* **281,** 36560-36568.

Kanneganti TD, Ozoren N, Body-Malapel M, Amer A, Park JH, Franchi L, Whitfield J, Barchet W, Colonna M, Vandenabeele P, Bertin J, Coyle A, Grant EP, Akira S & Nunez G. (2006b). Bacterial RNA and small antiviral compounds activate caspase-1 through cryopyrin/Nalp3. *Nature* **440,** 233-236.

Karni A, Koldzic DN, Bharanidharan P, Khoury SJ & Weiner HL. (2002). IL-18 is linked to raised IFN-gamma in multiple sclerosis and is induced by activated CD4(+) T cells via CD40-CD40 ligand interactions. *J Neuroimmunol* **125,** 134-140.

Kleemann R, Zadelaar S & Kooistra T. (2008). Cytokines and atherosclerosis: a comprehensive review of studies in mice. *Cardiovasc Res* **79,** 360-376.

Kloft N, Busch T, Neukirch C, Weis S, Boukhallouk F, Bobkiewicz W, Cibis I, Bhakdi S & Husmann M. (2009). Pore-forming toxins activate MAPK p38 by causing loss of cellular potassium. *Biochem Biophys Res Commun*.

Kokkola R, Andersson A, Mullins G, Ostberg T, Treutiger CJ, Arnold B, Nawroth P, Andersson U, Harris RA & Harris HE. (2005). RAGE is the major receptor for the proinflammatory activity of HMGB1 in rodent macrophages. *Scand J Immunol* **61,** 1-9.

Kumar H, Kawai T & Akira S. (2009a). Toll-like receptors and innate immunity. *Biochem Biophys Res Commun* **388,** 621-625.

Kumar H, Kumagai Y, Tsuchida T, Koenig PA, Satoh T, Guo Z, Jang MH, Saitoh T, Akira S & Kawai T. (2009b). Involvement of the NLRP3 inflammasome in innate and humoral adaptive immune responses to fungal beta-glucan. *J Immunol* **183,** 8061-8067.

Lamkanfi M, Amer A, Kanneganti TD, Munoz-Planillo R, Chen G, Vandenabeele P, Fortier A, Gros P & Nunez G. (2007). The Nod-like receptor family member Naip5/Birc1e restricts Legionella pneumophila growth independently of caspase-1 activation. *J Immunol* **178,** 8022-8027.

Lamkanfi M, Kanneganti TD, Van Damme P, Vanden Berghe T, Vanoverberghe I, Vandekerckhove J, Vandenabeele P, Gevaert K & Nunez G. (2008). Targeted peptidecentric proteomics reveals caspase-7 as a substrate of the caspase-1 inflammasomes. *Mol Cell Proteomics* **7,** 2350-2363.

Lange SS & Vasquez KM. (2009). HMGB1: the jack-of-all-trades protein is a master DNA repair mechanic. *Mol Carcinog* **48,** 571-580.

Le Feuvre RA, Brough D, Iwakura Y, Takeda K & Rothwell NJ. (2002). Priming of macrophages with lipopolysaccharide potentiates P2X7-mediated cell death via a caspase-1-dependent mechanism, independently of cytokine production. *J Biol Chem* **277,** 3210-3218.

Leslie KS, Lachmann HJ, Bruning E, McGrath JA, Bybee A, Gallimore JR, Roberts PF, Woo P, Grattan CE & Hawkins PN. (2006). Phenotype, genotype, and sustained response to anakinra in 22 patients with autoinflammatory disease associated with CIAS-1/NALP3 mutations. *Arch Dermatol* **142,** 1591-1597.

Li H, Willingham SB, Ting JP & Re F. (2008). Cutting edge: inflammasome activation by alum and alum's adjuvant effect are mediated by NLRP3. *J Immunol* **181,** 17-21.

Lich JD, Arthur JC & Ting JPY. (2006). Cryopyrin: In from the Cold. *Immunity* **24,** 241-243.

Lichtman AH, Chin J, Schmidt JA & Abbas AK. (1988). Role of interleukin 1 in the activation of T lymphocytes. *Proc Natl Acad Sci U S A* **85,** 9699-9703.

Lightfield KL, Persson J, Brubaker SW, Witte CE, von Moltke J, Dunipace EA, Henry T, Sun YH, Cado D, Dietrich WF, Monack DM, Tsolis RM & Vance RE. (2008). Critical function for Naip5 in inflammasome activation by a conserved carboxy-terminal domain of flagellin. *Nat Immunol* **9,** 1171-1178.

Liu S, Stolz DB, Sappington PL, Macias CA, Killeen ME, Tenhunen JJ, Delude RL & Fink MP. (2006). HMGB1 is secreted by immunostimulated enterocytes and contributes to cytomix-induced hyperpermeability of Caco-2 monolayers. *Am J Physiol Cell Physiol* **290,** C990-999.

Lochner M & Forster I. (2002). Anti-interleukin-18 therapy in murine models of inflammatory bowel disease. *Pathobiology* **70,** 164-169.

Locovei S, Scemes E, Qiu F, Spray DC & Dahl G. (2007). Pannexin1 is part of the pore forming unit of the P2X7 receptor death complex. *FEBS Letters* **581,** 483-488.

Lotze MT & Tracey KJ. (2005). High-mobility group box 1 protein (HMGB1): nuclear weapon in the immune arsenal. *Nat Rev Immunol* **5,** 331-342.

Lyons-Giordano B, Pratta MA, Galbraith W, Davis GL & Arner EC. (1993). Interleukin-1 differentially modulates chondrocyte expression of cyclooxygenase-2 and phospholipase A2. *Exp Cell Res* **206,** 58-62.

Maedler K, Dharmadhikari G, Schumann DM & Storling J. (2009). Interleukin-1 beta targeted therapy for type 2 diabetes. *Expert Opin Biol Ther* **9,** 1177-1188.

Maksimovic L, Stirnemann J, Caux F, Ravet N, Rouaghe S, Cuisset L, Letellier E, Grateau G, Morin AS & Fain O. (2008). New CIAS1 mutation and anakinra efficacy in overlapping of Muckle-Wells and familial cold autoinflammatory syndromes. *Rheumatology (Oxford)* **47,** 309-310.

Malley R, Henneke P, Morse SC, Cieslewicz MJ, Lipsitch M, Thompson CM, Kurt-Jones E, Paton JC, Wessels MR & Golenbock DT. (2003). Recognition of pneumolysin by Toll-like receptor 4 confers resistance to pneumococcal infection. *Proc Natl Acad Sci U S A* **100,** 1966-1971.

Mariathasan S, Newton K, Monack DM, Vucic D, French DM, Lee WP, Roose-Girma M, Erickson S & Dixit VM. (2004). Differential activation of the inflammasome by caspase-1 adaptors ASC and Ipaf. *Nature* **430,** 213-218.

Mariathasan S, Weiss DS, Newton K, McBride J, O'Rourke K, Roose-Girma M, Lee WP, Weinrauch Y, Monack DM & Dixit VM. (2006). Cryopyrin activates the inflammasome in response to toxins and ATP. *Nature* **440,** 228-232.

Martin MU & Wesche H. (2002). Summary and comparison of the signaling mechanisms of the Toll/interleukin-1 receptor family. *Biochim Biophys Acta* **1592,** 265-280.

Martinon F, Mayor A & Tschopp J. (2009). The inflammasomes: guardians of the body. *Annu Rev Immunol* **27,** 229-265.

Martinon F, Petrilli V, Mayor A, Tardivel A & Tschopp J. (2006). Gout-associated uric acid crystals activate the NALP3 inflammasome. *Nature* **440,** 237-241.

Masters SL, Simon A, Aksentijevich I & Kastner DL. (2009). Horror autoinflammaticus: the molecular pathophysiology of autoinflammatory disease (*). *Annu Rev Immunol* **27,** 621-668.

Matsui K, Tsutsui H & Nakanishi K. (2003). Pathophysiological roles for IL-18 in inflammatory arthritis. *Expert Opin Ther Targets* **7,** 701-724.

Matzinger P. (2002). The Danger Model: A Renewed Sense of Self. *Science* **296,** 301-305.

Mayor A, Martinon F, De Smedt T, Petrilli V & Tschopp J. (2007). A crucial function of SGT1 and HSP90 in inflammasome activity links mammalian and plant innate immune responses. *Nat Immunol* **8,** 497-503.

Medzhitov R. (2001). Toll-like receptors and innate immunity. *Nat Rev Immunol* **1,** 135-145.

Mehta VB, Hart J & Wewers MD. (2001). ATP-stimulated release of interleukin (IL)-1beta and IL-18 requires priming by lipopolysaccharide and is independent of caspase-1 cleavage. *J Biol Chem* **276,** 3820-3826.

Meissner F, Molawi K & Zychlinsky A. (2008). Superoxide dismutase 1 regulates caspase-1 and endotoxic shock. *Nat Immunol* **9,** 866-872.

Mendes AF, Carvalho AP, Caramona MM & Lopes MC. (2001). Diphenyleneiodonium inhibits NF-kappaB activation and iNOS expression induced by IL-1beta: involvement of reactive oxygen species. *Mediators Inflamm* **10,** 209-215.

Mertens M & Singh JA. (2009). Anakinra for rheumatoid arthritis: a systematic review. *J Rheumatol* **36,** 1118-1125.

Miao EA, Andersen-Nissen E, Warren SE & Aderem A. (2007). TLR5 and Ipaf: dual sensors of bacterial flagellin in the innate immune system. *Semin Immunopathol* **29,** 275-288.

Miao EA, Ernst RK, Dors M, Mao DP & Aderem A. (2008). Pseudomonas aeruginosa activates caspase 1 through Ipaf. *Proc Natl Acad Sci U S A* **105,** 2562-2567.

Mitchell TJ, Andrew PW, Saunders FK, Smith AN & Boulnois GJ. (1991). Complement activation and antibody binding by pneumolysin via a region of the toxin homologous to a human acute-phase protein. *Mol Microbiol* **5,** 1883-1888.

Mitsui K, Mitsui N, Kobashi K & Hase J. (1982). High-molecular-weight hemolysin of Clostridium tetani. *Infect Immun* **35,** 1086-1090.

Morgan PJ, Hyman SC, Rowe AJ, Mitchell TJ, Andrew PW & Saibil HR. (1995). Subunit organisation and symmetry of pore-forming, oligomeric pneumolysin. *FEBS Lett* **371,** 77-80.

Mosser EM & Rest RF. (2006). The Bacillus anthracis cholesterol-dependent cytolysin, Anthrolysin O, kills human neutrophils, monocytes and macrophages. *BMC Microbiol* **6,** 56.

Munoz-Planillo R, Franchi L, Miller LS & Nunez G. (2009). A critical role for hemolysins and bacterial lipoproteins in Staphylococcus aureus-induced activation of the Nlrp3 inflammasome. *J Immunol* **183,** 3942-3948.

Nakae S, Asano M, Horai R, Sakaguchi N & Iwakura Y. (2001). IL-1 enhances T cell-dependent antibody production through induction of CD40 ligand and OX40 on T cells. *J Immunol* **167,** 90-97.

Nakae S, Komiyama Y, Yokoyama H, Nambu A, Umeda M, Iwase M, Homma I, Sudo K, Horai R, Asano M & Iwakura Y. (2003). IL-1 is required for allergen-specific Th2 cell activation and the development of airway hypersensitivity response. *Int Immunol* **15,** 483-490.

Nakanishi K, Yoshimoto T, Tsutsui H & Okamura H. (2001a). Interleukin-18 is a unique cytokine that stimulates both Th1 and Th2 responses depending on its cytokine milieu. *Cytokine Growth Factor Rev* **12,** 53-72.

Nakanishi K, Yoshimoto T, Tsutsui H & Okamura H. (2001b). Interleukin-18 regulates both Th1 and Th2 responses. *Annu Rev Immunol* **19,** 423-474.

Nakouzi A, Rivera J, Rest RF & Casadevall A. (2008). Passive administration of monoclonal antibodies to anthrolysin O prolong survival in mice lethally infected with Bacillus anthracis. *BMC Microbiol* **8,** 159.

Netea MG, Van der Meer JW & Kullberg BJ. (2004). Toll-like receptors as an escape mechanism from the host defense. *Trends Microbiol* **12,** 484-488.

Newman ZL, Leppla SH & Moayeri M. (2009). CA-074Me protection against anthrax lethal toxin. *Infect Immun*.

Ng G, Sharma K, Ward SM, Desrosiers MD, Stephens LA, Schoel WM, Li T, Lowell CA, Ling CC, Amrein MW & Shi Y. (2008). Receptor-independent, direct membrane binding leads to cell-surface lipid sorting and Syk kinase activation in dendritic cells. *Immunity* **29,** 807-818.

Nishibori T, Xiong H, Kawamura I, Arakawa M & Mitsuyama M. (1996). Induction of cytokine gene expression by listeriolysin O and roles of macrophages and NK cells. *Infect Immun* **64,** 3188-3195.

Nomura T, Kawamura I, Kohda C, Baba H, Ito Y, Kimoto T, Watanabe I & Mitsuyama M. (2007). Irreversible loss of membrane-binding activity of Listeria-derived cytolysins in non-acidic conditions: a distinct difference from allied cytolysins produced by other Gram-positive bacteria. *Microbiology* **153,** 2250-2258.

Okamoto I, Kohno K, Tanimoto T, Ikegami H & Kurimoto M. (1999). Development of CD8+ effector T cells is differentially regulated by IL-18 and IL-12. *J Immunol* **162,** 3202-3211.

Olofsson A, Hebert H & Thelestam M. (1993). The projection structure of perfringolysin O (Clostridium perfringens theta-toxin). *FEBS Lett* **319,** 125-127.

Palmer M. (2001). The family of thiol-activated, cholesterol-binding cytolysins. *Toxicon* **39,** 1681-1689.

Palmer RM, Hickery MS, Charles IG, Moncada S & Bayliss MT. (1993). Induction of nitric oxide synthase in human chondrocytes. *Biochem Biophys Res Commun* **193,** 398-405.

Pang L & Knox AJ. (1997). Effect of interleukin-1 beta, tumour necrosis factor-alpha and interferon-gamma on the induction of cyclo-oxygenase-2 in cultured human airway smooth muscle cells. *Br J Pharmacol* **121,** 579-587.

Park JM, Ng VH, Maeda S, Rest RF & Karin M. (2004a). Anthrolysin O and Other Gram-positive Cytolysins Are Toll-like Receptor 4 Agonists. *J Exp Med* **200,** 1647-1655.

Park JS, Svetkauskaite D, He Q, Kim JY, Strassheim D, Ishizaka A & Abraham E. (2004b). Involvement of toll-like receptors 2 and 4 in cellular activation by high mobility group box 1 protein. *J Biol Chem* **279,** 7370-7377.

Park S, Cheon S & Cho D. (2007). The dual effects of interleukin-18 in tumor progression. *Cell Mol Immunol* **4,** 329-335.

Paton JC. (1996). The contribution of pneumolysin to the pathogenicity of Streptococcus pneumoniae. *Trends in Microbiology* **4,** 103-106.

Paton JC, Andrew PW, Boulnois GJ & Mitchell TJ. (1993). Molecular Analysis of The Pathogenicity of Streptococcus Pneumoniae: The Role of Pneumococcal Proteins. *Annual Review of Microbiology* **47,** 89-115.

Pedra JH, Cassel SL & Sutterwala FS. (2009). Sensing pathogens and danger signals by the inflammasome. *Curr Opin Immunol* **21,** 10-16.

Pelegrin P & Surprenant A. (2006). Pannexin-1 mediates large pore formation and interleukin-1beta release by the ATP-gated P2X7 receptor. *EMBO J* **25,** 5071-5082.

Petty RD, Sutherland LA, Hunter EM & Cree IA. (1995). Comparison of MTT and ATP-based assays for the measurement of viable cell number. *Journal of Bioluminescence and Chemiluminescence* **10,** 29-34.

Pinkney M, Beachey E & Kehoe M. (1989). The thiol-activated toxin streptolysin O does not require a thiol group for cytolytic activity. *Infect Immun* **57,** 2553-2558.

Polekhina G, Giddings KS, Tweten RK & Parker MW. (2005). Insights into the action of the superfamily of cholesterol-dependent cytolysins from studies of intermedilysin. *Proceedings of the National Academy of Sciences* **102,** 600-605.

Puren AJ, Fantuzzi G, Gu Y, Su MS & Dinarello CA. (1998). Interleukin-18 (IFNgamma-inducing factor) induces IL-8 and IL-1beta via TNFalpha production from non-CD14+ human blood mononuclear cells. *J Clin Invest* **101,** 711-721.

Qu Y, Franchi L, Nunez G & Dubyak GR. (2007). Nonclassical IL-1 beta secretion stimulated by P2X7 receptors is dependent on inflammasome activation and correlated with exosome release in murine macrophages. *J Immunol* **179,** 1913-1925.

Ratner AJ, Hippe KR, Aguilar JL, Bender MH, Nelson AL & Weiser JN. (2006). Epithelial cells are sensitive detectors of bacterial pore-forming toxins. *J Biol Chem* **281,** 12994-12998.

Rendon-Mitchell B, Ochani M, Li J, Han J, Wang H, Yang H, Susarla S, Czura C, Mitchell RA, Chen G, Sama AE & Tracey KJ. (2003). IFN-gamma induces high mobility group box 1 protein release partly through a TNF-dependent mechanism. *J Immunol* **170,** 3890-3897.

Reuter BK & Pizarro TT. (2004). Commentary: the role of the IL-18 system and other members of the IL-1R/TLR superfamily in innate mucosal immunity and the pathogenesis of inflammatory bowel disease: friend or foe? *Eur J Immunol* **34,** 2347-2355.

Robinson D, Shibuya K, Mui A, Zonin F, Murphy E, Sana T, Hartley SB, Menon S, Kastelein R, Bazan F & O'Garra A. (1997). IGIF does not drive Th1 development but synergizes with IL-12 for interferon-gamma production and activates IRAK and NFkappaB. *Immunity* **7,** 571-581.

Rossjohn J, Feil SC, McKinstry WJ, Tweten RK & Parker MW. (1997). Structure of a cholesterol-binding, thiol-activated cytolysin and a model of its membrane form. *Cell* **89,** 685-692.

Rossjohn J, Gilbert RJ, Crane D, Morgan PJ, Mitchell TJ, Rowe AJ, Andrew PW, Paton JC, Tweten RK & Parker MW. (1998). The molecular mechanism of pneumolysin, a virulence factor from Streptococcus pneumoniae. *J Mol Biol* **284,** 449-461.

Salter RD, Tuma-Warrino RJ, Hu PQ & Watkins SC. (2004). Rapid and extensive membrane reorganization by dendritic cells following exposure to bacteria revealed by high-resolution imaging. *J Leukoc Biol* **75,** 240-243.

Saunders FK, Mitchell TJ, Walker JA, Andrew PW & Boulnois GJ. (1989). Pneumolysin, the thiol-activated toxin of Streptococcus pneumoniae, does not require a thiol group for in vitro activity. *Infect Immun* **57,** 2547-2552.

Scaffidi P, Misteli T & Bianchi ME. (2002). Release of chromatin protein HMGB1 by necrotic cells triggers inflammation. *Nature* **418,** 191-195.

Schotte P, Van Criekinge W, Van de Craen M, Van Loo G, Desmedt M, Grooten J, Cornelissen M, De Ridder L, Vandekerckhove J, Fiers W, Vandenabeele P & Beyaert R. (1998). Cathepsin B-mediated activation of the proinflammatory caspase-11. *Biochem Biophys Res Commun* **251,** 379-387.

Shannon JG, Ross CL, Koehler TM & Rest RF. (2003). Characterization of Anthrolysin O, the Bacillus anthracis Cholesterol-Dependent Cytolysin. *Infect Immun* **71,** 3183-3189.

Sharp FA, Ruane D, Claass B, Creagh E, Harris J, Malyala P, Singh M, O'Hagan DT, Petrilli V, Tschopp J, O'Neill LA & Lavelle EC. (2009). Uptake of particulate vaccine adjuvants by dendritic cells activates the NALP3 inflammasome. *Proc Natl Acad Sci U S A* **106,** 870-875.

Shepard LA, Shatursky O, Johnson AE & Tweten RK. (2000). The mechanism of pore assembly for a cholesterol-dependent cytolysin: formation of a large prepore complex precedes the insertion of the transmembrane beta-hairpins. *Biochemistry* **39,** 10284-10293.

Shoma S, Tsuchiya K, Kawamura I, Nomura T, Hara H, Uchiyama R, Daim S & Mitsuyama M. (2008). Critical involvement of pneumolysin in production of interleukin-1alpha and caspase-1-dependent cytokines in infection with Streptococcus pneumoniae in vitro: a novel function of pneumolysin in caspase-1 activation. *Infect Immun* **76,** 1547-1557.

Shumway CN & Klebanoff SJ. (1971). Purification of Pneumolysin. *Infect Immun* **4,** 388-392.

Simi A, Tsakiri N, Wang P & Rothwell NJ. (2007). Interleukin-1 and inflammatory neurodegeneration. *Biochem Soc Trans* **35,** 1122-1126.

Singh J & Dixon GH. (1990). High mobility group proteins 1 and 2 function as general class II transcription factors. *Biochemistry* **29,** 6295-6302.

Solini A, Chiozzi P, Morelli A, Fellin R & Di Virgilio F. (1999). Human primary fibroblasts in vitro express a purinergic P2X7 receptor coupled to ion fluxes, microvesicle formation and IL-6 release. *J Cell Sci* **112 (Pt 3),** 297-305.

Soltani CE, Hotze EM, Johnson AE & Tweten RK. (2007). Specific Protein-Membrane Contacts Are Required for Prepore and Pore Assembly by a Cholesterol-dependent Cytolysin. *J Biol Chem* **282,** 15709-15716.

Srivastava A, Henneke P, Visintin A, Morse SC, Martin V, Watkins C, Paton JC, Wessels MR, Golenbock DT & Malley R. (2005). The Apoptotic Response to Pneumolysin Is Toll-Like Receptor 4 Dependent and Protects against Pneumococcal Disease. *Infect Immun* **73,** 6479-6487.

Suadicani SO, Brosnan CF & Scemes E. (2006). P2X7 Receptors Mediate ATP Release and Amplification of Astrocytic Intercellular Ca2+ Signaling. *J Neurosci* **26,** 1378-1385.

Sutterwala FS, Mijares LA, Li L, Ogura Y, Kazmierczak BI & Flavell RA. (2007). Immune recognition of Pseudomonas aeruginosa mediated by the IPAF/NLRC4 inflammasome. *J Exp Med* **204,** 3235-3245.

Sutterwala FS, Ogura Y, Szczepanik M, Lara-Tejero M, Lichtenberger GS, Grant EP, Bertin J, Coyle AJ, Galan JE, Askenase PW & Flavell RA. (2006). Critical Role for NALP3/CIAS1/Cryopyrin in Innate and Adaptive Immunity through Its Regulation of Caspase-1. *Immunity* **24,** 317-327.

Sutton C, Brereton C, Keogh B, Mills KH & Lavelle EC. (2006). A crucial role for interleukin (IL)-1 in the induction of IL-17-producing T cells that mediate autoimmune encephalomyelitis. *J Exp Med* **203,** 1685-1691.

Suzuki T, Franchi L, Toma C, Ashida H, Ogawa M, Yoshikawa Y, Mimuro H, Inohara N, Sasakawa C & Nunez G. (2007). Differential regulation of caspase-1 activation, pyroptosis, and autophagy via Ipaf and ASC in Shigella-infected macrophages. *PLoS Pathog* **3,** e111.

Tiemi Shio M, Eisenbarth SC, Savaria M, Vinet AF, Bellemare MJ, Harder KW, Sutterwala FS, Bohle DS, Descoteaux A, Flavell RA & Olivier M. (2009). Malarial hemozoin activates the NLRP3 inflammasome through Lyn and Syk kinases. *PLoS Pathog* **5,** e1000559.

Tilley SJ, Orlova EV, Gilbert RJ, Andrew PW & Saibil HR. (2005). Structural basis of pore formation by the bacterial toxin pneumolysin. *Cell* **121,** 247-256.

Timmer AM, Timmer JC, Pence MA, Hsu LC, Ghochani M, Frey TG, Karin M, Salvesen GS & Nizet V. (2009). Streptolysin O promotes group A Streptococcus immune evasion by accelerated macrophage apoptosis. *J Biol Chem* **284,** 862-871.

Tohyama Y & Yamamura H. (2009). Protein tyrosine kinase, syk: a key player in phagocytic cells. *J Biochem* **145,** 267-273.

Tsan MF & Gao B. (2004). Endogenous ligands of Toll-like receptors. *J Leukoc Biol* **76,** 514-519.

Tschopp J, Martinon F & Burns K. (2003). NALPs: a novel protein family involved in inflammation. *Nat Rev Mol Cell Biol* **4,** 95-104.

Tweten RK. (2005). Cholesterol-Dependent Cytolysins, a Family of Versatile Pore-Forming Toxins. In *Infect Immun*, pp. 6199-6209.

Uhlik MT, Abell AN, Johnson NL, Sun W, Cuevas BD, Lobel-Rice KE, Horne EA, Dell'Acqua ML & Johnson GL. (2003). Rac-MEKK3-MKK3 scaffolding for p38 MAPK activation during hyperosmotic shock. *Nat Cell Biol* **5,** 1104-1110.

Valeva A, Palmer M & Bhakdi S. (1997). Staphylococcal alpha-toxin: formation of the heptameric pore is partially cooperative and proceeds through multiple intermediate stages. *Biochemistry* **36,** 13298-13304.

van der Goot FG, Pattus F, Wong KR & Buckley JT. (1993). Oligomerization of the channel-forming toxin aerolysin precedes insertion into lipid bilayers. *Biochemistry* **32,** 2636-2642.

van Zoelen MA, Yang H, Florquin S, Meijers JC, Akira S, Arnold B, Nawroth PP, Bierhaus A, Tracey KJ & van der Poll T. (2009). Role of toll-like receptors 2 and 4, and the receptor for advanced glycation end products in high-mobility group box 1-induced inflammation in vivo. *Shock* **31,** 280-284.

Vancompernolle K, Van Herreweghe F, Pynaert G, Van de Craen M, De Vos K, Totty N, Sterling A, Fiers W, Vandenabeele P & Grooten J. (1998). Atractyloside-induced release of cathepsin B, a protease with caspase-processing activity. *FEBS Lett* **438,** 150-158.

Vicenova B, Vopalensky V, Burysek L & Pospisek M. (2009). Emerging role of interleukin-1 in cardiovascular diseases. *Physiol Res* **58,** 481-498.

Vinzing M, Eitel J, Lippmann J, Hocke AC, Zahlten J, Slevogt H, N'Guessan P D, Gunther S, Schmeck B, Hippenstiel S, Flieger A, Suttorp N & Opitz B. (2008). NAIP and Ipaf control Legionella pneumophila replication in human cells. *J Immunol* **180,** 6808-6815.

Walev I, Bhakdi SC, Hofmann F, Djonder N, Valeva A, Aktories K & Bhakdi S. (2001a). Delivery of proteins into living cells by reversible membrane permeabilization with streptolysin-O. *Proceedings of the National Academy of Sciences* **98,** 3185-3190.

Walev I, Hombach M, Bobkiewicz W, Fenske D, Bhakdi S & Husmann M. (2001b). Resealing of large transmembrane pores produced by streptolysin O in nucleated cells is accompanied by NF-kB activation and downstream events. *FASEB J***,** 237-239.

Walev I, Reske K, Palmer M, Valeva A & Bhakdi S. (1995). Potassium-inhibited processing of IL-1 beta in human monocytes. *EMBO J* **14,** 1607-1614.

Wang H, Bloom O, Zhang M, Vishnubhakat JM, Ombrellino M, Che J, Frazier A, Yang H, Ivanova S, Borovikova L, Manogue KR, Faist E, Abraham E, Andersson J, Andersson U, Molina PE, Abumrad NN, Sama A & Tracey KJ. (1999). HMG-1 as a late mediator of endotoxin lethality in mice. *Science* **285,** 248-251.

Wang H, Yang H & Tracey KJ. (2004). Extracellular role of HMGB1 in inflammation and sepsis. *J Intern Med* **255,** 320-331.

Wang S, Miura M, Jung YK, Zhu H, Li E & Yuan J. (1998). Murine caspase-11, an ICE-interacting protease, is essential for the activation of ICE. *Cell* **92,** 501-509.

Watanabe H, Gaide O, Petrilli V, Martinon F, Contassot E, Roques S, Kummer JA, Tschopp J & French LE. (2007). Activation of the IL-1beta-processing inflammasome is involved in contact hypersensitivity. *J Invest Dermatol* **127,** 1956-1963.

Watanabe I, Nomura T, Tominaga T, Yamamoto K, Kohda C, Kawamura I & Mitsuyama M. (2006). Dependence of the lethal effect of pore-forming haemolysins of Gram-positive bacteria on cytolytic activity. *J Med Microbiol* **55,** 505-510.

Weaver CT, Harrington LE, Mangan PR, Gavrieli M & Murphy KM. (2006). Th17: an effector CD4 T cell lineage with regulatory T cell ties. *Immunity* **24,** 677-688.

Wei Z, Schnupf P, Poussin MA, Zenewicz LA, Shen H & Goldfine H. (2005). Characterization of Listeria monocytogenes expressing anthrolysin O and phosphatidylinositol-specific phospholipase C from Bacillus anthracis. *Infect Immun* **73,** 6639-6646.

Willingham SB, Allen IC, Bergstralh DT, Brickey WJ, Huang MT, Taxman DJ, Duncan JA & Ting JP. (2009). NLRP3 (NALP3, Cryopyrin) facilitates in vivo caspase-1 activation, necrosis, and HMGB1 release via inflammasome-dependent and -independent pathways. *J Immunol* **183,** 2008-2015.

Willingham SB, Bergstralh DT, O'Connor W, Morrison AC, Taxman DJ, Duncan JA, Barnoy S, Venkatesan MM, Flavell RA, Deshmukh M, Hoffman HM & Ting JP. (2007). Microbial pathogen-induced necrotic cell death mediated by the inflammasome components CIAS1/cryopyrin/NLRP3 and ASC. *Cell Host Microbe* **2,** 147-159.

Willingham SB & Ting JP. (2008). NLRs and the dangers of pollution and aging. *Nat Immunol* **9,** 831-833.

Wilmsen HU, Leonard KR, Tichelaar W, Buckley JT & Pattus F. (1992). The aerolysin membrane channel is formed by heptamerization of the monomer. *EMBO J* **11,** 2457-2463.

Yoshikawa H, Kawamura I, Fujita M, Tsukada H, Arakawa M & Mitsuyama M. (1993). Membrane damage and interleukin-1 production in murine macrophages exposed to listeriolysin O. *Infect Immun* **61,** 1334-1339.

Yoshimoto T, Okamura H, Tagawa YI, Iwakura Y & Nakanishi K. (1997). Interleukin 18 together with interleukin 12 inhibits IgE production by induction of interferon-gamma production from activated B cells. *Proc Natl Acad Sci U S A* **94,** 3948-3953.

Zwaferink H, Stockinger S, Hazemi P, Lemmens-Gruber R & Decker T. (2008). IFN-beta increases listeriolysin O-induced membrane permeabilization and death of macrophages. *J Immunol* **180,** 4116-4123.